

How Cyanobacteria Bore

by

Edgardo L. Ramírez-Reinat

A Dissertation Presented in Partial Fulfillment  
of the Requirements for the Degree  
Doctor of Philosophy

Approved November 2010 by the  
Graduate Supervisory Committee:

Ferran Garcia-Pichel, Chair  
Douglas Chandler  
Jack Farmer  
Susanne Neuer

ARIZONA STATE UNIVERSITY

December 2010

## ABSTRACT

Some cyanobacteria, referred to as boring or euendolithic, are capable of excavating tunnels into calcareous substrates, both mineral and biogenic. The erosive activity of these cyanobacteria results in the destruction of coastal limestones and dead corals, the reworking of carbonate sands, and the cementation of microbialites. They thus link the biological and mineral parts of the global carbon cycle directly. They are also relevant for marine aquaculture as pests of mollusk populations. In spite of their importance, the mechanism by which these cyanobacteria bore remains unknown. In fact, boring by phototrophs is geochemically paradoxical, in that they should promote precipitation of carbonates, not dissolution. To approach this paradox experimentally, I developed an empirical model based on a newly isolated euendolith, which I characterized physiologically, ultrastructurally and phylogenetically (*Mastigocoleus testarum* BC008); it bores on pure calcite in the laboratory under controlled conditions. Mechanistic hypotheses suggesting the aid of accompanying heterotrophic bacteria, or the spatial/temporal separation of photosynthesis and boring could be readily rejected. Real-time  $\text{Ca}^{2+}$  mapping by laser scanning confocal microscopy of boring BC008 cells showed that boring resulted in undersaturation at the boring front and supersaturation in and around boreholes. This is consistent with a process of uptake of  $\text{Ca}^{2+}$  from the boring front, trans-cellular mobilization, and extrusion at the distal end of the filaments (borehole entrance).  $\text{Ca}^{2+}$  disequilibrium could be inhibited by ceasing illumination, preventing ATP generation, and more specifically, by blocking P-type  $\text{Ca}^{2+}$

ATPase transporters. This demonstrates that BC008 bores by promoting calcite dissolution locally at the boring front through  $\text{Ca}^{2+}$  uptake, an unprecedented capacity among living organisms. Parallel studies using mixed microbial assemblages of euendoliths boring into Caribbean, Mediterranean, North and South Pacific marine carbonates, demonstrate that the mechanism operating in BC008 is widespread, but perhaps not universal.

Dedicated to my wife Jennifer  
and my sons Alex and Orion; three lights in my life

## ACKNOWLEDGMENTS

This work could have not been possible without the mentoring, and out-of-the-box ideas of Dr. Ferran Garcia-Pichel, to whom I owe a strong foundation in science, and many of the core values that I use in teaching and mentoring students of my own. Dr. Garcia-Pichel helped me, in a joyful and swift way, to see the light at the end of the tunnel on the many times the solutions to a problem were not obvious to me. It is said in the FGP lab that graduate students are a simple block of marble, which with many years of chiseling, become full-fledged doctors. So Ferran, cheers to you and thanks for the chiseling!

To Dr. Lilliam Casillas from University of Puerto Rico in Humacao, a great mentor, who gave me the opportunity for undergraduate research and introduced me to microbial ecology. I recall with much affection the many fun and educational trips to the NSF Microbial Observatory in Cabo Rojo, Puerto Rico, which consequently inspired me to pursue my doctoral education (¡Doctora mil gracias!)

To past and present members of the Garcia-Pichel lab, who played an important part in my scientific development, as peers, mentors and friends. I would like to thank Dr. Scott Bates for the many ideas and insight in all stages of my project, not to mention his friendship, which I value deeply. To Dr. Tanya Soule (a.k.a. “Buddy”) for her cheerful and helpful insight in dealing with the rollercoaster of graduate school. To Dr. Hugo Beraldi-Campesi, for his support, friendship and guitar playing breaks in-between hard working hours. Thanks to Drs. Sathyanarayana Reddy Gundlapally,

Quinje “Jason” Gao, Doerte Hoffman and Cosmin Sicora. Thanks to Ruth Potrafka (“La Jefa”) for her strong support on the many years of graduate school.

To Drs. Page Baluch, Bret Judson and Douglas Chandler of the Keck Lab Bioimaging Facility at Arizona State University for their immense help with confocal microscopy.

To the Hispanic Research Fund at ASU (especially Laura Serrano and Elizabeth Lúquez,) who made my participation in the NSF Bridge to the Doctorate and MGE@MSA (AGEP) fellowships possible, and to whom I owe my very Ph.D. degree; without them, this endeavor would have been impossible. Thank you.

And to all those that I have failed to mention, who made the many years of graduate school a gratifying journey, thank you!

# TABLE OF CONTENTS

	Page
LIST OF TABLES.....	ix
LIST OF FIGURES.....	x
CHAPTER	
INTRODUCTION .....	1
Bioerosion as a geobiological process and its biological agents....	1
Cyanobacteria and their boring members .....	3
Diversity of boring cyanobacteria .....	8
Mechanisms of cyanobacterial boring and the thermodynamics of dissolution.....	10
The boring mechanism in cyanobacteria .....	13
Ca <sup>2+</sup> transport and homeostasis.....	16
Research approach and considerations.....	18
1 POLYPHASIC CHARACTERIZATION OF A MARINE EUENDOLITHIC CYANOBACTERIUM AND THE REDESCRIPTION OF THE GENUS MASTIGOCOLEUS LAGERHEIM .....	27
Abstract .....	28
Introduction .....	28
Materials and Methods.....	31
Results .....	38
Discussion .....	42
Acknowledgements .....	48

CHAPTER	Page
2 HOW CYANOBACTERIA BORE .....	58
Abstract .....	59
Introduction .....	59
Materials and Methods.....	65
Results .....	72
Discussion .....	78
Conclusions .....	82
Acknowledgements .....	82
3 UNIVERSALITY OF THE Ca <sup>2+</sup> ATPASE-MEDIATED CARBONATE BORING MECHANISM IN CYANOBACTERIAL EUENDOLITHS .....	90
Abstract .....	91
Introduction .....	92
Materials and Methods.....	94
Results .....	99
Discussion .....	103
Conclusions .....	107
Acknowledgements .....	107
4 A METHOD FOR THE EXHUMATION OF LIVE ENDOLITHS FROM CARBONATE .....	112
Abstract .....	113
Introduction .....	113
Materials and Methods.....	115



	Page
Discussion .....	119
Acknowledgements .....	120
REFERENCES .....	123

## LIST OF TABLES

Table		Page
1.	Euendolithic genera .....	20
2.	Boring in various solid substrates .....	89

## LIST OF FIGURES

Figure		Page
1.	Marine carbonates infested by metazoans and microborers .....	23
2.	Model of boring by calcium pumping .....	24
3.	Calcite chips infested with <i>Mastigocoleus testarum</i> BC008.....	25
4.	<i>Mastigocoleus testarum</i> BC008; free living and boring filaments, colonies .....	26
5.	BC008; lateral heterocysts, tapering, boring into calcite, hormogonia .....	50
6.	Morphological changes of BC008 boring filaments.....	51
7.	Ultrastructure of BC008 cells.....	52
8.	Complementary chromatic adaptation in BC008 .....	53
9.	Phylogenetic tree of BC008 and cyanobacteria; 16S rRNA .....	54
10.	Phylogenetic tree of BC008 and cyanobacteria; <i>nifH</i> .....	55
11.	Phylogenetic tree of BC008 and cyanobacteria; <i>rbcL</i> .....	56
12.	Phylogenetic tree of BC008 and cyanobacteria; <i>kaiC</i> .....	57
13.	BC008; phase-contrast, autofluorescence, boring in chips, boring into calcite.....	83
14.	Growth rates of BC008 & photopigments in boring cells .....	84
15.	Photosynthetic rates of boring BC008 filaments .....	85
16.	Calcium microprofiles & fluorophor enabled Ca <sup>2+</sup> mapping .....	86
17.	Effect of light/dark shift and calcium transport inhibitors in Ca <sup>2+</sup> release by BC008 .....	87

Figure	Page
18. Effect of calcium transport inhibitors on photosynthesis; oxygen optode time courses.....	88
19. Diversity of field euendoliths as imaged by laser scanning confocal microscopy .....	108
20. Morphological diversity of field euendoliths .....	109
21. Effect of light/dark shift and calcium transport inhibitors in Ca <sup>2+</sup> release by field euendoliths.....	110
22. Phylogenetic tree (16S rRNA) of all field clone sequences.....	111
23. Exhumation steps .....	121
24. Exhumation steps, cont. ....	122



## INTRODUCTION

### *Bioerosion as a geobiological process and its biological agents*

Erosion is a natural weathering process that occurs on Earth's landmasses as a consequence of geomorphologically relevant phenomena, typically understood as a combination of the destructive actions of wind, water, ice, or gravity, and ultimately involves the transport of solids such as rocks, sediments, soil and other particles. Living organisms can contribute, exacerbate and even drive the weathering processes through bioerosion, which is defined as the erosion of a hard substrate by biological means (Neumann, 1966). Bioerosion is a common process in marine, freshwater and terrestrial environments and many animals and microorganisms can colonize exposed substrates, either inorganic or biogenic in origin, actively eroding them as they create cavities that are in many cases incidental to their trophic or metabolic strategies. One typical mode of bioerosion is the case of herbivores, such as snails or sea urchins, that feed upon primary producers attached to a mineral substrate, such as the case of an algal biofilm and that in so doing, scrape off part of the mineral solid. Another example is the case of sulfide oxidizing bacteria growing on concrete sewer pipes, which release corrosive metabolic by-products, and by doing so weaken the pipe's structure. A third mode of bioerosion is the result of active tunneling or burrowing on the part of the biological agents, such as the case of polychaetes or sponges who will initially create small burrows into a substrate surface, or the case of algae that actively excavate galleries into calcareous substrates as means of

securing a living space.

Many metazoans are agents of bioerosion, and erode hard substrates by mechanical means or a combination of mechanical and chemical dissolution, and do their impact by grazing, scraping or swallowing (Flugel, 2004). Examples include echinoids (sea urchins and sand-dollars) (Carreiro-Silva and McClanahan, 2001, Herrera-Escalante, et al., 2005, Toro-Farmer, et al., 2004), gastropods (snails) (Carriker and Gruber, 1999, Herbert, et al., 2009, Wayne, 1987), polychaetes (worms) (Blake, 1969, Buschbaum, et al., 2006, Riascos, et al., 2009, Wayne, 1987), sponges (Nava and Carballo, 2008, Neumann, 1966, Zundeleovich, et al., 2007), holothurians (sea cucumbers) (Hammond, 1981, Jansen and Ahrens, 2004), chitons (Barbosa, et al., 2008, Rasmussen and Frankenberg, 1990) and fish (Ong and Holland, 2010, Peyrot-Clausade, et al., 2000, Rotjan and Lewis, 2005). Many of these contribute to the typical look of a maritime coast (i.e. sea urchins, sponges and chitons), colonizing exposed calcareous surfaces. Among metazoans, sponges and polychaetes can be considered true macroborers, as they will tunnel into the carbonate to attach themselves to the substrate. At the microscopic level, microborers including fungi (Bentis, et al., 2000, Golubic, et al., 2005), algae (green, brown and red) and cyanobacteria (Tribollet, 2008, Le Campion-Alsumard, et al., 1995, Golubic, 1969) that can actively excavate tunnels in carbonates by means of chemical dissolution. They colonize calcareous and calcophosphatic substrates, including bone, shells, skeletal carbonate, limestones and dolostones (Campbell, 1983). Among the agents of bioerosion, microborers are some of the most common, widespread and environmentally

significant (Garcia-Pichel, 2006), found in variable geographic regions, from the cold (Wisshak, et al., 2005, Young and Nelson, 1988), to the temperate (Kaehler, 1999, Webb and Korrubel, 1994, Young and Nelson, 1988), subtropical (Al-Thukair, 2002, Peyrot-Clausade, et al., 2000, Sheppard, et al., 2002, Zubia and Peyrot-Clausade, 2001) and tropical (Chazottes, 1995, Che, et al., 1996, Laurenti and Montaggioni, 1995, Le Campion-Alsumard, 1991).

Bioerosion rates for many systems are in the order of kilograms of carbonate per meter squared per year. For example, in coral reefs one study found that grazers eroded  $2.6 \text{ kg CaCO}_3 \text{ m}^{-2} \text{ yr}^{-1}$ , while bioerosion by microborers was measured at  $0.6 \text{ kg CaCO}_3 \text{ m}^{-2} \text{ yr}^{-1}$  (Chazottes, 1995 ). In another study, sponges were found to have bioerosion rates that varied between 4 to  $16 \text{ kg m}^{-2} \text{ year}^{-1}$  (Holmes, et al., 2009). In yet a third study, five genera and 6 species of cyanobacteria, green and red algae and different kinds of heterotrophic microendoliths were found to erode  $0.2\text{--}0.3 \text{ kg CaCO}_3 \text{ m}^{-2} \text{ yr}^{-1}$  (Vogel, et al., 2000). These examples illustrate the impact of bioerosion in many communities and its importance in carbonate biogeochemical cycling.

### *Cyanobacteria and their boring members*

Among the microborers, cyanobacteria contribute significantly to bioerosion. Cyanobacteria are a unique and diverse phylum of oxygenic, photosynthetic bacteria capable of synthesizing chlorophyll a, splitting water as a source of electrons. Intrinsic to the light gathering apparatus in cyanobacteria, the phycobilisome, are the phycobiliproteins phycocyanin and



allophycocyanin and in some cases phycoerythrin. Different expression levels of these pigments will promote the display of a variety of colors, blue-green being the most typical, but including brown, red, olive, black, violet and other shades. Some cyanobacteria are able to express ultraviolet sunscreens, such as scytonemin (Garcia-Pichel, et al., 1992, Proteau, et al., 1993, Soule, et al., 2007), which imparts a dark brown color to the sheaths of those that do so; other sunscreens, such the mycosporine-like aminoacids, are found in some cyanobacteria as well (Garcia-Pichel, et al., 1993). These bacteria were described initially by botanists, and referred to as *blue-green algae* or cyanophytes within the botanical taxonomy. Even today, a complete bacteriological treatment is missing and most of the descriptions available follow the botanical traditions, with all of their inherent shortcomings. Some the oldest microfossils of cyanobacteria reach back to 3.5 billion years ago (Lee, et al., 1999). Cyanobacteria are the oldest known oxygen-producing organisms, with the appearance of cyanobacteria on Earth and the oxygenation of the planet going hand in hand (Dismukes, et al., 2001).

Cyanobacteria are cosmopolitan, found in a variety of geographical settings across the globe. Their generic niche is limited to temperatures above 4°C, and below 74 °C (Ward, 2002); many cyanobacteria have adapted to cold climates and contribute to primary productivity such as the case of Antarctic lakes (Pandey, et al., 2004) as well as being extremely important in hot spring mats (Miller and Castenholz, 2000). In terms of pH, cyanobacteria grow at neutral and alkaline pH and very rarely under acidic conditions, generally found in pHs above 4-5 (Brock, 1973). The upper limit for pH in

cyanobacteria is closer to 11, with some members thriving in very alkaline environments, such as the case of soda lakes in Eastern Africa (Mikhodyuk, et al., 2008) and Russia (Kupriyanova, et al., 2003). Their general habitat is not necessarily limited by salinity, as they are found in freshwaters, seawater, brackish waters and hypersaline environs; some with extreme halotolerance, such as *Halotheca*, growing in salinities close to 12% w/v (ca. 3.5 times open ocean salinity) (Garcia-Pichel, et al., 1998) and 3.0 M NaCl for *Aphanotheca halophytica* (close to 17% w/v or almost 5 times open ocean salinity) (Takabe, et al., 1988, Waditee, et al., 2001). Cyanobacteria account for 20–30% of Earth's primary productivity and convert solar energy into biomass-stored chemical energy at the rate of ~450 TW (Waterbury, et al., 1979). Many members are able to fix gaseous nitrogen from the atmosphere into organic chemical species; the vast majority (with the exception of some pelagic unicellular species) do it with specialized, thick-walled cells called heterocysts, which harbor the oxygen-sensitive enzyme nitrogenase, responsible for nitrogen fixation. Heterocystous species are considered truly multicellular organisms as their cells exchange nutrients and regulatory molecules (Flores, et al., 2006). Cyanobacteria have been used as food source by many cultures; the Mayans supplemented their diets with dried *Spirulina* cakes, which were sold in the antique markets of Tenochtitlan (today's Mexico City) (Diaz del Castillo, 1928). In modern times *Spirulina* is consumed in China (Roney, et al., 2009), India (Kumar, 2004), Peru (Johnson, et al., 2008) and Sudan (Ciferri, 1983), as well as part of a health-conscious diet in the United States. Cyanobacteria have a rich nutritional value due to their

high protein content, in addition to being a source of chemical and pharmaceutical products (Rodríguez, et al., 1989).

Several groups of cyanobacteria colonize carbonate rocks. Epilithic forms live on the surface, while chasmoliths take advantage of space provided in cracks or fissures. Cryptoendolithic cyanobacteria are those that live in natural pores or cavities in the rocks. Finally, euendolithic cyanobacteria (Golubic, et al., 1984) will actively excavate tunnels or burrows within the mineral solid. The latter are also referred to in the literature as boring, excavating, penetrating or tunneling cyanobacteria. Some of the earlier botanical articles from the late 19<sup>th</sup> and early 20<sup>th</sup> centuries mention them regularly, a variety being described as “perforating algae” (Bornet, 1888, Bornet, 1889, Ercegović, 1927, Frémy, 1936). Typical boring substrates include solid limestone and dolomite rocks as well as loose sand-size carbonate particles, shells and shell hash and other skeletal fragments (Golubic, 1975). In many cases, a common visual indication of boring by cyanobacteria is the formation of green bands within the substrate (Le Campion-Alsumard, et al., 1995). Microborers play a considerable role in the diagenesis of carbonates, producing fine grain sediments as a result of the crisscrossing tunnels in the mineral (Golubic, et al., 2005). The work of euendoliths is not always destructive, as they are known to also promote lithification in stromatolitic communities. Some cyanobacterial borers will excavate tunnels in carbonate sand grains, which eventually get filled with micrite (microcrystalline aragonite) that precipitates as the microorganism advances (Reid and Macintyre, 2000), likely due to calcium excretion by the

borers. The encrypted filaments become part of the scaffolding that holds the sand grains together and multiple cycles of this dissolution and re-precipitation completely cements them, creating a solid substrate. Nevertheless, a euendolith's impact is not restricted to just geologically relevant phenomena. Euendoliths will take advantage of the plentiful carbonate substrate provided by mollusk shells of clams, mussels and oysters. The infestation of bivalves by species such as *Mastigocoleus testarum* makes the shells brittle and the animals more prone to disease (Che, et al., 1996, Kaehler, 1999, Webb and Korrubel, 1994). This has large implications for commercial bivalve aquaculture operations.

Through the process of boring, euendoliths will leave clear traces of their activity in the substrates that they excavate, and these fossilize well. The fossil record presents evidence of euendoliths populating the Earth since the Precambrian. The oldest cyanobacterial euendolithic microfossil, *Eohyella campbellii*, was recorded in carbonate rocks as old as 1.5 billion years (Zhang, 1987). Other evidence of euendolithic fossils is found in microbial assemblages from the Neoproterozoic, some 700-800 million year ago, where the cells penetrated aragonitic ooid grains (Knoll, et al., 1986, Knoll, et al., 1989). Such is the case in ooid grains from the Upper Riphean/Vendian (570-700 Myr), which were originally carbonaceous and underwent silicification after boring occurred, pointing to microbial boring evolving before the appearance of skeleton-bearing metazoans in the geological record (Campbell, 1982). Some of these microfossils are commonly used, for example, in paleobathymetric reconstructions that use models based on the distribution

of microborers in ancient microbial assemblages (Budd and Perkins, 1980, Chazottes, et al., 2009, Vogel and Brett, 2009).

#### *Diversity of boring cyanobacteria*

The first publications that describe some of the most common euendoliths date back to the late 1800's, including the genera *Mastigocoleus* (Lagerheim, 1886), *Plectonema* (Thuret, 1875) and *Hyella* (Bornet, 1888). Common euendolithic genera (illustrated in Table 1) include *Cyanosaccus*, *Hormathonema*, *Hyella*, *Solentia*, *Plectonema*, *Kyrthutrix*, *Schizotrix*, *Iyengariella* and *Mastigocoleus*, which all have been described according to the botanical code. These morphogenera are fairly cosmopolitan, judging from literature reports, and are found boring in a variety of calcareous substrates. Some other forms have been described as being "euendolithic" (e.g. *Lithococcus*, *Placoma*, *Chloroglea*, *Paracapsa*, *Lithocapsa* ) but have questionable true boring capabilities (e.g. *Enthophysalis deusta*) (Golubic, 1975, Le Campion-Alsumard, 1970). All of them are of uncertain phylogenetic placement and even some of dubious taxonomic status. Their potential morphological plasticity and the lack of cultivated representatives or any phylogenetic information define the present situation of these "euendoliths". Thus, these genera are not included in the table. A much less stringent listing was presented in a paper by May and Perkins (May and Perkins, 1979).

We note that even using a conservative list, the cyanobacterial borers display a remarkable diversity, spanning 4 out of 5 Orders in the phylum.

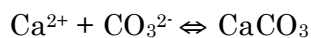
This can be interpreted as a synapomorphy, in which a common ancestor already had a capability to bore. The boring capability, was kept only in certain species, according to its selective value, but lost in most others; a rather unlikely explanation considering the overwhelming diversity of cyanobacteria in the tree of life. Alternatively, we may have a case of lateral transfer of a capacity that evolved at some point in one of the groups. Yet a third possibility is that boring represents a case of convergent evolution, in which the ability evolved multiple times as a result of selective pressure. The first 2 explanations would allow us to predict a common mechanism and genetic basis in all, whereas the last would call for different mechanisms or genetic elements. These alternatives have not been studied explicitly.

In terms of evolutionary advantage, the reasons why euendoliths penetrate into carbonates are not entirely clear. As always the 'why' questions lie at the fringe of biological reasoning. Many habitats where euendoliths are found such as intertidal and supra-tidal zones, are considered extreme. Selection pressures such as temperature variation, desiccation, nutrient acquisition, excessive solar irradiance, and herbivore grazing activity could promote boring; none of these pressures is mutually exclusive and they probably act in concert to favor the development of microorganisms that bore (Garbary, 2007). Carbonates being a relatively soft and ample substrate, offer some protection from these demanding circumstances, and allow the establishment of a habitat only a few organisms can take advantage of.

*Mechanisms of microbial boring and the thermodynamics of dissolution*

But how do cyanobacteria bore? Our knowledge of the physiological mechanisms that drive euendolithic boring has remained in the shadows. There is minimal information, and many hypotheses, on how cyanobacteria bore into carbonates with no comprehensive experiments, before this dissertation, that aimed at testing these hypotheses. This may be a result of a lack of available cultures, as euendoliths have been mostly described *in situ*, and when cultures have been obtained, they have either not been submitted to collections or have lost their boring capacity. There have been some efforts in establishing cultures to better understand euendoliths (Al-Thukair and Golubic, 1991, Montoya-Terreros, 2006, Pari, et al., 1998, Vogel, et al., 2000) mostly with identification and characterization in mind. To bore into the carbonate, regardless of the mechanism, cyanobacteria must follow basic thermodynamic constraints that govern carbonate dissolution. To understand how a carbonate is dissolved, I will refer to Le Châtelier's equilibrium reaction, which states that if a system in equilibrium is disturbed by changes in determining factors (temperature, pressure, and concentration of components) the system will tend to shift its equilibrium position so as to counteract the effect of the disturbance. The solubility equilibrium thus governs when a substrate precipitates or dissolves.

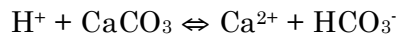
The formation/dissolution of calcium carbonate is expressed as:



Carbonate ions are a constituent part of the carbonate system in water, expressed as:



whose equilibrium depends on pH. At a neutral to slightly alkaline pH (within oceanic range), the equation can be expressed as:



It is obvious from this equation that to dissolve the carbonate, one has to either increase concentration of protons (lower pH), or decrease concentration of bicarbonate or  $\text{Ca}^{2+}$ , or a combination of both. Both mechanisms affect the thermodynamics of the reaction by shifting the equilibrium towards dissolution.

The reactions of dissolution and precipitation of ionic compounds are governed by the solubility equilibrium, a dynamic equilibrium, which depends on the compound's specific solubility product ( $K_{sp}$ ) and the activities of the specific ions (IAP).

In an ionic dissociation reaction (calcium carbonate is used as an example) the equilibrium would be expressed as:

$$K^{\theta} = \frac{[\text{Ca}^{2+}(aq)][\text{CO}_3^{2-}(aq)]}{[\text{CaCO}_3(s)]} = [\text{Ca}^{2+}(aq)][\text{CO}_3^{2-}(aq)]$$



where  $K^\theta$  is the solubility equilibrium constant and the brackets indicate ion activity. The activity of solids is one by definition. In insoluble salts, (i.e. calcium carbonate) the ion activities are close to one, which reduces the equation to:

$$K_{sp} = [Ca^{2+}][CO_3^{2-}]$$

When the reaction is in equilibrium, the activities of the ions equal the solubility product ( $IAP = K_{sp}$ ) and the solid remains intact. When the activities of either of the ions increase stoichiometrically, the value of IAP becomes higher than the solubility product ( $IAP > K_{sp}$ ) and thus precipitation of carbonates becomes thermodynamically favorable. When the activity of either of the ions decreases, the value of the IAP becomes lower than the solubility product constant ( $IAP < K_{sp}$ ) and thus dissolution is thermodynamically favored. An approach that reduces the ion activity product must be used by cyanobacteria to excavate into the mineral.

The oceans are supersaturated with respect to  $Ca^{2+}$ , with the average concentration close to 10mM. The spontaneous solubility of calcium carbonate in seawater does not happen readily under standard pH conditions (ca. pH = 8.1-8.3). Boring into a carbonate seems like a rather difficult endeavor, analogous to swimming against the current. Under normal pH conditions, the thermodynamics in seawater favor precipitation, not dissolution. Thus, seems obvious that the dissolution of carbonates in such an environments can only happen at the expense of energy. This of course, is dependent on concentration of carbonate ions, as the concentration on calcium does not

change significantly in the oceans. A direct example of this dependency can be seen in the recent work by Tribollet (2009) in which ocean acidification as the result of an increase in partial pressures of CO<sub>2</sub> favor dissolution of calcium carbonate by euendoliths.

### *The boring mechanism in cyanobacteria*

The boring mechanism of euendolithic cyanobacteria remains obscure. The fact that dissolution happens in an environment where the opposite would be expected (i.e. the case of CaCO<sub>3</sub> in seawater), adds a degree of complexity to the study of the mechanism. Some plausible mechanisms of boring had been suggested. Most authors call on the use of acidic substances secreted by the cells, that dissolve the carbonate and allow the cells to grow into the mineral (Schneider and Le Campion-Alsumard, 1999). This is the most widely accepted theory amongst scholars. Some have even wanted to see specialized organelles that would sustain this function (Alexandersson, 1975), but this could not be corroborated by ensuing decades of independent research. The big problem with this is that cyanobacteria are autotrophs and by nature will consume CO<sub>2</sub> through photosynthesis, thereby increasing the pH of their environment. Garcia Pichel (2006) tried to elucidate theoretical alternatives that would not contradict known metabolic pathways or the thermodynamics of the systems in which boring occurs. Strategies that utilize dissolution by acids for example could involve the temporal separation of the boring process, in which the euendoliths only bore at night, using the by-products of respiration as the driver of boring. Another is the spatial

separation of the process, in which cells are photosynthetically active outside the carbonate matrix, and as they penetrate, the cells switch to respiration exclusively to power the carbonate dissolution. The proposed acid-dissolution mechanism, although plausible, has many conflicting physiological consequences. Additionally, cyanobacteria do not survive at pH levels below 4, possibly due to proton damage to the cell membrane (Brock, 1973). Small-molecular weight organic acids (products of carbon fixation) are metabolically unsustainable, with the maximal number of carboxyl moieties in such acids (1 in formic, 2 in oxalic, 3 in citric...) corresponding stoichiometrically to the moles of CO<sub>2</sub> taken up from the medium and consequently to the protons already consumed (Garcia-Pichel, 2006). Using this method means that a great deal of carbon fixed has to go exclusively to the production of acids, which would be extremely expensive metabolically.

Apart from the acidic by-product hypotheses, another mechanism is the removal of the metal ion (in this case Ca<sup>2+</sup>) from the water by the action of Ca<sup>2+</sup> transporting, energy-dependent enzymes. The dissolution process, under many of the geochemical conditions in which it has been described, occurs in waters saturated or supersaturated with respect to calcite and aragonite, and is thermodynamically unfavorable, therefore excavation would only be possible at the cost of energy (Garcia-Pichel, 2006). Removing Ca<sup>2+</sup> from the water in the interstitial space (between cell and mineral) would create an under-saturated environment at the boring front, and consequently cause a small amount of the mineral to be dissolved, a result of thermodynamic equilibrium. The Ca<sup>2+</sup> is mobilized intracellularly, and eventually released by

the cells opposite to the boring front. This alternative was previously suggested by Garcia-Pichel (2006), in which the primary driver in the boring process is  $\text{Ca}^{2+}$  transport, and not acid-dissolution.

The model for carbonate boring using  $\text{Ca}^{2+}$  transport is illustrated in Fig 2. Initially, free-living filaments of the euendolith attach as a biofilm to the calcium carbonate. The cell in closest proximity to the mineral, initiates the boring process by mobilizing  $\text{Ca}^{2+}$  from the water in the interstitial space between the cell and the mineral. The  $\text{Ca}^{2+}$  activity is lowered, and the thermodynamic equilibrium is thus shifted towards dissolution. The mineral dissolves, giving off free  $\text{Ca}^{2+}$  to compensate for the lower ion activity. Once a small amount of the mineral is dissolved, the apical cell will grow to fill the void, and the process of dissolution is resumed. The  $\text{Ca}^{2+}$  taken is mobilized, from cell to cell, and eventually released from the distal cell (the one closest to the mineral's surface) maintaining  $\text{Ca}^{2+}$  homeostasis in the cytoplasm. Dissolution will free  $\text{CO}_3^{2-}$  in solution, and under normal seawater pH conditions, buffering will shift  $\text{CO}_3^{2-}$  to  $\text{HCO}_3^-$ , which can be taken by the cells as source of inorganic carbon, achieving charge balance in the process.

#### *$\text{Ca}^{2+}$ transport and homeostasis*

The previous model implicates transport processes of  $\text{Ca}^{2+}$ ; it is thus advisable to review some of the principles and condition of  $\text{Ca}^{2+}$  transport in living systems. In higher organisms,  $\text{Ca}^{2+}$  plays an important role as secondary messenger. For example it acts as a secondary messenger in cardiac myocytes (Kabakov and Hilgemann, 1995, Tan, et al., 1988, Wilde, et

al., 1991), skeletal muscle (Dirksen and Beam, 1995, Lynch, et al., 1997, Zhao, et al., 1996) and cancerous cells (Flourakis and Prevarskaya, 2009, Furuya, et al., 1993), as well as in processes like apoptosis (Criddle, et al., 2007, Porn-Ares, et al., 1998), cell proliferation (Schreiber, 2005, Sperti and Colucci, 1991), motility (Hong, et al., 1985, Moon, et al., 2004, Young and Nelson, 1974) and signaling (Domínguez, 2004, Norris, et al., 1996). In bacteria,  $\text{Ca}^{2+}$  regulates processes like chemotaxis (Ordal, 1977, Snyder, et al., 1981), chromosomal regulation and replication (Norris, et al., 1988). Cellular  $\text{Ca}^{2+}$  homeostasis is necessary and levels are kept rather constant at the cost of energy (Pandey, et al., 1999), with normal levels of intracellular  $\text{Ca}^{2+}$  maintained very low, ranging from 0.1–0.2  $\mu\text{M}$ , to prevent toxicity to the cell metabolism, although transient levels may rise to 5  $\mu\text{M}$  in some cyanobacteria (Torrecilla, et al., 2001). This homeostasis is achieved by the uptake and export of  $\text{Ca}^{2+}$  in the cell. A variety of  $\text{Ca}^{2+}$  transport strategies are described in living systems and include passive permeability,  $\text{Ca}^{2+}$ -specific channels,  $\text{Ca}^{2+}/\text{H}^{+}$  antiporters and  $\text{Ca}^{2+}$ -ATPases (Kretsinger and Nelson, 1976). Passive permeability does not use energy and typically occurs when extracellular concentration of  $\text{Ca}^{2+}$  is higher.  $\text{Ca}^{2+}$  channels allow the selective transport of  $\text{Ca}^{2+}$  across membranes or between cells.  $\text{Ca}^{2+}$ -proton antiporters are powered by proton motive force and the enzymes are involved in  $\text{Ca}^{2+}$  efflux, exchanging  $\text{Ca}^{2+}$  and protons across energized membranes.  $\text{Ca}^{2+}$ -ATPases are linked to ATP hydrolysis and the enzymes are involved in  $\text{Ca}^{2+}$  transport against concentration gradients.

Ca<sup>2+</sup> channels are found in cyanobacteria and thought to be involved in gliding motility (Hoiczuk, 2000, Hoiczuk and Baumeister, 1997, Hoiczuk and Baumeister, 1998) and phototaxis (Moon, et al., 2004, Toh, et al., 2009). Ca<sup>2+</sup>-ATPases, which are responsible in actively exporting the cation out of the cell, have been described in cyanobacteria as well (Berkelman, et al., 1994, Geisler, et al., 1993). It appears that the building blocks needed for the Ca<sup>2+</sup> pump-enabled dissolution can be present in cyanobacteria, so it is not difficult to envision the possibility of one or many of these mechanisms involved the carbonate excavation; the problem lies in identifying specifically (1) if is indeed caused by the transporting of Ca<sup>2+</sup> enzymes and (2) by what type of enzyme it is and how does it do it. If euendoliths are dissolving the carbonate by Ca<sup>2+</sup> mobilization, they must be using an equal or similar strategy to the ones previously described above.

Regardless of the cellular approach, without a culture, there is little that can be done to shed light on the mechanism. Therefore, there is a need for a thorough investigation of the specifics that drive boring in euendolithic cyanobacteria in at least one model organism. Any knowledge acquired, apart from being a significant contribution, would motivate the further characterization of other euendoliths alike.

### *Research approach and considerations*

The primary goal of this dissertation is to unveil the mechanism by which euendolithic (boring) cyanobacteria bore into carbonates. This dissertation is divided in four chapters, each following the format of a scientific journal

article. In Chapter 1, I address our model organism, (illustrated in Fig. 4) which is a euendolithic cyanobacterium isolated from marine carbonates in Cabo Rojo, Puerto Rico. To resolve the mechanism of boring, the first requirement is to have a model in which it can be studied. This chapter presents the polyphasic approach used to characterize the organism, including its ecology, morphology, ultra-structure, adaptations and phylogeny.

In Chapter 2, I focus on the physiology and molecular basis of the boring mechanism in *Mastigocoleus*, which was cultivated and allowed to bore under controlled laboratory conditions (Fig. 3). This chapter presents data on the dynamics of the mechanism, and its relationship with the  $\text{Ca}^{2+}$  - pumping model. It will present as well the effects of blockers of  $\text{Ca}^{2+}$  transporters, including channels and ATPases, which were added to try to impair boring. Finally, we attempted to find genes encoding for  $\text{Ca}^{2+}$  - specific transporting enzymes and these findings are presented as well.

In Chapter 3, I evaluate the commonalities of the mechanism amongst a variety of euendolithic cyanobacteria by returning to the field. Euendolithic cyanobacteria are widespread and there is the possibility of alternative strategies being used to bore that differ from the proposed model. Euendolithic representative communities from all over the world, collected from beaches in Baja California, Mexico, Cabo Rojo, Puerto Rico, Sardinia, Italy and Whakatane, New Zealand, were evaluated with culture independent methods. Euendolithic populations were evaluated

simultaneously for the phylogenetic composition using the 16S rRNA gene, and for the response to specific boring inhibitors.

Lastly, Chapter 4 will present, both in written and video format, a modified method of disinterring live filaments from carbonates. This method derives from an original protocol by Wade (Wade and Garcia-Pichel, 2003) and allowed the exhumation of the filaments while still alive. This method was key for the analyses presented in Chapter 2.

It is my greatest desire that this dissertation provides some insight on how the mechanism of cyanobacterial boring works, unveiling its obscurity. Hopefully, it will inspire the comprehensive study of other euendoliths as well.



Table 1. Genera of common euendolithic cyanobacteria. Classification of groups according to the botanical nomenclature. Drawings of typical morphotypes are shown for comparison. *Bar, 10 μm.*

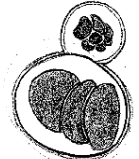
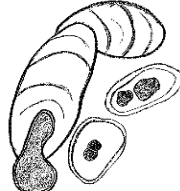
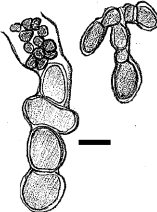
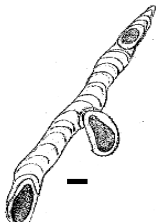
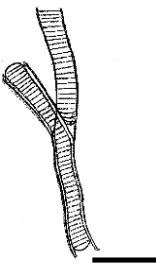
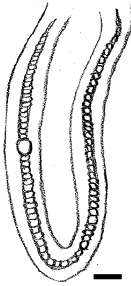
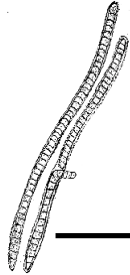
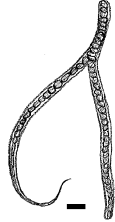

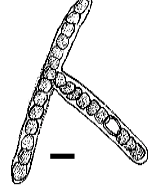
Order Pleurocapsales (Group 2)	Ecology	Substrate	Reference	Morphology
<b><i>Cyanosaccus</i></b> ( <i>C. aegeus</i> , <i>C. atticus</i> <i>C. piriformis</i> )	Greece, Spain	Estuarine and marine mollusk shells, cave carbonates and other limestone substrates	(Anagnostidis, 1985, Anagnostidis, 1988, Lukas and Golubic, 1981, Martinez, 2010, Pantazidou, et al., 2006)	
<b><i>Hormathonema</i></b> ( <i>H. violaceo-nigrum</i> , <i>H. luteo-brunneum</i> )	Adriatic Sea, Mediterranean Sea, Indian Ocean, Puerto Rico	Marine limestones	(Budd and Perkins, 1980, Ercegović, 1929, Golubic, 1969)	
<b><i>Hyella</i></b> ( <i>H. caespitosa</i> , <i>H.</i> <i>inconstans</i> , <i>H. reptans</i> , <i>H.</i> <i>conferta</i> , <i>H.</i> <i>salutans</i> , <i>H. stella</i> , <i>H. immanis</i> )	Arabian Gulf, Greece, Puerto Rico, Red Sea	Marine mollusk shells, estuarine bivalve and gastropod shells and other limestone substrates	(Al-Thukair and Golubic, 1991, Al- Thukair, et al., 1994, Budd and Perkins, 1980, Le Campion- Alsumard, 1991, Radtke and Golubic, 2005)	
<b><i>Solentia</i></b> ( <i>S. achromatica</i> , <i>S.</i> <i>foveolarum</i> , <i>S.</i> <i>intricate</i> , <i>S.</i> <i>paulocellulare</i> , <i>S.</i> <i>sanguinea</i> , <i>S. stratosa</i> )	Arabian Gulf, Bahamas, Mediterranean Sea, Red Sea	Marine limestone shores, marine mollusk shells, estuarine bivalve and gastropod shells and other limestone substrates	(Ercegović, 1927, Golubic, 1996, Le Campion- Alsumard, 1996, Radtke and Golubic, 2005, Schneider and Le Campion- Alsumard, 1999, Stolz, et al., 2001)	

Table 1, Cont.

Order Oscillatoriales (Group 3)	Ecology	Substrate	Reference	Morphology
<p><b>*Plectonema</b> (<i>P. capitatum</i>, <i>P. litorale</i> <i>P. radiosum</i>, <i>P. terebrans</i> [<i>Leptolyngbya terebrans</i>] <i>P. tomasinianum</i> <i>P. wollei</i>)</p>	<p>Belize, French Polynesia, Greece, India, Mexico</p>	<p>Marine mollusk shells, estuarine bivalve and gastropod shells, calcareous skeletons of coralline alga.</p>	<p>(Che, et al., 1996, Kaehler, 1999, Le Campion-Alsumard, et al., 1995, Pantazidou, et al., 2006, Raghukumar, et al., 1991, Thuret, 1875)</p>	
Order Nostocales (Group 4)				
<p><b>Kyrtuthrix</b> (<i>K. dalmatica</i> <i>K. maculans</i>)</p>	<p>Mediterranean Sea, Sweden</p>	<p>Marine limestones and calcareous substrates</p>	<p>(Ercegović, 1957, Ercegović, 1929, Golubić and Le Campion-Alsumard, 1973, Silva, 1996)</p>	
<p>†<b>Schizothrix</b> (<i>S. calcicola</i>, <i>S. coriacea</i>, <i>S. perforans</i>)</p>	<p>England, Bermuda</p>	<p>Freshwater carbonates, marine stromatolites,</p>	<p>(Drouet, 1963, Gomont, 1892, Hoffmann, 1989, Pentecost, 1992, Sharp, 1969)</p>	

\*Not all the species actively bore into carbonates. † More than 80 species have been described for the genus, and only those that are suspected of boring are included.

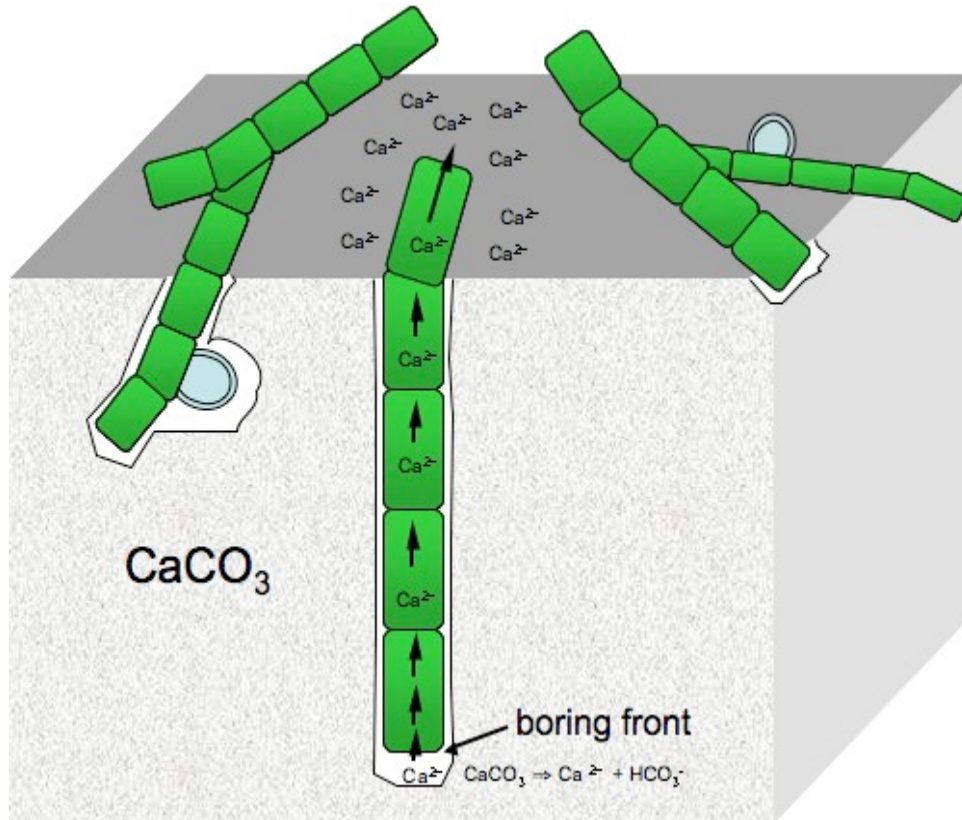
Table 1, Cont.

Order Stigonematales (Group 5)	Ecology	Substrate	Reference	Morphology
<b>*<i>Iyengariella</i></b> ( <i>I. endolithica</i> , <i>I. tirupatiensis</i> )	Mexico, India	Freshwater carbonates	(Desikachary, 1953, Seeler and Golubic, 1991)	
<b><i>Mastigocoleus</i></b> ( <i>M. testarum</i> )	Canada, New Zealand, Mexico, Peru, Puerto Rico, South Africa, Sweden, West Indies	Marine mollusk shells, calcareous skeletons of dead coral and algae	(Golubić and Le Campion-Alsumard, 1973, Kaehler, 1999, Lagerheim, 1886, Montoya-Terreros, 2006, Tribollet, et al., 2006, Webb and Korrubel, 1994)	
<b><i>Matteia</i></b> ( <i>Matteia conchicola</i> )	Mediterranean Sea, Israel	Marine carbonates and terrestrial limestones	(Borzi, 1907, Friedman, 1993)	

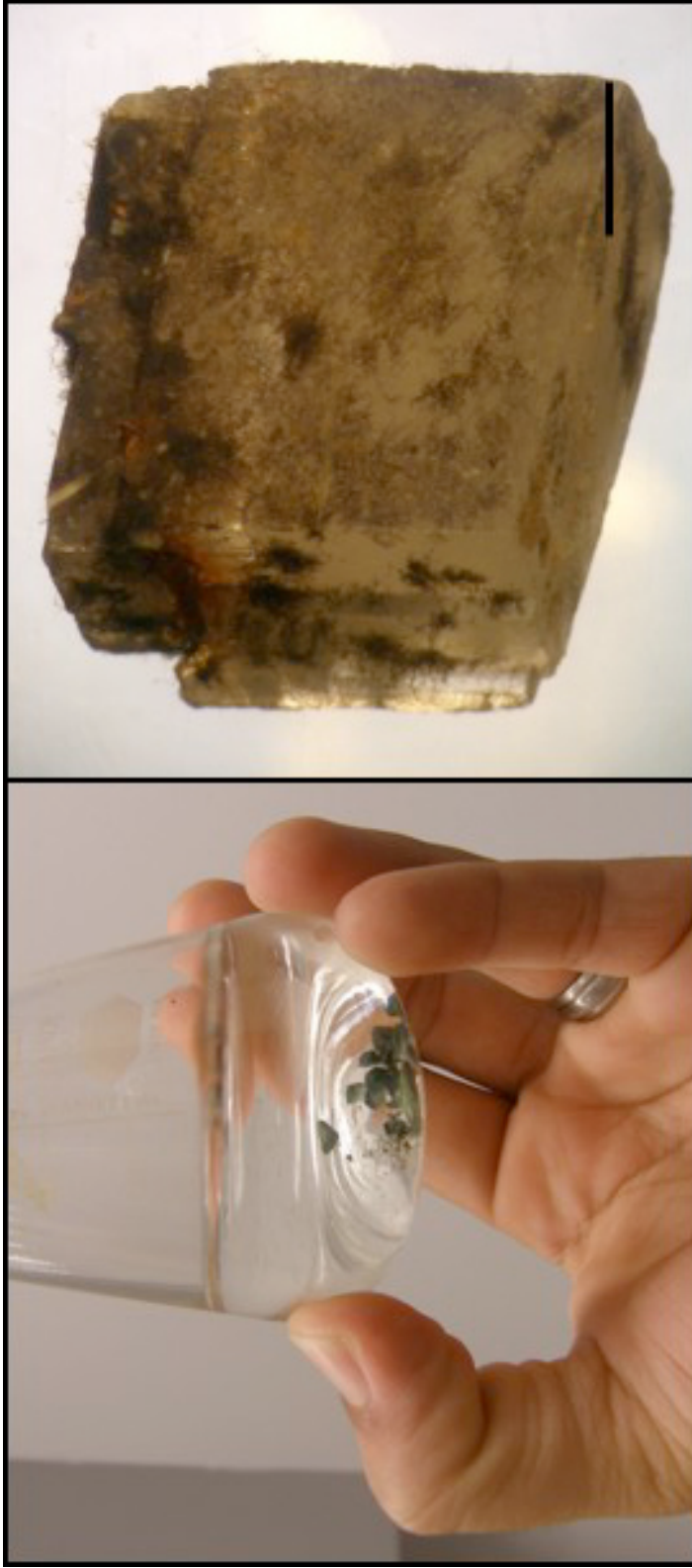
\*Not all the species actively bore into carbonates.



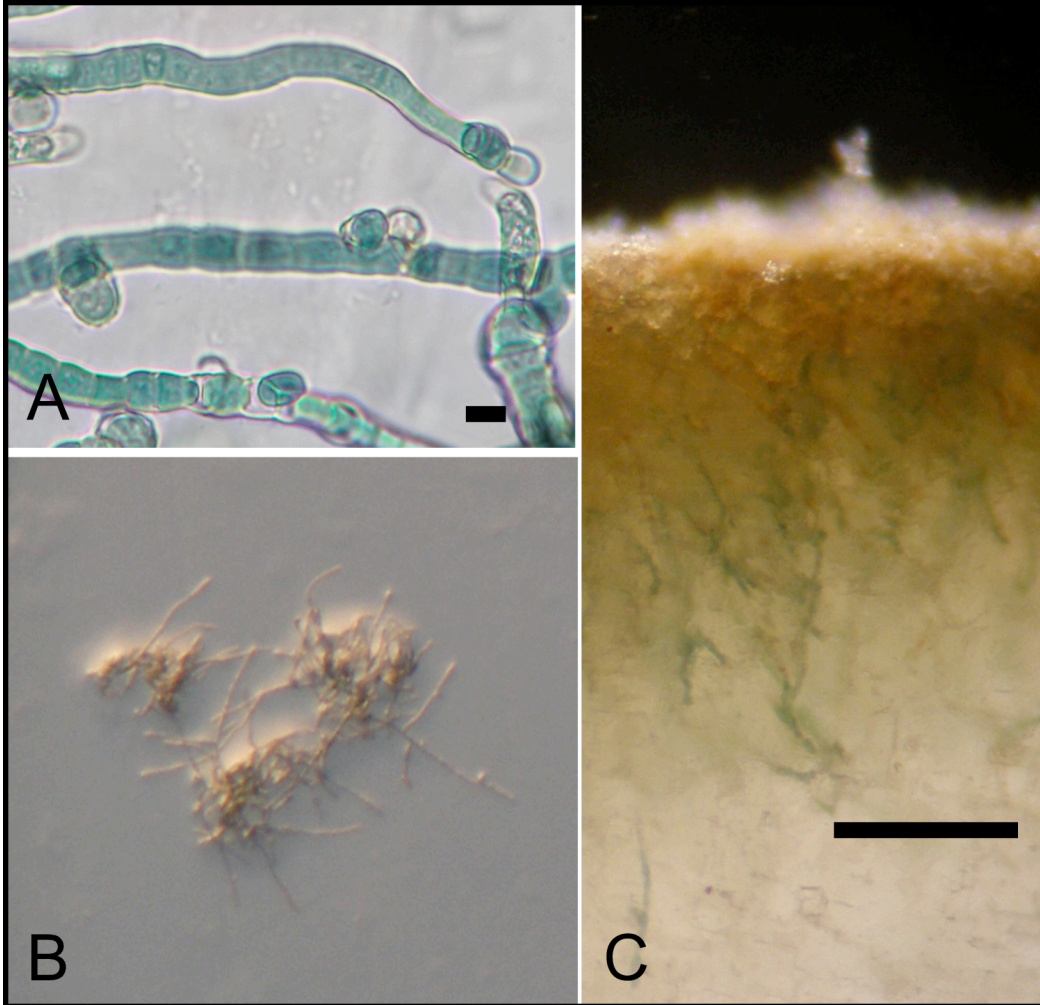
**FIG. 1** An example of marine carbonates exposed to both physical and biological erosion on the Southwest coast of Puerto Rico, in the town of Cabo Rojo. The dark areas at the bottom of the carbonate cliff are extensively infested by metazoans and microborers (image courtesy of Lilliam Casillas).



**FIG. 2** Model of boring by calcium pumping. One or more calcium pumping enzymes transport calcium ions from the water in the interstitial space (at the boring front) into the apical cell. This reduces the ion activity product of calcium, causing a small amount of the calcite to dissolve. The calcium is transported, cell-to-cell, and eventually released by the distal cell, closest to the mineral's surface. Cartoon illustrates typical morphology of *Mastigocoleus*, with lateral heterocysts.



**FIG. 3** Calcite chips infested by *Mastigocoleus testarum*, strain BC008. Bar, 2 mm



**FIG. 4** Morphology of strain BC008, a euendolith isolated from marine carbonates. A. Free-living filaments. *Bar, 10  $\mu\text{m}$* ; B. Typical colony morphology, grown on PES agar; C. Vertical cross-section of an infested chip, with boring filaments. *Bar, 100  $\mu\text{m}$*

CHAPTER 1  
POLYPHASIC CHARACTERIZATION OF A MARINE EUENDOLITHIC  
CYANOBACTERIUM AND THE REDESCRIPTION OF THE GENUS  
MASTIGOCOLEUS LAGERHEIM



## ABSTRACT

Despite the well-described nature of euendolithic (true-boring) cyanobacteria, no actively boring culture exists in any of the public culture collections. A culture of a marine, filamentous, true-branching heterocystous cyanobacterium capable of boring into pure calcite under laboratory conditions, strain BC008, was characterized using a polyphasic approach that involved the study of its morphology, ultrastructure, physiology and evolutionary history. The strain contained many of the characters intrinsic to the *Mastigocoleus* genus, one of the key features being the display of lateral heterocysts. Collectively, these observations point at BC008 being a representative of the genus *Mastigocoleus*, which allowed us to do a comprehensive redescription of the genus that includes those characters not mentioned in its original description by Lagerheim (1886). The new description includes new characters, such as morphological changes boring cells undergo inside the solid substrate, the display of complementary chromatic adaptation, ultrastructural features and multi-gene phylogeny.

## INTRODUCTION

Endolithic microbial communities in the photic zone of coastal marine carbonates are typically dominated by cyanobacteria that actively bore into the mineral substrate (Thuret, 1875, Frey, 1936, Le Campion-Alsumard, et al., 1995, Radtke and Golubic, 2005, Stockfors and Peel, 2005, Vogel and Brett, 2009). Boring cyanobacteria can also be found in other aquatic and terrestrial habitats where carbonates are present (Campbell, 1983, Friedmann, 1993). Euendolithic cyanobacteria, as they are known, have a

rich and ancient fossil record (Knoll, et al., 1986, Seong-Joo and Golubic, 1998), and even today are important agents of bioerosion (Tribollet, 2008, Le Campion-Alsumard, et al., 1995, Tribollet, et al., 2006). They are responsible for the weakening of carbonate shells of mussels, abalone and other mollusks in aquaculture settings (Dunphy and Wells, 2001, Webb and Korrubel, 1994), and are involved in the formation of lithified laminae in modern stromatolites (Macintyre, et al., 2000). Genera of cyanobacteria with members that have been described as true-boring include *Cyanosaccus* (Anagnostidis, 1985, Pantazidou, et al., 2006), *Hormathonema* (Budd and Perkins, 1980, Golubic, 1969), *Hyella* (Al-Thukair and Golubic, 1991, Le Campion-Alsumard, 1991), *Solentia* (Macintyre, et al., 2000, Radtke and Golubic, 2005), *Plectonema* (Berman-Frank, et al., 2003, Forsterra and Haussermann, 2008), *Kyrtuthrix* (Ercegovic, 1957, Le Campion-Alsumard, 1973), *Schizothrix* (Drouet, 1963, Pentecost, 1992) *Iyengariella* (Seeler and Golubic, 1991), *Mastigocoleus* (Kaehler, 1999, Tribollet, et al., 2006) and *Matteia* (Friedmann, 1993).

Our knowledge of cyanobacterial euendolith biology comes mainly from field observations, as does largely the present classification of the genera and species involved. Microscopic accounts can be done better: observations can be conducted after exhumation from the substrate (Perkins and Tsentas, 1976, Vogel, et al., 2000) or by studying their boring marks or boreholes (Golubic, 1970). In some occasions petrographic thin sections with contrast-enhancing chromophores such as Toluidine blue have been used (Tribollet, 2008), or ethylene-diamine-tetraacetic acid (EDTA) solutions (Chacon, et al., 2006). Recently, we have also used laser scanning confocal

microscopy of boring filaments to aid in their observation *in situ* (see Chapter 2 of this dissertation). Some descriptive work has been done on cultivated isolates (e.g. Al-Thukair, 1991, Seeler and Golubic, 1991, Montoya-Terreros et al., 2006) but this has not involved any genetic, physiological or ultrastructural characterization, being restricted to morphological characterization only. All of these aspects are required for sound phylogenetic description (Castenholz, 2001). Not a single complete 16 S rRNA sequence, has been submitted to public databases stemming from an isolation of euendolithic members [a partial 16S rRNA sequence of BC008 was submitted by Chacon (2006)]

The genus *Mastigocoleus* and its only species, *Mastigocoleus testarum* Lagerheim, is one of the first described euendoliths (Lagerheim, 1886). It is a marine form, found originally boring in shells on the coast of Kristineberg, Sweden. By now, it is commonly recognized in surveys around the world (Chazottes, et al., 2009, Che, et al., 1996, Le Campion-Alsumard, et al., 1995, Raghukumar, et al., 1991, Tribollet, et al., 2006). It is a morphologically unique and easily recognizable morphogenus that develops lateral heterocysts, the only marine cyanobacterium to do so. There are currently no cultivated *Mastigocoleus* representatives in public culture collections, and no information regarding this genus in public sequence databases.

We undertook a polyphasic study with the triple aim of providing an assessment of the old generic description that was based on restricted morphological observations, as well as enhancing the characterization of these morphogenus by including physiological, ultrastructural and genetic

data, and, finally, establishing a firm phylogenic placement of these important euendoliths.

## MATERIALS AND METHODS

**Cultivation.** Strain BC008 was isolated from a marine snail shell in Cabo Rojo, Puerto Rico (latitude N 17.93386, longitude W 67.1924) (Chacón, et al., 2006). These cultures were kept growing and boring on small calcite chips, submerged in liquid sterile Provasoli's Enriched Seawater (PES) medium (Provasoli, 1968) containing 30 grams per liter of Instant Ocean® salts (Spectrum Brands Inc., Atlanta, GA, USA) at a salinity of 35 ‰ and pH of 8.3. For transferring stock cultures, infested chips were cleaned of any superficial growth with a small brush and rinsed in medium, and then transferred into new culture flasks alongside sterile chips of commercially available blocky calcite (CaCO<sub>3</sub>; WARD'S Natural Science, Rochester, NY). The chips were prepared by cleaving blocks of calcite into suitable size (2 mm<sup>3</sup> to 6 mm<sup>3</sup>) fragments with the aid of a flame-sterilized hammer. After cleaving, the chips were placed in ethanol 95% and each one flame-sterilized before transferring to the culture flasks. The purity of the calcite was evaluated by powder X-ray diffraction and confirmed against the ICDD Powder Diffraction Database. Stock cultures were kept at 25°C, under white incandescent light bulbs providing 30 μmoles of photons with no period of darkness. Cultures were monitored for growth and boring activity by visual inspection using a dissecting microscope.

**Obtaining axenic cultures.** BC008 filaments were collected and transferred to a fresh PES-medium 1.5% agar Petri plate. Under the dissecting microscope, filaments were dragged across the surface of the agar plate using a small glass hook, to clean the filaments and reduce the number of heterotrophic contaminants (Vischer, 1937). Afterwards, the filaments were placed in additional fresh PES agar plates and allowed to grow for a period of 3 to 4 weeks. Filaments were again collected from the plates, and the drag-and-transfer continued for several months, monitoring the number of heterotrophic colonies that grew around the filaments under the dissecting microscope. After several transfers, we choose the cleanest filaments from the agar and washed them 5 times in small volumes (approx. 3 mL) of sterile PES medium in a small, sterile flask with a magnetic stirring bar. After washing, the filaments were then re-plated in PES agar, and monitored once more for contaminants. This process was repeated until no more bacterial colonies were observed under the microscope. Axenicity was verified by plating filaments in PES agar supplemented with peptone, glucose and yeast (PGY-PES; Reddy). Filaments were incubated in the light, on PGY-PES plates for 48h at 25° C. Plates were monitored once more for bacterial growth, and only those that showed no signs of heterotrophic growth after 48 hours were kept as stock inoculums. Filaments were observed with Phase contrast optics.

**Microscopy of free-living filaments.** Wet mounts of BC008 were prepared with fresh, free-living filaments PES medium and observed under

the compound microscope with phase-contrast optics. Cell color, cellular types, branching pattern, and filament tapering were recorded. Cell, length and width, sheath thickness, and heterocysts frequencies were measured on approximately 200 individual cells to attain statistical significance. Sheaths were stained with a 1% alcian blue solution (EMS, Hatfield, PA) to improve contrast. Heterocyst were classified as terminal or lateral, with intercalary heterocysts being the least common, and thus omitted from our counts. Hormogonia production was evaluated by plating filaments in PES agar, and allowing them to grow for approximately 4 months. Hormogonia were located as peripheral short filaments with a typical EPS trail moving away from the central inoculum. Their size and shape were recorded under the dissecting microscope.

**Microscopy of boring filaments.** To address morphological variability during boring, cells were grown and allowed to infest calcite chips for a period of approximately 3 months. Afterwards, chips were harvested and cleaned of any superficial growth with a small watercolor brush in sterile PES medium. Filaments were disintegrated from the carbonate matrix using a modified ethylene-diamine-tetraacetic-acid (EDTA) carbonate dissolution method (Wade and Garcia-Pichel, 2003). Chips were placed on a small, stainless steel basket at the top of the column of a glass, 15 mL vacuum filtration apparatus. A peristaltic pump was used to deliver a 200 mM sodium-EDTA solution at pH 5, on top of the chip at a rate of 1ml per minute. Filaments were gradually exposed, and at 30 minute intervals, the filaments

were gently brushed from the chip, washed with sterile distilled water and collected on a 2  $\mu\text{m}$  pore polycarbonate filter on the filtration apparatus. Each dissolution interval removed 5 mg of calcium carbonate and each fraction collected corresponded to a 50  $\mu\text{m}$  layer. Fractions were classified as superficial, intermediate and deep. After collecting the fractions, filaments were rinsed in 10 mL of sterile PES to remove any excess precipitate, centrifuged for 10 minutes at 4,000 RPM and then the pellet re-suspended in PES medium. Cells were placed on a microscope slide under a microscope and observed at 400X magnification with brightfield optics. Measurements were then carried out as explained above.

**Transmission electron microscopy.** Ultra-structural characteristics were determined for free-living filaments as well as disintegrated filaments. Cells were concentrated by centrifugation (10 min. @ 10,000g) and prepared for microscopy following van de Meene, et al. (2006). Briefly, pellets were transferred to a Bal-Tec HPM010 high pressure freezing apparatus for cryofixation using B type planchettes and dextran as a cryoprotectant. After cryofixation, the samples were submerged in liquid nitrogen and freeze-substituted in a 1% glutaraldehyde: 1% tannic acid in acetone solution for 72 hours at  $-80^{\circ}\text{C}$ . Afterwards, samples were gradually warmed to room temperature for 3 hours in a 1% osmium tetroxide in acetone solution. Samples were embedded in Spurr's resin at  $61^{\circ}\text{C}$  overnight and thin sections ranging from 65 to 75 nm in thickness were cut with a microtome onto 300 mesh copper grids. Post-staining followed with 1% uranyl acetate in

methanol and Sato's lead citrate solutions respectively. Samples were observed using a Phillips CM12 microscope with an accelerating voltage of 80kV.

**Determination of complementary chromatic adaptation.** BC008 cultures, containing calcite chips, were grown under different light wavelengths, attained with Rosco polyester-based light filters (Rosco Laboratories Inc., Stamford, CT), placed in front of white fluorescent lights. The filters achieved peak percent transmittance in the 400nm (blue), 520nm (green) and 620 (red) regions, verified with a Shimadzu UV-1601 spectrophotometer. Controls were grown under white fluorescent lights with no filters. All cultures were exposed to constant light with similar intensities, averaging 15  $\mu$ mol of photons, and grown for a period of approximately 3 months.

**DNA extraction.** Genomic DNA was extracted from BC008 cells using the phenol:chloroform:isoamyl alcohol (PCI) extraction method, described elsewhere (Countway, et al., 2005). Briefly, cells were pelleted by centrifugation and lysed by zirconium-silica bead beating, with alternating 10 minute cycles of heating at 70°C. Sodium chloride (NaCl) and cetyltrimethyl ammonium bromide (CTAB) were added to a final concentration of 0.7M NaCl and 0.01% CTAB respectively and the mixture heated at 70°C for 10 minutes. An equal volume of PCI solution (25:24:1) was added and after gentle vortexing the supernatant was removed and placed in a fresh



microcentrifuge tube, where another addition of PCI followed, repeated twice. Afterwards an equal volume of chloroform:isoamyl alcohol (CI) (24:1) added and repeated twice. Nucleic acids were precipitated overnight at -20°C with 95% ethanol and 10.5 M ammonium acetate. Next day the nucleic acids were centrifuged at 14,000 RPMs, 4°C for 30 minutes. The nucleic acid pellet was rinsed with 70% ice-cold ethanol, centrifuged once more and air-dried in a laminar flow hood. Nucleic acids were re-suspended in 40 uL of sterile water. DNA concentration was quantified by gel electrophoresis on a 4% agarose gel stained with ethidium bromide using the Quantity One analysis software (Biorad Laboratories, CA, USA).

**PCR amplification and sequencing.** Four genes were chosen to independently measure phylogeny in strain BC008 including the small subunit ribosomal RNA gene (16S rRNA), the nitrogenase reductase gene (*nifH*), the large subunit ribulose-bisphosphate carboxylase enzyme gene (*rbcL*) and a member of the circadian clock genes (*kaiC*). Approximately 10 ng of DNA extract was used as template for Polymerase Chain Reaction (PCR) amplification. A 1100 bp-long 16S rRNA gene fragment was amplified, using the primer set BAC-GM5F / BAC-907R, universal for the domain Bacteria (Nagy, et al., 2005). The thermal cycle consisted of an initial denaturation at 94°C for 5 min, 40 cycles of 94°C for 45 s, 51°C for 45s, and 72°C for 1:30 min, and a final extension at 72°C for 7min.

A ca. 400 bp-long *nifH* gene fragment was amplified, using the primer set PolF / PolR (Poly, et al., 2001). The thermal cycle consisted of an initial

denaturation at 94°C for 2 min, 40 cycles of 94°C for 1 min, 52°C for 1 min, and 72°C for 1 min, and a final extension at 72°C for 10 min.

A ca. 500 bp-long *rbcl* gene fragment was amplified, using the primer set RbclF / RbclR (Rajaniemi, et al., 2005) with a thermal cycle consisting 94°C for 2 min, 40 cycles of 94°C for 1 min, 45°C for 1 min, and 72°C for 1 min, and a final extension at 72°C for 10 min.

Lastly, a ca. 600 bp-long *kaiC* gene fragment was amplified, using the primer set kaiC 488F / kaiC 489R (Lorne, et al., 2000), with a thermal cycle consisting of an initial denaturation at 94°C for 5 min, 40 cycles of 94°C for 45 s, 51°C for 45 s, and 72°C for 1 min, and a final extension at 72°C for 5 min.

Each 100 µL reaction contained the following: 10 µL of 10× Takara Ex Taq DNA polymerase, 8 µL of Takara dNTP mixture (2.5 mM each), 50 pmol of each primer (synthesized by Operon Technologies, Inc., Alameda, CA, USA) and 5–10 ng of template DNA. Quantification of PCR products was verified as described for genomic DNA.

**Phylogeny reconstruction.** To establish the molecular evolutionary history of the strain, a phylogenetic reconstruction was performed using the four independent genes sequenced. For the 16S rRNA, a partial sequence was obtained by sequencing the 16S rRNA amplified PCR product in triplicate and aligning forward and reverse complement sequences with MEGA 4.0 (Tamura, et al., 2007). Sequences were checked for non-coding bases, which accounted for less than 1% of the total sequence number and all non-coding

ends were cleaned. A high-quality consensus sequence of 1094 bp was obtained, and this sequence was verified against other cyanobacterial members using the Basic Local Alignment Search Tool (BLAST). The closest cyanobacterial sequences were used to establish the initial alignment, and representative cyanobacteria of all groups were used thereafter to populate the alignment, as well as plant plastids and one heterotrophic bacterium. A final alignment of 35 taxa was used to construct phylogenetic trees. Two algorithms were used, the Neighbor-Joining (NJ) and the Maximum Parsimony (MP), both with 10,000 bootstrap replicates. Trees were bottom-rooted with a heterotrophic bacterium. The percentage of replicate trees, where the sequences clustered together in the bootstrap test, is shown next to the branches. All positions containing gaps and missing data were eliminated. Sequences for all other genes were obtained in a similar way, with final consensus sequences for *nifH* being a 325 bp partial sequence, a 438 bp partial sequence for *rbcl* and a 594 bp partial sequence for *kaiC*. Trees with translated protein sequences were made for *nifH* and *rbcl*, and showed similar topologies to DNA ones.

## RESULTS

**Microscopic characterization.** Observation by light microscopy of free-living filaments revealed a heterocystous, true-branching cyanobacterium. Trichomes produce a dense exopolysaccharide sheath (Fig. 1D). True branching occurs when a cell changes its plane of division by 90°, and branches taper towards the apex (Fig. 1B), elongating into thin filaments of about half the width of mature vegetative cells. The filaments are always

uniseriate. *Calothrix*-like terminal hairs are not formed under standard conditions. This strain develops intercalary, lateral and terminal heterocysts, even in a single branch, which are paler, having a slight green-yellow tint. Heterocyst formation is constitutive, regardless of the presence of fixed nitrogen sources. Intercalary heterocysts are barrel-shaped, while terminal and lateral heterocysts are dome-shaped, and without apparent pore plug. Seven to ten-celled motile hormogonia are formed, whose cell resemble vegetative cells in shape, but are only about half as wide. No akinetes were detected. Individual cells in mature filaments are  $12.4 \pm 1.8 \mu\text{m}$  in width and  $9.9 \pm 1.5 \mu\text{m}$  in length. BC008 varies from reddish-brown, brownish-green, to blue-green, to violet depending on illumination, due to changes in phycobilin complement. No scytonemin nor other sheath pigments are present, nor are they formed under UV exposure. The cytoplasm is remarkably heterogeneous and granular.

**Morphological changes during boring.** BC008 filaments can penetrate solid, crystalline calcite, and will branch and produce heterocysts inside the solid while boring (Fig. 1C). The filaments do not seem to prefer a particular angle of penetration with respect to the surface, and do not necessarily follow the crystal's cleavage planes, as has been reported for other endoliths (Golubic, 1969). However, this strain undergoes clear changes in cell size, heterocyst frequency, and the frequency of particular heterocyst types as the filaments penetrate the mineral. Fig. 2A illustrates these changes with the most superficial filaments having an average width of  $6.9 \pm 1.7 \mu\text{m}$  and

length of  $7.3 \pm 3.5 \mu\text{m}$ . Deeper filaments are  $5.7 \pm 0.9 \mu\text{m}$  wide and  $8.9 \pm 1.6 \mu\text{m}$  long. The deepest filaments are  $5.2 \pm 0.9 \mu\text{m}$  wide and  $7.9 \pm 1.5 \mu\text{m}$  long. Student T tests were calculated taking into account all possible comparisons for cell width and length, with values being significantly different (p value of at least 0.039 and 0.018, respectively). The results indicate a trend in which cells become thinner and longer as they bore. As for the heterocysts, lateral, terminal and intercalary types are found in all fractions, albeit the latter were quite rare. Lateral heterocyst frequency, relative to other types, increases as filaments bore deeper into the mineral (Fig. 2B). In contrast, overall frequency of heterocysts (Fig. 2C) decreases as filaments bore deeper (linear regression,  $r^2 = 0.9823$ ). Only the ratio of lateral vs. terminal was measured, as intercalary ones are not as common in this strain.

**Ultrastructure.** BC008's thylakoid membranes have no preferred orientation, and are found randomly arranged, with no apparent stacking. The cytoplasm is conspicuously granular owing to the presence of a multitude of structures of about 20-40 nm in size, that sometimes appear polyhedral at high magnification. These granules are widespread, filling in most of the cytoplasm, but are never found in the intrathylakoidal lumen. Both boring and non-boring vegetative cells contain these structures, but heterocysts do not. The sheath appears as a laminated and dense structure surrounding the trichomes, ranging from 0.2 to 1  $\mu\text{m}$  in thickness. Heterocysts are transparent, with thickened cell walls, and do not contain granules or inclusion bodies inside and have no junctional pores. In vegetative cells

intracellular bodies such as carboxysomes, cyanophycin granules, lipid bodies, and polyphosphate granules were observed (data not shown).

**Complementary chromatic adaptation.** BC008 cells exhibit complementary chromatic adaptation when grown under variable light wavelengths. When grown under red light (maximum peak  $\lambda = 620$  nm) cultures display a bright green color, likely due to a decrease of phycoerythrin levels (Fig 4). Cultures grown under green light (maximum peak  $\lambda = 520$  nm) display a reddish-brown color, a result of higher phycoerythrin. These color changes reflect the predicted shift of constituents of the phycobilisome (phycoerythrin and phycocyanin) during red and green light exposure. Changes in the expression of phycoerythrin were verified by whole-cell spectra measurements (data not shown) and correspond to observed changes in coloration (e.g. higher levels of phycoerythrin under green light). Blue light had a detrimental effect on the cells caused by photobleaching and the vast majority of them did not survive. The bleaching effect of blue light on the phycobilins has been described in other cyanobacteria elsewhere (Sinha, et al., 2002), so this result was not surprising.

**Phylogeny. Phylogenetic** trees based on the neighbor joining (NJ) and the maximum parsimony (MP) algorithms were constructed for each gene with 10,000 bootstrap replicates to infer confidence values on phylogenetic trees. Independently of the algorithms used, the trees show a similar topology; we only show the NJ trees for the sake of simplicity. Trees constructed with both

nucleic acid sequences and (translated) protein sequences (for the cases of *nifH*, and *rbcL*) had a similar topology. Fig. 5 illustrates the phylogenetic analysis of 16S rRNA sequences of 35 taxa, placing BC008 amongst the heterocystous cyanobacteria, in a deep branch within the Nostocales. The strain fits basally to cyanobacteria within the *Rivularia* or *Calothrix* genera and has a 7% sequence divergence from the closest cyanobacterial taxa. Fig. 6 illustrates a phylogenetic reconstruction of 22 *nifH* partial sequences, placing the strain within the heterocystous group. The strain is found on a deep branch within members of the Nostocales. Fig. 7 shows a phylogenetic reconstruction of *rbcL* partial sequences of 20 taxa, placing the strain once more within the heterocystous group, on a deep branch, basal to cyanobacteria with *Calothrix* morphology. Fig. 8 illustrates a phylogenetic reconstruction in with 12 partial *kaiC* gene sequences. The strain appears once more, on a deep branch, within the heterocystous, between the Nostocales and Stigonematales.

## DISCUSSION

BC008 was successfully kept in the lab in its actively boring state for more than 5 years, without losing its boring ability, an improvement taking in account how common is for euendolith cultures, that are indeed established, not to keep their actively boring state in the laboratory for long. Such is the case of a culture of *Matteia conchicola*, provided to us by Friedmann, previously reported as boring (Friedmann *et al.*, 1993) which did not bore in our lab. We attribute our success to a more efficient sub-culturing method that excluded, for the most part, non-boring filaments, by using

infested chips rather than free-living filaments as inocula. We recommend this approach, in which the infested substrate is used instead of biomass in the upkeep of actively boring cultures.

The results show that strain BC008 has many of the diacritical morphological characters of *Mastigocoleus* according to its botanical description. The formation of lateral heterocysts, filament tapering and true branching are key features of the original genus description, even though its ability to bore is not. BC008 forms sheathed, uniseriate trichomes that exhibit true, irregular branching and tapering, display terminal and lateral heterocysts that only rarely appear in pairs, produce hormogonia, and do not produce akinetes (“spora”). Nevertheless, three characters mentioned in the original genus description that do not match. These are: (1) homogeneous cellular content, which is granular in BC008, (2) reproduction by chroococcoidal cells, absent in BC008 and (3) the absence of intercalary heterocysts, which although rare, are present in BC008. As for the species description (*M. testarum*), BC008 shares the majority of the characters as well. It forms vegetative cells that are cylindrical to semi cylindrical in shape, and display a bluish color. Heterocysts for the most part are small and dense, vary in form (dome vs. barrel shaped) and have a thickened (“firmae”) “membrane” (cell wall) with a yellowish content. In the description, trichomes are said to range from 6 to 10  $\mu\text{m}$  in width and vegetative cells range from 3.5 to 6  $\mu\text{m}$  in width. The only two mismatches found in BC008 are: (1) the ability of vegetative cells to change color (i.e. violets, reds, browns and greens) which is a result to its ability for complementary chromatic



adaptation, and (2) the size range of cells, which varies significantly from those in the description (4-19  $\mu\text{m}$ , taking into account all growth modes). It is not difficult to envision the reasons why characters that we see in BC008 were not included in the original description; non-boring mode morphology and life cycle observations can only happen with a culture in hand. Altogether, BC008 seems to be a likely good representative for the original description and a good candidate for a recharacterization that includes aspects beyond simple morphology.

The obvious changes in morphology that we detected in BC008 (Fig. 2) are also intriguing and of unknown physiological significance. According to our calculations, an average cell in free-living mode is 7 times more voluminous, than a deeply boring cell is (1130  $\mu\text{m}^3$  vs. 153  $\mu\text{m}^3$  respectively). Heterocyst frequency also diminishes as the filaments bore deeper, with free-living filaments producing approximately 1 heterocyst per every 12 vegetative cells, compared to 1 per every 33 at depth. Lateral heterocysts become clearly more prominent while boring: inside the mineral heterocysts are almost exclusively lateral. One cannot help to wonder if such morphological adaptations might be related to the efficiency or mechanism of boring, an aspect that will be probed in the following chapters.

The reasons for the reduction in heterocysts frequency as the strain bores are not immediately obvious, but an explanation can be approached logically, if the frequency of heterocyst diminishes as a result of reduced need for nitrogen, as it is known in other cyanobacteria (Castenholz, 2001). In this case one and alternative nitrogen source would be needed, such as nitrogen-

containing impurities or traces in the substrate, which would partially supply the cellular needs. This of course, is not the case, as we know that the calcite used in our experiments is pure. This explanation assumes that both cell volume and nitrogen need remain constant. However, our data show that in reality cell volume in BC008 decreases with depth and naturally, a smaller cell would be expected to have less of a nitrogen requirement than a bigger cell. An average heterocyst in free-living mode has a volume of  $144 \mu\text{m}^3$  and provides N to a cellular volume of  $13,560 \mu\text{m}^3$  (12 vegetative cells). At depth, however, a heterocyst has an average volume of only  $57 \mu\text{m}^3$  (data not shown) and provides nitrogen to an overall cellular volume of  $5049 \mu\text{m}^3$  (33 vegetative cells). Both situations indicate a similar need of cell volume allocation to heterocysts, around 1%, which would indicate that the N needs have not varied, and that the change in heterocyst frequency, is an adjustment needed as a result of the change in cell dimensions.

The ability of BC008 to chromatically adapt could maximize their efficiency during photosynthesis under a changing light quality. This may enable *Mastigocoleus* members to bore into calcareous benthic substrates at varying depth in the water column, and might also play an important role inside the substrates, as light availability and quality can also change, for example, due to self-shading or multiple scattering. By contrast, no known function can yet be attributed to the unusually small structures that fill in the cytoplasm of BC008, as they are the first reported of their kind, in terms of size and shape. Although smaller in size and much more numerous than the previously described bacterial micro-compartments found in

*Synechococcus* PCC7942 and some heterotrophic bacteria (Yeates, et al., 2008), these intracellular bodies do share some structural analogy with them, as they are all polyhedral or pseudo-spherical in shape.

In terms of evolutionary placement, our multiple, independent reconstructions place the strain clearly within Group IV (REF) of the cyanobacteria, amongst the “Nostocales”, and not close to members of the “Stigonematales” (Group V), even though BC008 shares defining morphological characteristics with the latter, like true branching. The genus *Mastigocoleus* has traditionally been placed in the “Stigonematales” since its inception (Desikachary, 1959, Geitler, 1932, Komárek, 1999). BC008 was significantly divergent from any other cyanobacteria represented in the public databases with respect to sequences from any of our four loci, to suggest that *Mastigocoleus*, as represented by BC008, is very likely a well-defined genetic entity. In fact, in all phylogenetic trees, the strain emerges as branches with deep nodes, basal to some groups of *Calothrix* /*Rivularia*. Morphologically, BC008 shares with this group the presence of tapering filaments. Even so, its 16S rRNA sequence is 7% divergent from its closest cyanobacterial neighbor, *Rivularia* sp. PCC7116, a marine form, which typically is sufficiently different to classify it as a separate genus (Stackebrandt 1994). Thus, it appears that it is convenient to maintain the standing of the original taxon of Lagerheim’s, if perhaps with a revised characterization.

*Mastigocoleus* represents a widespread taxon. Among euendoliths, the genus and its only described species, *Mastigocoleus testarum* Lagerheim is

found abundantly in marine endolithic communities around the world (Chazottes, et al., 2009, Che, et al., 1996, Le Campion-Alsumard, et al., 1995, Raghukumar, et al., 1991, Tribollet, et al., 2006). It is the only marine member of the heterocystous cyanobacteria that develops lateral heterocysts, a trait that is rare in cyanobacteria, reported in only two other genera, *Nostochopsis* (Tiwari, 1978) and *Mastigocladopsis* (Hoffmann, 1990), both from freshwater settings. There is at least one modern, published attempt to culture the microbe (Montoya-Terreros, 2006) but there are no *Mastigocoleus* in public culture collections.

Our novel physiological and molecular data allows a more comprehensive re-characterization of *Mastigocoleus* and *M. testarum*, that integrates its ecology, morphology, physiology and evolutionary placement. A redescription of the genus and species is presented below.

***Mastigocoleus* (ex Lagerheim) Ramírez-Reinat & Garcia-Pichel**

Marine, benthic, filamentous, heterocystous cyanobacteria, capable of boring in calcareous substrates, developing mostly lateral and terminal, but sometimes also intercalary heterocysts. In boring mode, most heterocysts are lateral. Filaments are uniseriate, true-branch by a 90° change in division plane, and display tapering. Mature trichomes are cylindrical averaging 12 (ranging from 4 to 19) µm in width in free-living filaments and 5 µm in width in boring filaments. Hormogonia are produced. No akinetes are observed. Thylakoid membranes have a random arrangement, with no stacking. No junctional pores are observed. Molecular phylogeny reconstructions of 16S

rRNA, *nifH*, *rbcl* and *kaiC* genes place the organism among the heterocystous cyanobacteria, on a deep branch amongst the “Nostocales”.

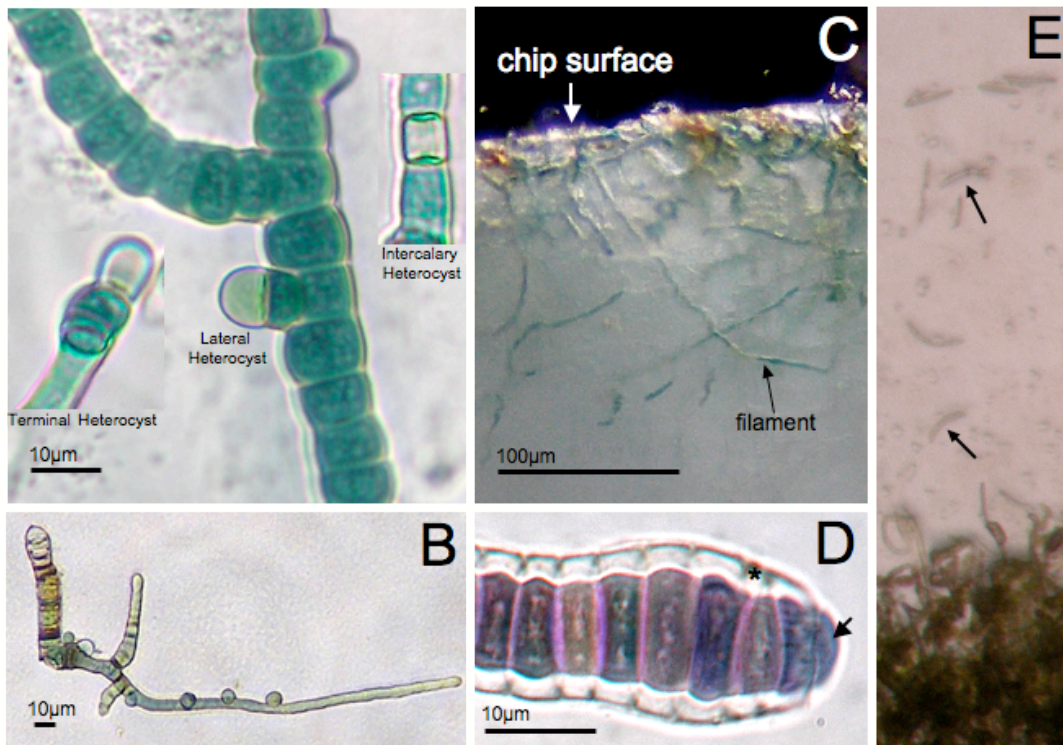
***Mastigocoleus testarum* (ex Lagerheim) Ramírez-Reinat & Garcia-Pichel**

Cells are barrel-shaped, averaging 9 µm in length. Growth optimum temperature ranges from 15-42 °C. Capable of complementary chromatic adaptation, with colors varying from dark brown, blue-green, olive-green, reddish-brown to violet. Sheaths are transparent and colorless. Cytoplasmatic content of vegetative cells has a granular consistency, with small, 20-40 nm granular bodies comprising most of its volume which are never found in the intrathylakoidal lumen, or inside heterocysts. A translucent sheath, averaging 1µm in width surrounds the trichomes. Heterocysts have thickened cell walls and display a yellowish-green tint. Hormogonia are produced, ranging from 7 to 10 cells in length. Type strain is BC008, isolated from submerged snail shells, in sunlit ponds of the intertidal zone of a carbonate beach, on the southwest coast of Cabo Rojo, Puerto Rico.

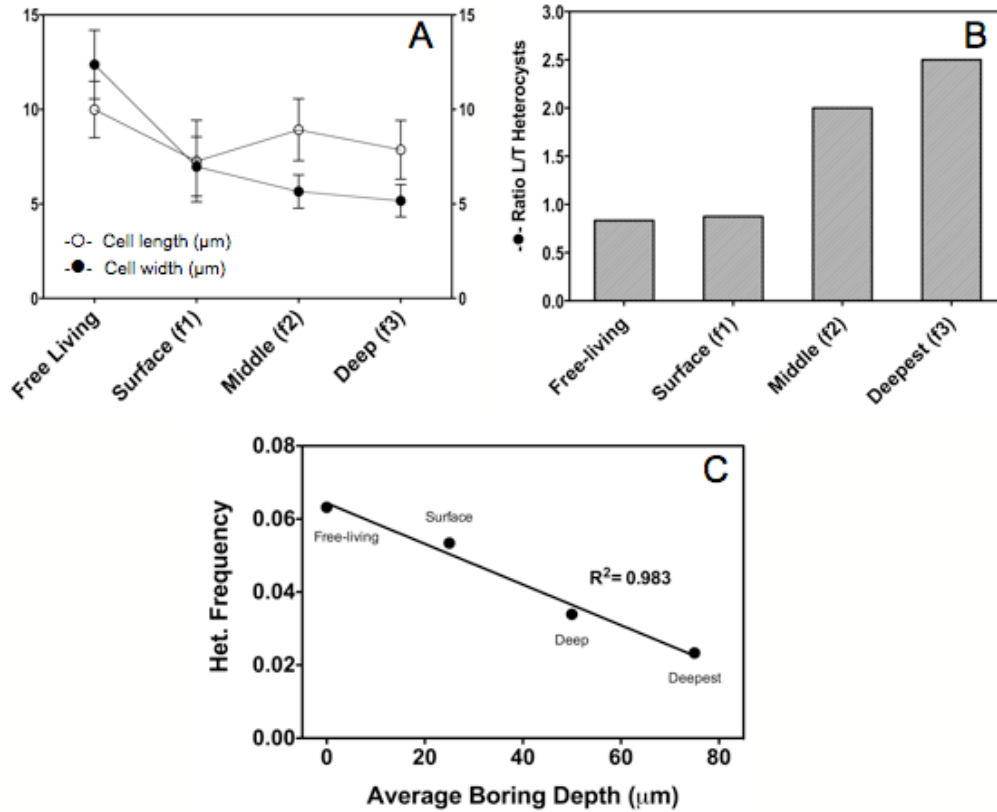
**AKNOWLEDGEMENTS**

We thank Robert Morris and Johanna Rodríguez for their help with microscopy cell counts. We would also like to thank Hugo Beraldi for his help with the X-ray diffraction analysis.

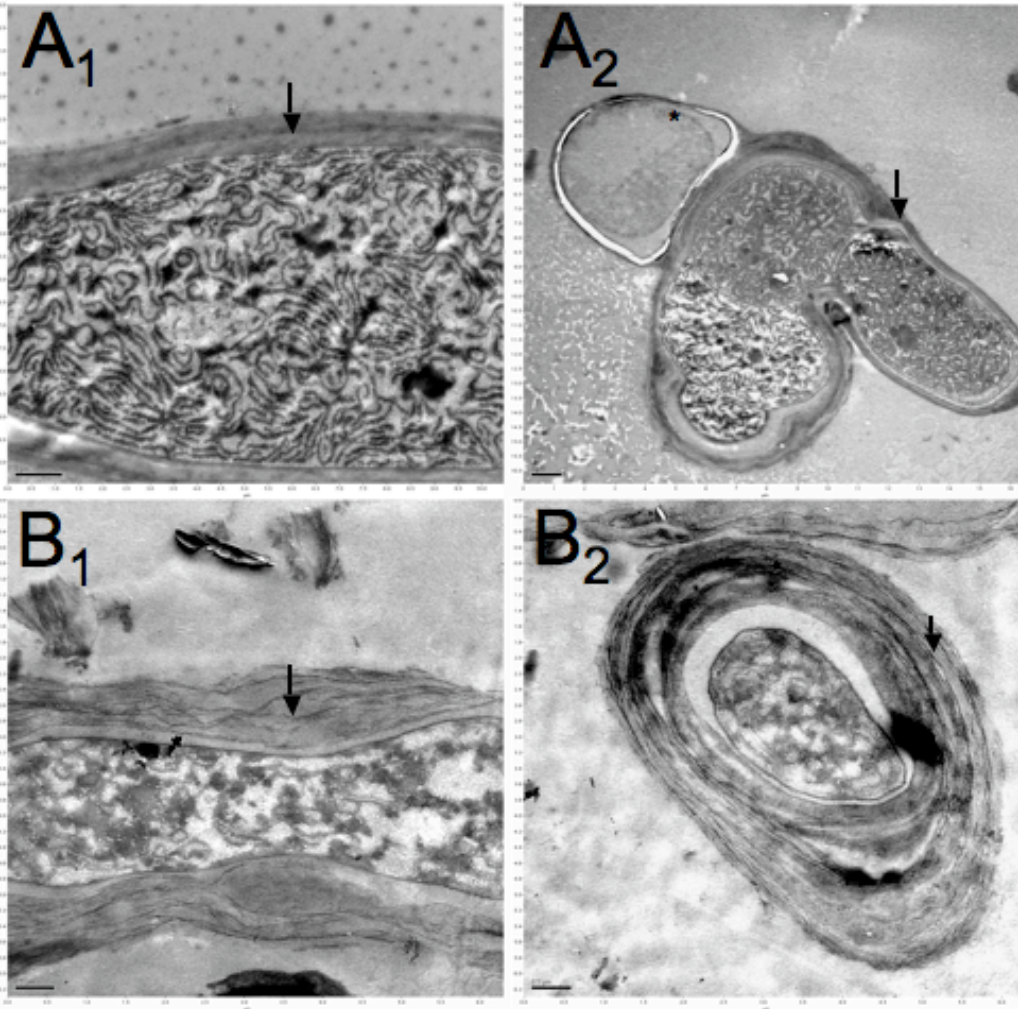
This work was supported by a National Science Foundation grant 0311945.



**FIG. 1** (A) Morphology of strain BC008 as seen by brightfield optics, showing the typical morphology of a filamentous, true branching, and heterocystous cyanobacterium. Formation of lateral heterocysts (\*), characteristic of the strain, can be observed as well as the granular consistency of the cytoplasm. (B) Tapering filament, with lateral heterocysts alongside. (C) Boring filaments penetrating a chip of Iceland spar calcite, down to a depth of approx. 200  $\mu\text{m}$ . Micritization can be observed at the surface of the chip. (D) A transparent exopolysaccharide sheath (\*) surrounds the filaments. Arrow shows terminal cell growing past the EPS sheath. (E) Hormogonia can be produced by the strain, and range from 7 to 10 cells in length and about half the width of mature vegetative cells.

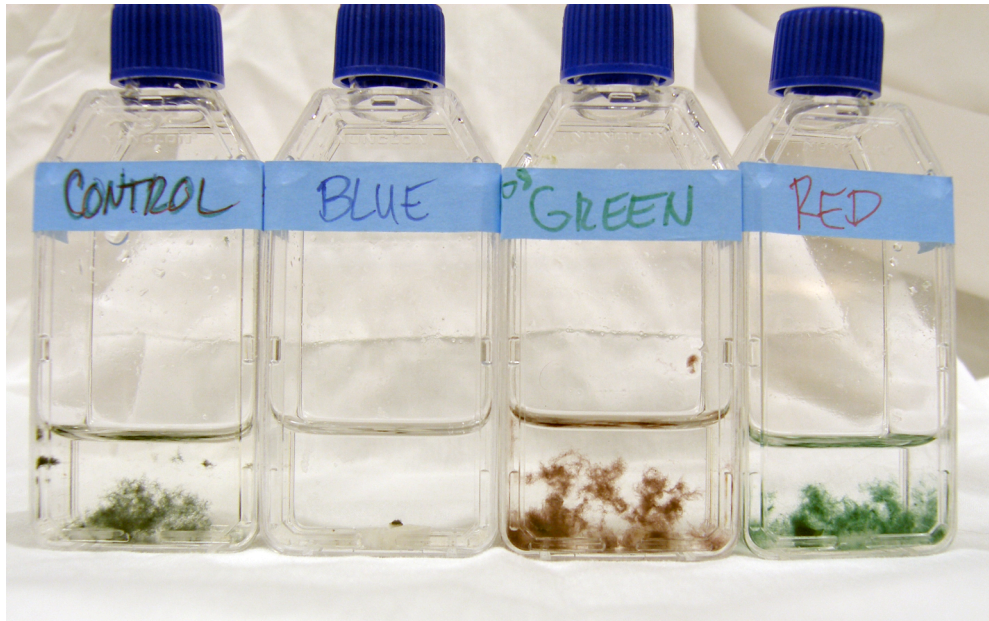


**FIG. 2** Morphological changes of boring filaments. (A) Average cell length (white circle) and width (black circle) measurements with standard deviation from free-living cells,  $n=225$ , surface cells (1<sup>st</sup> fraction),  $n=180$ , middle cells (2<sup>nd</sup> fraction),  $n=208$  and the deepest cells (3<sup>rd</sup> fraction),  $n=210$ . (B) Ratio of lateral vs. terminal heterocysts in free-living and boring fractions. (C) Heterocysts frequency in free-living and boring fractions, with best-fit linear regression.

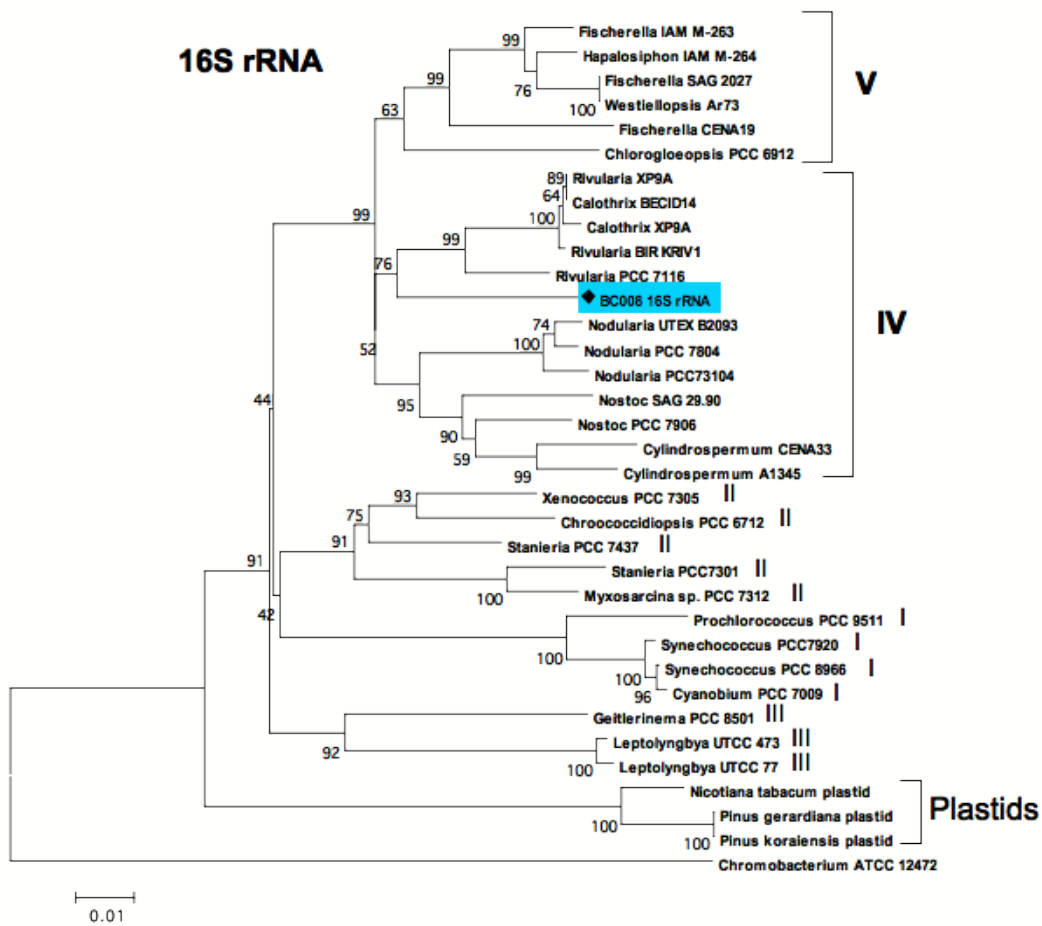


**FIG. 3** Ultrastructure of BC008 cells, observed by transmission electron microscopy. (A) Free-living cell as growing in liquid culture without calcite. (B) Actively boring BC008 cells after exhumation with EDTA. Granular bodies are observed in vegetative cells, but not in heterocysts under both growing conditions. Arrows point at filament sheath. Asterisk indicates a heterocyst. Scale bar on panel A is 1  $\mu\text{m}$ , and 0.5  $\mu\text{m}$  in panel B.

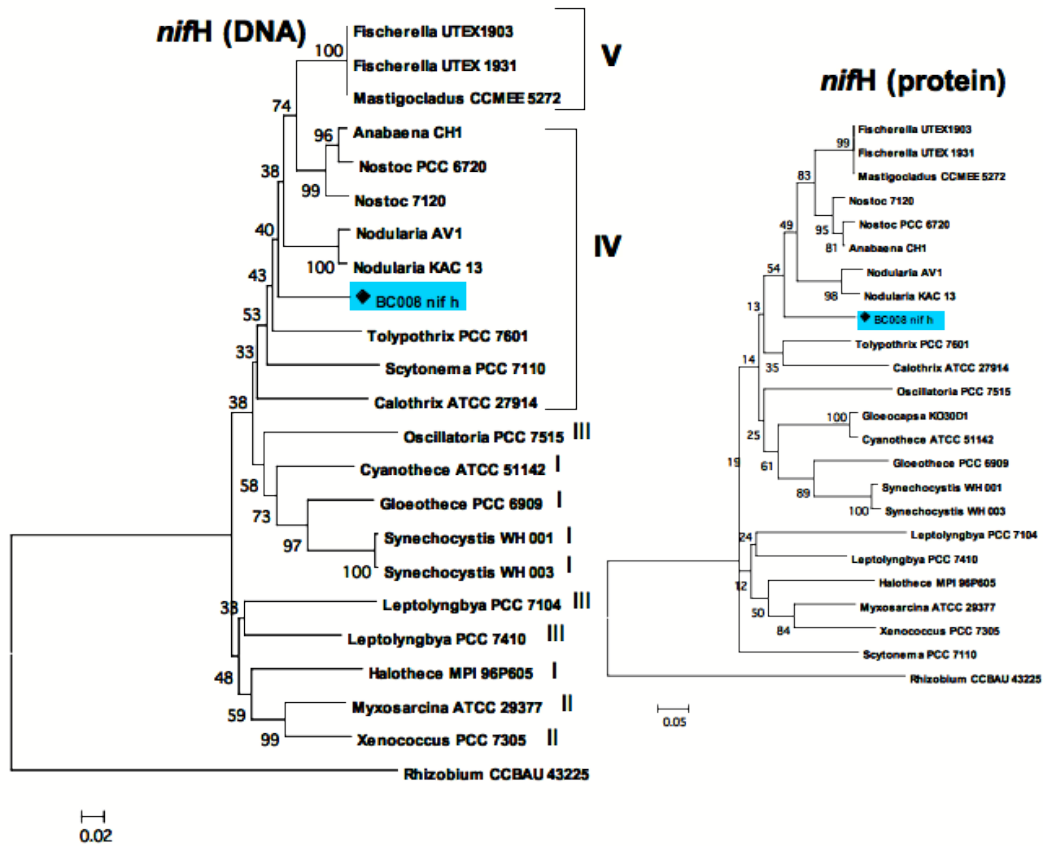




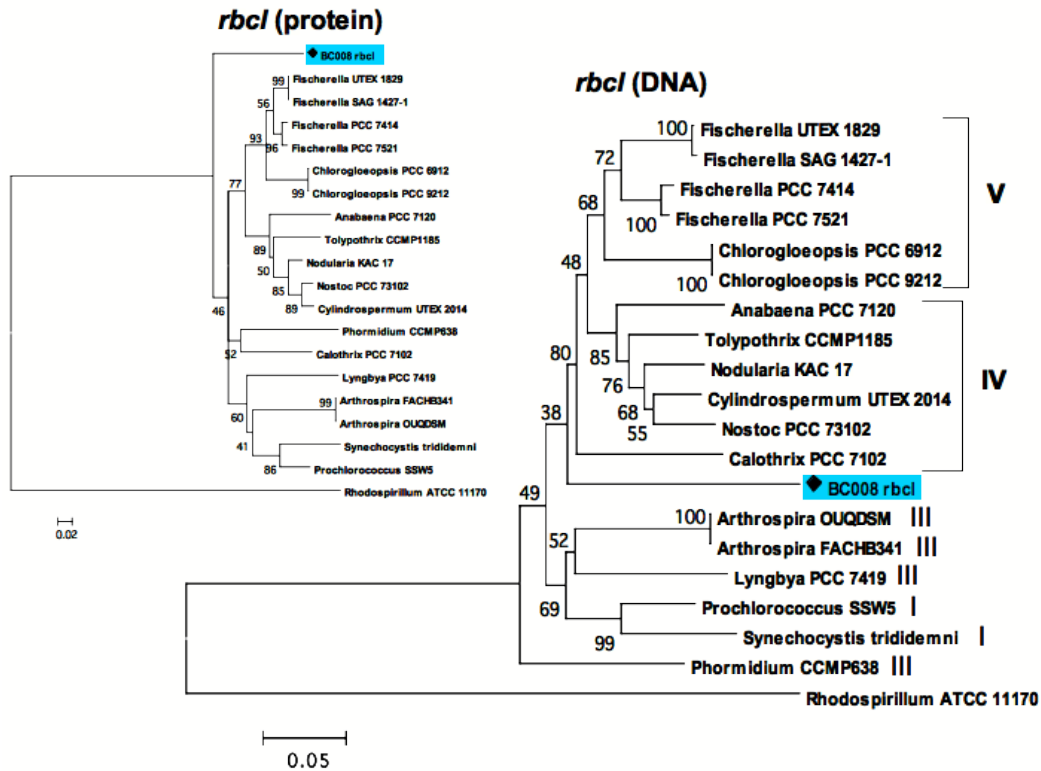
**FIG. 4** Cultures displaying complementary chromatic adaptation when grown in white light (“Control”), green light (“Green”) and red light (“Red”). Blue light proved to be detrimental, and cells did not grow under it (“Blue”). Light intensity = 3  $\mu$ moles of photons.



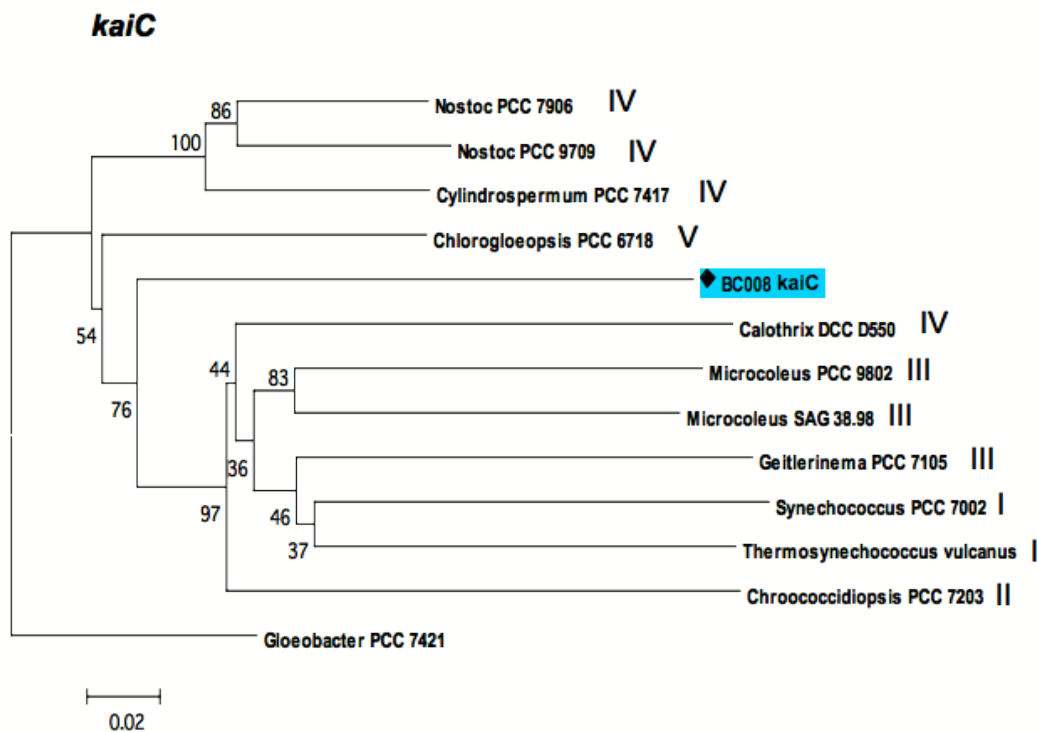
**FIG. 5** Neighbor-Joining phylogenetic tree based on 35 16S rRNA complete sequences. Other trees constructed with partial 16S rRNA sequences (ca. 600 bp-long, not shown) show a similar topology. The sequence of *Chromobacterium violaceum* (ATCC12472) was used as the outgroup. Brackets and roman numerals illustrate cyanobacterial groups and plastid sequences. Denomination of particular strains corresponds to those in the database, and are not necessarily taxonomically correct. Bootstrap values of 10,000 trees are included and indicated at the nodes. Scale bar represent 1% estimated sequence divergence.



**FIG. 6** Neighbor-Joining phylogenetic tree based on 23 *nifH* partial sequences. The sequence of *Rhizobium* CCBAU was used as the outgroup. Brackets and roman numerals illustrate botanical cyanobacterial groups. Denomination of particular strains corresponds to those in the database, and are not necessarily taxonomically correct. Bootstrap values of 10,000 trees are included and indicated at the nodes. Scale bar represent 2% estimated sequence divergence.



**FIG. 7** Neighbor-Joining phylogenetic tree based on 20 *rbcL* partial sequences. The sequence of *Rhodospirillum* ATCC 11170 was used as the outgroup. Brackets and roman numerals illustrate botanical cyanobacterial groups. Denominations of particular strains correspond to those given in the database, and are not necessarily taxonomically correct. Bootstrap values of 10,000 trees are included and indicated at the nodes. Scale bar represent 5% estimated sequence divergence.



**FIG. 8** Neighbor-Joining phylogenetic tree based on 12 *kaiC* partial sequences. The sequence of *Gloeobacter* PCC7421 was used as the outgroup. Brackets and roman numerals delimit “botanical” cyanobacterial groups. Denominations of particular strains correspond to those in the database, and are not necessarily taxonomically correct. Bootstrap values of 10,000 trees are included and indicated at the nodes. Scale bar represent 2% estimated sequence divergence.

CHAPTER 2  
HOW CYANOBACTERIA BORE

## ABSTRACT

Cyanobacteria bore into carbonates by a mechanism that has remained elusive. We present evidence that clarifies the key aspects of this mechanism in one euendolithic cyanobacterium, *Mastigocoleus testarum* strain BC008. Temporal separation of photosynthesis and the boring process does not play a role, since cells are able to bore under constant illumination. Spatial separation is also not involved, as cells remain photosynthetically active in deep layers of the bored mineral. The evidence is consistent with a carbonate dissolution mechanism driven by the cellular uptake of free  $\text{Ca}^{2+}$  at the boring front. This is an alternative strategy to simple acidification that still allows dissolution to become thermodynamically favorable. Boring entails a measurable release and accumulation of free- $\text{Ca}^{2+}$  on the surface of the mineral (opposite of the boring front), which was quantified using the fluorescent reporter Calcium Green-5N and laser scanning confocal microscopy. This accumulation of free  $\text{Ca}^{2+}$  is not due to spontaneous chemical dissolution of the mineral and is (1) dependent on light, (2) dependent on chemical energy and (3) dependent on calcium-transporting ATPase enzymes as demonstrated by exposure to light and dark cycles and the addition of oxidative-phosphorilation inhibitors, ATP-production inhibitors and calcium-transport inhibitors.

## INTRODUCTION

Cyanobacterial euendoliths, otherwise referred as boring, excavating, perforating or tunneling cyanobacteria, are widespread. They are found in many geographically distinct locations, in both marine (Al-Thukair and

Golubic, 1991, Fremy, 1936, Golubic, et al., 1970, Lagerheim, 1886, Le Campion-Alsumard, 1991, Vogel, et al., 2000) and terrestrial (Campbell, 1983, Friedmann, et al., 1993) settings. This notwithstanding, a comprehensive study of the physiological mechanism that enables cyanobacterial boring has never taken place, possibly due to the lack of appropriate cultivated isolates. Typically, euendoliths have been mostly described *in situ* (Golubic, et al., 1970, Le Campion-Alsumard, et al., 1995, Tribollet, et al., 2006), with only a few efforts made to try to establish cultures (Al-Thukair and Golubic, 1991, Friedmann, 1993, Montoya-Terreros, 2006, Pari, et al., 1998, Vogel, et al., 2000) mostly with identification and characterization in mind. However, in cases where cultures have been obtained, they have either not been submitted to collections or have lost their boring capacity.

The generally accepted hypothesis regarding the boring mechanism is that dissolution of carbonates is enabled in these organisms by the excretion of acidic byproducts of respiration (Golubic, et al., 1984, Haigler, 1969), although no experiments have been done to prove or disprove this conclusively. Conversely, boring by euendolithic phototrophs is nothing less than a geochemical paradox due to the fact that photosynthesis consumes CO<sub>2</sub> (a weak acid), raising the pH of the medium and promoting the precipitation of carbonates, rather than their dissolution. Yet, euendoliths are able to penetrate into carbonates regardless of this fact. One explanation for the dissolution of carbonates under these conditions is the temporal separation of boring and photosynthesis, which would allow boring only in



the absence of light. Intracellular glycogen accumulated during the daytime could provide the energy, and the release of products of respiration, namely CO<sub>2</sub> and/or organic acids (e.g. formic and lactic) would promote carbonate dissolution in the same manner proposed for most acid-producing microorganisms. This type of temporal metabolic exclusion has been demonstrated for non-boring *Oscillatoria* and other cyanobacteria in the case of nitrogen fixation (Berman-Frank, et al., 2001, Stal and Krumbein, 1987). A second explanation is based on the spatial separation of boring and photosynthesis. Here, cells at the boring front would exclusively respire, producing the acidic moieties necessary for localized dissolution, but would benefit from photosynthate provided from cells away from the boring front, as a result of net intracellular transport. This proposed acid-dissolution mechanism, although plausible, has many conflicting physiological consequences. Small-molecular weight organic acids (products of carbon fixation) are metabolically unsustainable, with the maximal number of carboxyl moieties in such acids (1 in formic, 2 in oxalic, 3 in citric...) corresponding stoichiometrically to the moles of CO<sub>2</sub> taken up from the medium and consequently to the protons already consumed (Garcia-Pichel, 2006). Additionally, it has been demonstrated that cyanobacteria do not survive at pH levels below 4, possibly due to proton damage to the cell membrane (Brock, 1973); sustained acidification would prove detrimental to the cells. All these consequences point to deposition of acids not being physiologically favorable to euendolithic phototrophs, and acid deposition

might not necessarily be what drives phototrophic boring, at least exclusively.

An alternative explanation, in which acids are not used to drive dissolution, involves the active transport of  $\text{Ca}^{2+}$  by the cyanobacterial filament, so that low concentrations of  $\text{Ca}^{2+}$  at the excavation front of the boring tunnel are created, decreasing ion activity products to levels that would make dissolution plausible (Garcia-Pichel, 2006). Dissolution of a carbonate will occur if any of the activities of either ion,  $\text{Ca}^{2+}$  or  $\text{CO}_3^{2-}$ , are reduced shifting the thermodynamic equilibrium. Because this occurs in an environment where precipitation rather than dissolution is favored (alkaline pH,  $\text{Ca}^{2+}$  supersaturation), it will most likely require energy input. Calcium transporters in charge of calcium metabolism and homeostasis, analogous to those described in other eukaryotic and prokaryotic models, might play a role. Examples of these transporters include calcium antiporters, calcium channels, and energy-dependent, cation-specific enzymes such as (P-type) ATPases.  $\text{Ca}^{2+}$ -ATPases, which are responsible in actively exporting  $\text{Ca}^{2+}$  out of the cell, are found in some cyanobacteria (Berkelman, et al., 1994, Geisler, et al., 1993). It appears that the building blocks needed for the  $\text{Ca}^{2+}$  pump-enabled dissolution can be present in cyanobacteria, so it is not difficult to envision the possibility of one or many of these mechanisms involved the carbonate excavation; the problem lies in identifying specifically (1) if is indeed caused by the transporting of  $\text{Ca}^{2+}$  enzymes and (2) by what type of enzyme it is and how does it do it. If euendoliths are dissolving the carbonate

by Ca<sup>2+</sup> mobilization, they must be using an equal or similar strategy to the ones previously described above.

It is the main goal of this project to pursue a solid understanding of the dynamics of cyanobacterial excavation in at least one model organism by gathering comprehensive evidence using quantitative and qualitative techniques.

## MATERIALS AND METHODS

**Strain and growth conditions.** *Mastigocoleus testarum* BC008 was obtained from marine carbonates, and grown in blocky calcite chips as previously described (Chapter 1 of this dissertation). Briefly, calcite chips were prepared by cleaving crystalline blocky calcite into suitable size fragments (2-6 mm<sup>3</sup>) with the aid of a flame-sterilized hammer. After cleaving, the chips were placed in ethanol 95% and each one flame-sterilized before transferring to sterile culture flasks. Calcite purity was evaluated and confirmed by X-ray diffraction. Sub-culturing was performed with previously infested chips, in which superficial biomass was removed with a small watercolor paintbrush and rinsed twice in sterile PES 30. Cultures were inoculated only with infested chips, so that the amount of non-boring filaments was minimized and the useful life of the euendolith cultures was extended for long-term observations. Cultures were kept at 25° C under constant light provided by fluorescent lamps (light intensity = 30 μmoles of photons). Cultures were monitored for growth and boring activity by visual inspection using a dissecting microscope.

### **Determination of photosynthesis rates in exhumated filaments.**

Filaments were exhumated using a modified dissolution method, based on Wade (2003) and described in detail in Chapter 4 of this dissertation. Briefly, a solution of 200mM sodium-ethylenediamine-tetraacetic acid (EDTA), pH=5 was used to dissolve the carbonate. The solution was drawn using a peristaltic pump, and allowed to drip on top of infested chips (1mL/min) placed on a small screen basket atop of the column of a filtration apparatus. Filaments were gradually exposed, gently brushed from the chip, washed with sterile distilled water and collected on a 2 µm pore polycarbonate filter, on a vacuum filtration apparatus. Each progressive dissolved fraction corresponded to a 50 µm deep layer (measured by volume and weight loss). Fractions were classified as superficial (top 50 µm), middle (up to 100µm) and deep (up to 150 µm). Filaments were rinsed in 10mL of sterile PES, centrifuged for 10 minutes at 4,000 RPM and the pellet re-suspended in PES medium. Cells were allowed to rest overnight, in the light. A Hansatech liquid-phase oxygen electrode chamber (Hansatech Instruments, Norfolk, England) was used to measure oxygen evolution from the fractions. The electrode was calibrated in PES medium, achieving 100% O<sub>2</sub> saturation by stirring in the open chamber, and by adding sodium dithionite to establish 0% O<sub>2</sub> saturation. Oxygen evolution rates were measured under white fluorescent light at 500 µmoles of photons. After measuring, biomass was quantified by pelleting cells (4,000RPM, 10 min.) and re-suspending in 5ml of 90% acetone. Cells were incubated at 4° C for 48h in the dark, and total chlorophyll content measured in a TD-700 fluorometer.

**Determination of boring substrates.** Pure crystalline samples of andradite ( $\text{Ca}_3\text{Fe}_2(\text{SiO}_4)_3$ ), ankerite ( $\text{CaFe}(\text{CO}_3)_2$ ), aragonite ( $\text{CaCO}_3$ ), barite ( $\text{BaSO}_4$ ), brazilianite ( $\text{NaAl}_3(\text{PO}_4)_2(\text{OH})_4$ ), colemanite ( $\text{CaB}_3\text{O}_4(\text{OH})_3 \cdot \text{H}_2\text{O}$ ), dolomite ( $\text{CaMgCO}_3$ ), fluoroapatite ( $\text{Ca}_5(\text{PO}_4)_3\text{F}$ ), gypsum ( $\text{Ca}_2\text{SO}_4$ ), hematite ( $\text{Fe}_2\text{O}_3$ ), magnesite ( $\text{MgCO}_3$ ), malachite ( $\text{CuCO}_3 \cdot \text{Cu}(\text{OH})_2$ ), rhodochrosite ( $\text{MnCO}_3$ ), strontianite ( $\text{SrCO}_3$ ) and vivianite ( $\text{Fe}_3(\text{PO}_4)_2 \cdot 8(\text{H}_2\text{O})$ ) were obtained from mineral collections (eBAY) and prepared as described previously for calcite. Commercially available marble chips ( $\text{CaCO}_3$ ) were as well evaluated for potential infestation. To ensure the pure nature of the substrates, purity was verified by X-ray powder diffraction and checked against the ICDD Database ([The International Centre for Diffraction Data](#)). Chips were harvested, placed in 95% ethanol, flame-sterilized and inoculated with a BC008 infested calcite chip. A calcite control was kept with the cultures under the same experimental conditions to establish the baseline for typical (*in calcite*) boring success. To quantify the biomass of boring filaments infested chips were cleaned of any superficial growth with a small watercolor brush and rinsed in sterile PES medium. The chips were measured with a ruler (in mm) to calculate their total surface area. Chlorophyll a was extracted by placing the chips in 5 mL of 90 % acetone for 48 hours at 4 °C and measured in a TD-700 fluorometer (Turner Designs, Sunnyvale, CA, USA). Relative boring activity in all substrates was reported as percent of boring rate against calcite controls with levels of boring in calcite assumed at a 100% success rate.

**Laser scanning confocal microscopy.** Infested chips were cleaned of any superficial biomass with a small watercolor paintbrush, rinsed in PES sterile medium twice and incubated for one hour in PES medium with 1  $\mu\text{M}$  of Calcium Green-5N (Molecular Probes, Eugene, OR, USA) at room temperature under white incandescent light at 30  $\mu\text{mol}$ s of photons. CG5N is a low affinity calcium-sensitive fluorophore, excitable with visible light and having a maximum emission peak close to 540 nm (green). Incubation under incandescent light bulbs for 1 hour had no significant effect on CG5N fluorescence (no bleaching of the fluorophore was observed). After incubation, the chips were fixed to custom-made slides with “superglue” (cyanoacrylate). Custom-made slides consisted of a regular microscope glass slide containing a modeling clay ring of approximately two centimeters in diameter. The ring was then filled with PES containing CG5N at a final concentration of 1  $\mu\text{M}$ . A 22mm x 22mm glass coverslip of regular thickness was placed on top of the ring creating a chamber. The ring held the medium and allowed some cushion between the microscope and chip, preventing crushing. Volume inside the chamber was approximately 500  $\mu\text{L}$ . The slides were then placed on the stage of a Leica TCS-SP2 Laser Scanning Confocal Microscope and observed under an oil immersion 40X objective. An epifluorescence mercury arc lamp with visible light lines in the 488 nm and 546 nm was used to evaluate the sample for viability (presence of photosynthetic pigments in cells), prior to laser scanning. Visible laser lines of Ar/Kr (488 nm) and Kr (546 nm) were used to excite the samples and emission bandwidths were selected using the microscope’s acousto-optical tunable filter (AOTF). CG5N

fluorescence was recorded at a bandwidth of 500 to 540 nm and chlorophyll at a bandwidth of 670 to 690 nm. Images were recorded using pinhole values of one airy unit (82  $\mu\text{m}$ ), 400 Hz scanning speed, XYZ format and 1024 by 1024 pixel resolution. Vertical profiles were created by recording single-scan optical sections every 1.3  $\mu\text{m}$ , starting from the overhead medium and moving vertically with depth into the calcite chips. For time course experiments, individual filament fluorescence was measured on a single optical section focused on the surface of the chips at the entrance of the boreholes. Images were analysed with the Leica Confocal Software (Leica Microsystems Inc., Bannockburn, IL, USA).

**General calibration of Calcium Green-5N.** Initial calibration of CG5N was performed using a TD-700 fluorometer (Turner Designs, Sunnyvale, CA, USA) using a 530/30 FITC green filter to measure fluorescence in calcium standards, ranging from 0.1 mM-50 mM  $\text{CaCl}_2$  in  $\text{Ca}^{2+}$ -free Artificial Seawater medium ( $\text{Ca}^{2+}$ -free ASW) at a final concentration of 1  $\mu\text{M}$  CG5N. Performing this calibration outside the experimental setup allowed us to establish the useful range for CG5N and evaluate its efficiency in our medium. When working with calcium fluorophores in seawater, calibration offers some challenges as natural seawater contains approximately 10mM of free calcium ions and early saturation can be a problem even when using low affinity dyes. The dissociation constant ( $K_d$ ) of CG5N in buffered medium at pH of 7.2 is reported to be 14  $\mu\text{M}$  (Rajdev and Reynolds, 1993, Tucker and Fettiplace, 1995, Zhao, et al., 1996). However when CG5N was added to PES

medium at a pH of 8.3, we calculated  $K_d$ 's anywhere from 2 mM-5 mM using the following equation for a one site binding hyperbola:

$$Y=B_{\max} * X / (K_d + X)$$

in which Y equals fluorescence as relative fluorescent units (RFU),  $B_{\max}$  equals the maximum fluorescence (as relative fluorescent units) at saturation, X equals free calcium concentration (in mM) and  $K_d$  is the dissociation constant. It has been reported that the  $K_d$  of calcium fluorophores and the affinity of EGTA for calcium (EGTA being the core molecular scaffold of  $Ca^{2+}$  sensitive fluorophores) is dependent on temperature, pH and ionic strength (Eberhard and Erne, 1991, Harrison and Bers, 1989, Lattanzio and Bartschat, 1991) providing evidence that under different conditions the  $K_d$  of dyes can change. In our case, the reduced affinity of CG5N for calcium in PES medium at pH of 8.3, allowed the dye to report at seawater calcium levels without saturating. This demonstrates that the useful range of CG5N could be pushed beyond its standardized use in our experiments and even when a high-resolution calibration was not achieved, the dye proved useful in measuring changes in calcium concentration with a moderate amount of precision.

***In situ* calibration of CG5N.** To establish the calibration curve of CG5N *in situ*, a custom slide was used and calcium standards ranging from 0.1 mM-50 mM calcium chloride in calcium-free Artificial Seawater medium ( $Ca^{2+}$ -free ASW) and 1  $\mu$ M CG5N were added into the chamber at increasing levels of concentration. Fluorescence in all standards was measured using the Leica



Confocal Software. While measuring fluorescence, our effective resolution of free calcium concentrations was impaired after 30 mM. A linear model was assumed and calibration curve was established using the one site binding hyperbola equation explained previously.

**Oxidative phosphorylation inhibitors and calcium-transport inhibitors.** The inhibitors carbonyl cyanide m-chlorophenyl hydrazone (CCCP), oligomycin, verapamil, lanthanum chloride and sodium orthovanadate were obtained from Sigma-Aldrich (Sigma-Aldrich Corp., St. Louis, MO, USA). Thapsigargin was obtained from Alexis Biochemicals (Lausen, Switzerland). Tert-butyl hydroquinone (TBHQ) was obtained from Spectrum (Spectrum Chemicals, Gardena, CA, USA). Stocks were prepared by dissolving polar compounds in sterile deionized water and non-polar compounds in dimethyl sulfoxide (DMSO) (for thapsigargin) or ethanol (for verapamil). Working solutions were prepared with fresh sterile PES and adjusted to pH=8.3, having final concentrations containing less than 1% of the solvents.

**Effect of calcium-transport inhibitors on photosynthesis.** Oxygen optodes (PreSens-Precision Sensing GmbH, Regensburg, Germany) were used to assess the effects of calcium transport inhibitors on photosynthesis, if any, by monitoring oxygen evolution in infested chips. Oxygen optodes were calibrated by bubbling PES with nitrogen for 10 minutes to achieve oxygen starvation (0% O<sub>2</sub>) and by bubbling with air for 10 minutes to achieve oxygen

saturation (100% O<sub>2</sub>). A micromanipulator was used to lower the optodes in the medium for initial calibration, to establish oxygen profiles and time courses in live chips. All the oxygen profiles were recorded using an ABB SE 120 chart recorder (ABB industries, Zurich, Switzerland). Concentration of the compounds was equivalent to the ones used in the confocal microscope.

## RESULTS

**Boring in minerals other than calcite.** To test the boring ability of BC008 in other substrates, pure crystalline samples of andradite (Ca<sub>3</sub>Fe<sub>2</sub>(SiO<sub>4</sub>)<sub>3</sub>), ankerite (CaFe(CO<sub>3</sub>)<sub>2</sub>), aragonite (CaCO<sub>3</sub>), barite (BaSO<sub>4</sub>), brazilianite (NaAl<sub>3</sub>(PO<sub>4</sub>)<sub>2</sub>(OH)<sub>4</sub>), colemanite (CaB<sub>3</sub>O<sub>4</sub>(OH)<sub>3</sub>·H<sub>2</sub>O), dolomite (CaMgCO<sub>3</sub>), fluoroapatite (Ca<sub>5</sub>(PO<sub>4</sub>)<sub>3</sub>F), gypsum (Ca<sub>2</sub>SO<sub>4</sub>), hematite (Ca<sub>2</sub>SO<sub>4</sub>), magnesite (MgCO<sub>3</sub>), malachite (CuCO<sub>3</sub>·Cu(OH)<sub>2</sub>), rhodochrosite (MnCO<sub>3</sub>), strontianite (SrCO<sub>3</sub>), vivianite (Fe<sub>3</sub>(PO<sub>4</sub>)<sub>2</sub>·8(H<sub>2</sub>O)) as well as marble chips (CaCO<sub>3</sub>), were evaluated as possible candidates for infestation. Substrates were allowed infestation for a period of 3 months under identical light conditions. Table 1 illustrates positive or negative boring (with calcite, the highest rates, set as 100% rate) on all the minerals tested. Apart from pure calcite, only aragonite, strontianite (modestly) and marble chips (microcrystalline calcite rock) had significant evidence of boring as indicated by visual inspection and boring success quantification.

**Temporal separation. Temporal separation.** To address the temporal separation of boring and photosynthesis, growth rates (doubling time) and levels of infestation on calcite chips (Chl a /cm<sup>2</sup>) were measured as a function

of light exposure, illustrated in Fig.2A. Cells were able to bore under 24h of constant light, albeit doubling times and infestation were marginally affected by the lack of day-night cycle. Optimal doubling times and infestation rates were obtained at 4 hours and 16 hours of light exposure respectively.

To test the temporal separation of the boring process and photosynthesis, liquid cultures of BC008 were incubated under constant light (no period of darkness) for 5 weeks. Growth rates (doubling time) and levels of infestation on calcite chips (Chl a /cm<sup>2</sup>) were measured as a function of light exposure, illustrated in Fig.2A. Cells were able to bore under 24h of constant light, albeit doubling times and infestation were marginally affected by the lack of day-night cycle. Optimal doubling times and infestation rates were obtained at 4 hours and 16 hours of light exposure respectively.

**Spatial separation.** To test the spatial separation of the boring process, *in situ* emission spectra of individual cells were measured with LSCM spectrometry on filaments that were actively boring to assess photosynthetic pigment expression (Fig. 2B). Both surface filaments (50 μm in depth) and deeply-boring filaments (150 μm in depth) express chlorophyll and phycobilins peaks as seen in the emission spectrum, and no significant difference was found in pigment expression on cells at the surface versus cells deep inside chips. Fig. 3 illustrates photosynthesis rates of boring filaments disinterred by EDTA dissolution. Actively boring filaments were isolated by decalcification in consecutive fractions (surface, middle and deep) of 50 μm in

depth. Typical photosynthetic rates of 2 other cyanobacteria (*Gloeobacter violaceus* PCC 7421, *Synechocystis* sp. PCC 6803 (Koyama, et al., 2008)) are presented for comparison.

**Calcium mobilization by boring cells.** The calcium sensitive fluorophore CG5N was used to measure putative release of free calcium by distal cells. Following the proposed calcium model, our hypothesis suggests that euendolithic cyanobacteria gradually dissolve the carbonate by removing calcium from the interstitial space between the apical cell(s) at the boring front and the calcium carbonate, with a  $\text{Ca}^{2+}$  transporting enzyme(s). Once a small amount of the mineral is dissolved, caused by the carbonate giving  $\text{Ca}^{2+}$  to compensate for those lost, the apical cell will expand to fill the space, and the process of dissolution is resumed. The calcium is mobilized from cell to cell through the filament and eventually released from the distal cell (the one closest to the mineral's surface), maintaining internal calcium homeostasis. This release of  $\text{Ca}^{2+}$  can be used as a proxy for the boring process, providing evidence of its activity. If this is true, we should be able to measure the release of free  $\text{Ca}^{2+}$ , understanding that this measuring does not completely disprove a process that involves dissolution with acids. Even if we are able to measure the release of  $\text{Ca}^{2+}$  above saturation, we cannot disprove the possibility of boring being driven by acid attack, as dissolving calcium carbonate with acid will still release  $\text{Ca}^{2+}$ . The problem lies in that observing any changes in acidity within the tunnels is impossible, as protons released would react with the surrounding carbonate, and no free  $\text{H}^+$  would be

available to measured with a reporter (i.e. pH-sensitive fluorophores). The process may still happen, but we are yet to quantify it with efficiency. However, if we were to predict how the process would look when dissolution is indeed acid-driven, we would expect the concentration of calcium to decrease linearly towards the surface of the chip due to diffusion of free  $\text{Ca}^{2+}$  from the boring front. The concentration of free  $\text{Ca}^{2+}$  (interstitially) in the deepest part of the tunnels would rise above saturation, these being the closest to the boring front and the ionic products of dissolution forced to slowly diffuse outwards. As predicted, calcium release and eventual supersaturation can be measured at the surface of infested chips, which is consistent with our hypothetical model. Calcium microprofiles of infested chips were recorded (Fig. 4A) and calcium concentration inside the boreholes decreased to levels below saturation (less than 10 mM  $\text{Ca}^{2+}$ ) with depth. Imaging of a chip placed under 48h of darkness (Fig. 4B) as well as sterile chips and bleach killed infested chips revealed no accumulation of calcium. Figure 3C shows a vertical cross section of a BC008 infested calcite chip with observed accumulation of  $\text{Ca}^{2+}$  (bright green) at the surface of boreholes, the latter being excreted by the filaments (in red).

**Boring is light dependent.** To evaluate the effects of light in the boring process, experiments with light and dark shifting were performed. Cyanobacteria are phototrophs and a constant input of light is expected to maintain boring. Upon darkening, boring should stop or at least be reduced significantly, although respiration may still provide some energy. What is

expected is for the release of calcium to decrease or stop completely in the dark, when chemical energy is not available and when calcium-transporting proteins are inactivated. The concentration of calcium in the medium should remain at basal levels (close to 10 mM for seawater) and not change if the cell's transporting machinery is inactivated. Cells were incubated in the stage illumination (white light, 50  $\mu$ moles of photons) for 1 hour before initial imaging. To demonstrate light dependency, a characteristic of boring by phototrophs, illumination was turned off for at least one hour, and imaged again. To assess recovery, light was turned on once more and chips incubated for  $\sim$ 1 hour before repeating measurements. Time course experiments provide evidence that the release of  $\text{Ca}^{2+}$  by the filaments and the following  $\text{Ca}^{2+}$  supersaturation at the surface of the boreholes is light dependent. When light is turned off, the supersaturation of the cation decreases to saturation levels (same levels as the medium,  $\sim$ 10 mM) and when light is again turned on, the level becomes once more supersaturated (Fig. 5A). This process was dependent on light irradiance as well, as cells incubated under more intense light (100  $\mu$ moles of photons) had higher recovery super-saturation levels than those at lower light intensity (30  $\mu$ moles of photons) (Fig. 5B).

**Boring is energy dependent.** To evaluate the chemical energy contribution to the boring process, a cocktail of carbonyl cyanide *m*-chlorophenyl hydrazone (CCCP) 2  $\mu$ M and the antibiotic oligomycin 63  $\mu$ M at a 1:1 ratio was used to block oxidative phosphorylation in strain BC008. CCCP works by disrupting the integrity of cell membranes, effectively

decoupling the electron transport chain (Hirose, et al., 1974, Kasianowicz, et al., 1984). Oligomycin inhibits ATP synthase by blocking its proton channel, which is necessary for oxidative phosphorylation of ADP to ATP (Nakata, et al., 1995). If the energy generating processes such as the electron transport chain and ATP synthesis are hindered, boring is also expected to stop. Cells were imaged in the light, and when the CCCP/oligomycin cocktail was added, free calcium supersaturation levels at the surface of the chip decreased back to saturation levels equivalent to those in the media (Fig. 5C). Sodium orthovanadate 10 mM was also used to evaluate the effects of chemical energy starvation. Vanadate ions act as inhibitors a number of ATPases, most likely acting as a phosphate analogue (Gordon, 1991). A similar result was achieved (Fig. 5D) decreasing  $\text{Ca}^{2+}$  supersaturation levels at the surface of infested chips back to saturation levels. The experiments prove the relationship between chemical energy starvation and the inability of the boring filaments to release calcium at the surface of chips.

**Boring is partially impaired by the addition of a calcium channel blocker.** To evaluate the contribution of calcium channels in the boring process, the compound verapamil at a final concentration of 1 mM was used (Fig. 5E). Verapamil is a calcium antagonist and acts as a  $\text{Ca}^{2+}$  channel blocker (Andersen, et al., 2006, Bourget, 1982, Shainkin-Kestenbaum, et al., 1989). If calcium channels are involved in the process, then by blocking these with the respective compounds should have a measurable effect on the release of  $\text{Ca}^{2+}$  due to boring. Fig. 4E shows calcium supersaturation levels at

the surface of the chip decreased approximately to half of the initial levels recorded at time zero when verapamil was added to cultures incubated in the light. Note that the concentrations used to obtain this effect are much larger than those needed to affect channels elsewhere (Kirischuk, et al., 1996, Knight, et al., 1997, Teixeira, et al., 2004). Long-term experiments to observe verapamil effects on boring proved inconclusive (data not shown).

**Boring is impaired with the addition of lanthanide ions.** To evaluate the contribution of cation-transporting ATPases in the boring process, lanthanum chloride ( $\text{LaCl}_3$ ) was used. Lanthanum chloride has been used in several models to evaluate its effect on calcium-related processes, working as a competitive inhibitor of divalent cation channels and ATPases (Entman, et al., 1969, Fernandez-Belda, 1988, Fujimori and Jencks, 1990, Hanel and Jencks, 1990). In time course experiments, (Fig. 5F) when lanthanum chloride was added to infested chips in the light, superstauration levels of  $\text{Ca}^{2+}$  measured at the surface of chips decreased back to saturation levels with time. The process was concentration dependent (i.e competitive), with the fastest effect occurring with a final concentration of 10 mM lanthanum chloride.

**Boring is impaired with the addition of  $\text{Ca}^{2+}$  ATPase blockers.** Specific blockers of  $\text{Ca}^{2+}$  ATPases, the compounds thapsigargin and tert-butyl hydroquinone (TBHQ) were used in time course experiments to evaluate their effects on boring activity (Fig. 4H & 4D) Thapsigargin, a tight-binding



inhibitor of sarco / endoplasmic reticulum (SERCA)  $\text{Ca}^{2+}$  ATPase (Rogers, et al., 1995) has been used in several models to evaluate its effect on P-type ATPases (Geisler, et al., 1998, Lanini, et al., 1992, Moreno, et al., 2008). Tert-butyl hydroquinone (TBHQ) it is also a blocker of SERCA P-type  $\text{Ca}^{2+}$  ATPases (Gukovskaya, et al., 2000, Phillippe, et al., 1995, Robinson, et al., 1992). If calcium-transporting enzymes drive the process, then by blocking or decoupling these with inhibitors, the observed  $\text{Ca}^{2+}$  supersaturation around boreholes should cease. In time course experiments, when thapsigargin or TBHQ were added to infested chips in the light, calcium supersaturation levels measured at the surface of infested chips decreased to saturation levels with time. The effect on  $\text{Ca}^{2+}$  supersaturation was fastest with TBHQ, decreasing to saturation levels in 20 minutes. Both compounds had a concentration dependent effect, thapsigargin 1 mM and TBHQ 100  $\mu\text{M}$  having the fastest response.

**Effect of calcium transport inhibitors on photosynthesis.** To evaluate the effect of calcium transport inhibitors in photosynthesis, time course experiments for sodium orthovanadate, verapamil and lanthanum chloride (Fig. 6) as well as for thapsigargin and TBHQ were recorded in the light using optodes to measure oxygen evolution. Cells were evaluated for viability by recording supersaturation levels of oxygen in the light and undersaturation of oxygen by turning the light off. Neither compounds affected photosynthesis significantly over a period of several hours, and cells

remained viable as demonstrated by light and dark cycles performed after the treatments.

## DISCUSSION

BC008 cells were able to bore under constant light, and even when cells were at sub-optimal growth conditions (with best infestation rates at 16 hours of light), the results show that boring can occur alongside photosynthesis. The evidence disproves a temporal separation hypothesis of the boring mechanism, where the boring process is achieved exclusively under darkness by using acidic by-products of respiration as the driving force. Spatial separation of the process is disproved, as photosynthesis occurs even in the deepest layers of the chips, as demonstrated both by the presence of photosynthetic pigments in deep cells and oxygen evolution measurements.

In regards to the support by heterotrophic bacteria during boring, axenic filaments were still able to bore, so heterotrophs do not play a direct role in boring. It is interesting to mention, on the other hand, that non-axenic cultures colonized chips faster than axenic ones, probably due to increased efficiency in nutrient cycling with the presence of heterotrophs. With regards to the strain's boring potential, non-carbonate minerals or carbonates containing barium, copper, iron, magnesium, manganese, or sodium could not be bored, likely do to the inability of the ATPases to transport those cations. Our strain could not bore on carbonates including magnesite, dolomite, siderite, malachite, ankerite, and witherite. Among the sulfates, gypsum and barite were not attacked; neither were some calcium silicates like andesite. Contrary to reports in the literature (Konigshof and Glaub, 2004) none of the

phosphates in our trials (apatite, vivianite, brazilianite) could be bored by our strain, suggesting that its habitat is limited to calcium (or strontium) carbonates in Nature. This specific mineral requirement stands out against the utilization of acids as the exclusive boring force, at least in this model organism, as any carbonate could have been subject to acid attack. In the case of strontianite, the ability of BC008 to bore into this substrate, although modest, provides some evidence that the mechanism could employ specific enzymes for calcium transport, as strontium is atomically analogous to calcium and frequently interchanged in biological systems (e.g. Avery and Tobin, 1992, Uhrik and Zacharova, 1988, Vasington, 1966)

If acid-driven dissolution were the main driver, we would expect calcium concentrations in the interstitial space of the borehole to decrease linearly towards the surface of the chip due to diffusion from the boring front, and the concentration of  $\text{Ca}^{2+}$  inside the boreholes to rise above saturation. Instead, what is observed is an accumulation of  $\text{Ca}^{2+}$  at the surface of the chips, and undersaturation inside the boreholes, which can only mean energy-dependent transport as it happens against thermodynamic equilibrium. As predicted by our model, if boring happens with calcium “pumping”, the concentrations in the tunnels would be expected to be the lower than the basal concentration of the medium, as direct uptake would lower the ion activity product below saturation. Active transport through the filament and the necessity of intracellular calcium to remain stable, predicts the release of this excess  $\text{Ca}^{2+}$  afar from the boring front. Such a distinct gradient of saturation in conditions where spontaneous chemical dissolution

of calcium carbonate is unlikely to occur (pH = 8.3 and 10 mM Ca<sup>2+</sup>) can only be explained by biological action. The LSCM-acquired profiles and time course experiments demonstrate that the accumulation of calcium observed at the surface of infested chips is correlated to the action of boring, and that the process depends on light and energy input, which is consistent with the activity of photosynthetic organisms.

Energy-dependent transport seems to play an intrinsic role in the boring mechanism. The results demonstrate that when energy starvation is forced by turning off the light, or by the addition of the oxidative phosphorylation and ATP production inhibitors CCCP and oligomycin, the observed calcium accumulation is effectively stopped, returning to saturation. Sodium orthovanadate acting as an ATPase inhibitor was able to stop the process completely. These results validate our hypothesis and are consistent with our proposed energy-dependent model for boring in cyanobacteria.

When using calcium transport inhibitors, the calcium channel blocker verapamil had a partial effect in the boring mechanism by decreasing the accumulation of free calcium to about half of the control levels. Because the process is not inhibited completely, this suggests that calcium channels might be part of the molecular boring machinery or that the chemical might be exerting a partial effect on transporting enzymes. Lanthanum chloride working as a competitive inhibitor of divalent cation channels and ATPases was responsible for the loss of the calcium accumulation, probably acting as a broad-spectrum inhibitor of the mechanism. Specific calcium transporting inhibitors of P-type ATPases like thapsigargin and TBHQ effectively stopped

this release and accumulation of calcium. This suggests a mechanism of transport in which calcium is mobilized by the action of P-type  $\text{Ca}^{2+}$  (or similar) transporting proteins. The inhibitors action also suggests that the type of enzymes that are present in the boring cyanobacterium might have similar structures to described sarco / endoplasmic reticulum (SERCA) P-type  $\text{Ca}^{2+}$  ATPases in other models. No significant effect on photosynthesis was demonstrated by any of the treatments involving calcium-metabolism inhibitors, confirming that the results of the treatments are indeed due to their effect on calcium transport and not a mere effect on photosynthesis hindrance, which would inevitably stop the dissolution process.

The results of this study are the first quantitative proof that demonstrate how boring is performed in at least one cyanobacterium model. The evolutionary implications of the use of calcium-transporting proteins at the organism's advantage are many. Cell orchestration, achieving complex transport and a smart display of thermodynamic management is yet another proof of the true multicellularity of some of these phototrophic prokaryotes. The reasons for boring by calcium removal are not absolutely evident, but it seems that this process of dissolution uses an available asset (a transporting protein or proteins) that does not place the cells at a physiological disadvantage, like a constant production of acid would.

## CONCLUSIONS

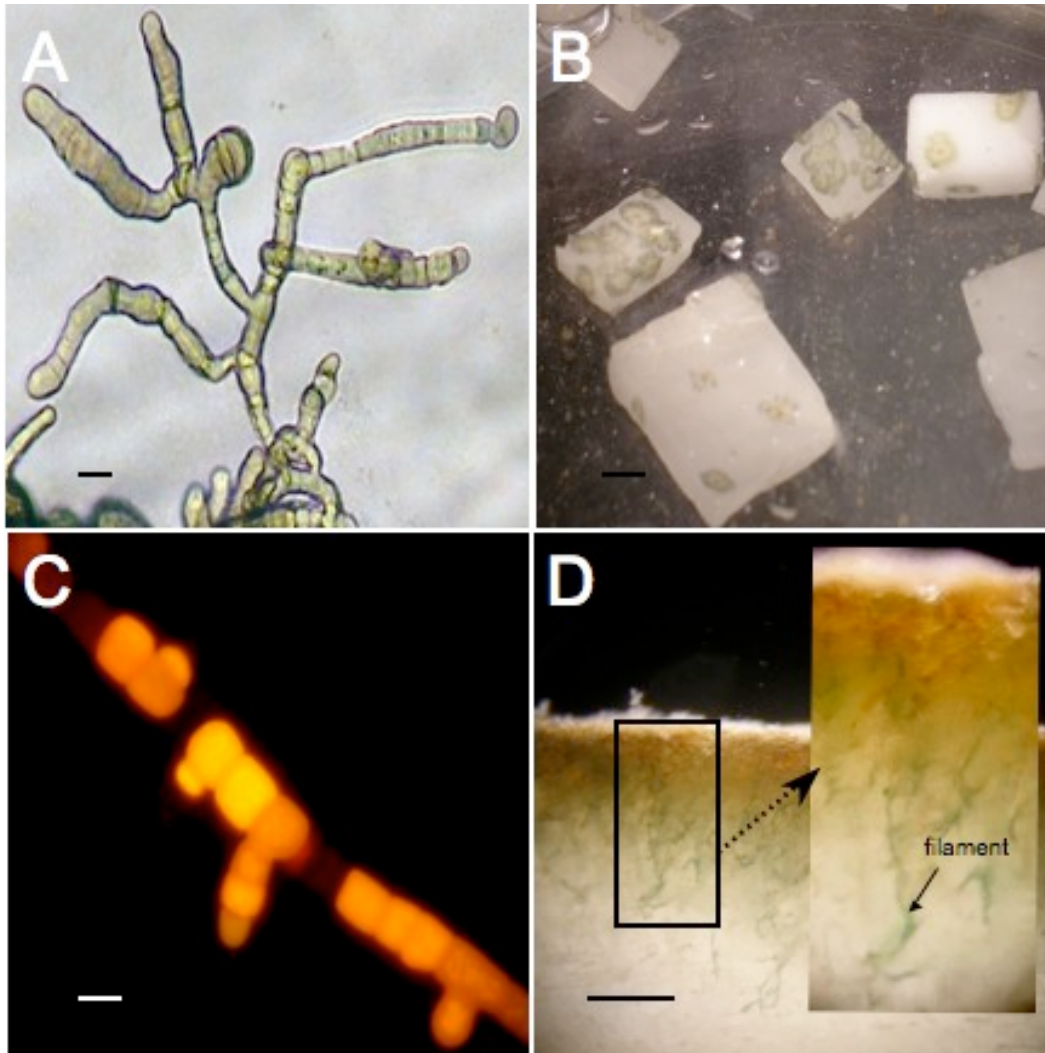
An axenic culture of a euendolithic cyanobacterium, *Mastigocoleus* strain BC008, can bore into calcium or strontium containing carbonates under controlled laboratory conditions. It is capable of boring into the

mineral using a calcium-transporting mechanism that allows dissolution of the carbonate by decreasing ion activity products in the interstitial space between cell and mineral. An accumulation of calcium at the distal end of the boring filaments can be observed due to excretion of  $\text{Ca}^{2+}$  after mobilization from the boring front, and this process is dependent on light, energy and the activity of P-type  $\text{Ca}^{2+}$  ATPases. This is the first and only evidence, to this date, that demonstrates that dissolution of carbonates other than acid attack is used by some cyanobacterial euendoliths. Work in progress is focused on probing the expression of P-type  $\text{Ca}^{2+}$ ATPases in the strain and assessing the universality of the boring mechanism among other euendolithic cyanobacteria from geographically distinct locations.

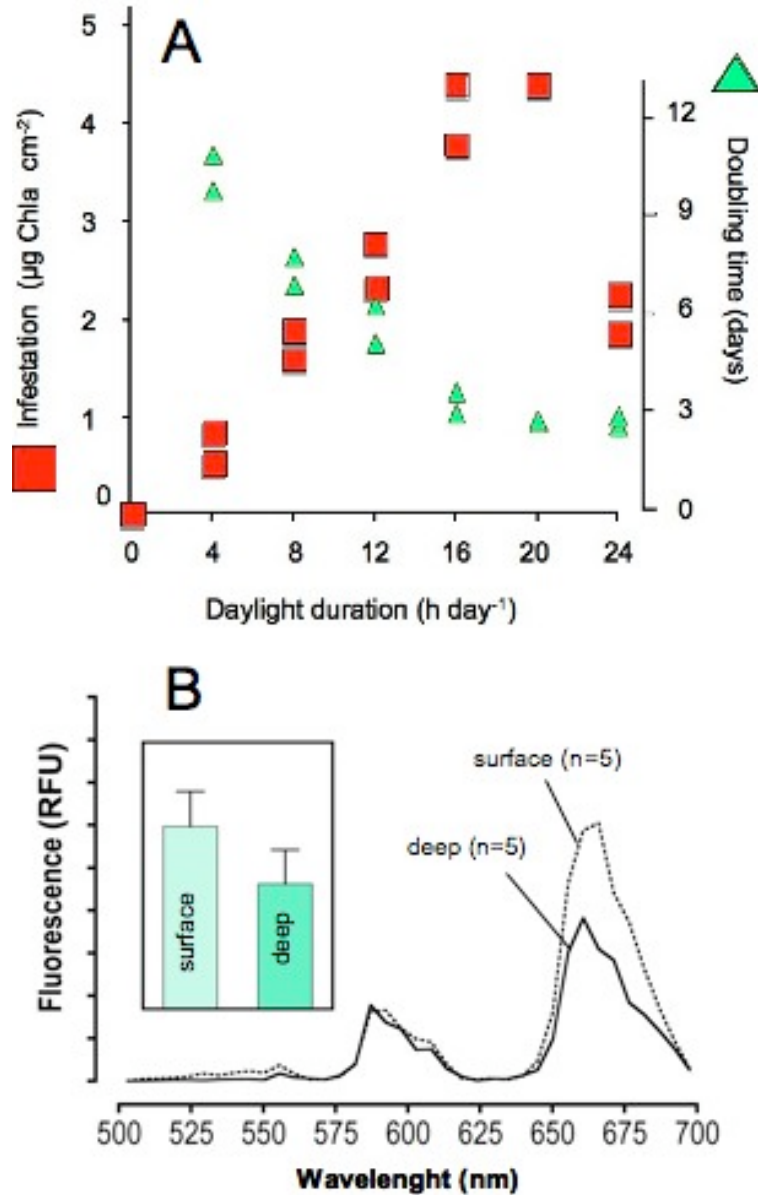
#### **ACKNOWLEDGMENTS**

We would like to thank Page Baluch and Bret Judson of the KeckLab Bioimaging Facility at Arizona State University for their immense help with confocal microscopy. We would also like to thank the members of the Garcia-Pichel lab for their helpful suggestions.

This work was supported by a National Science Foundation grant 0311945.

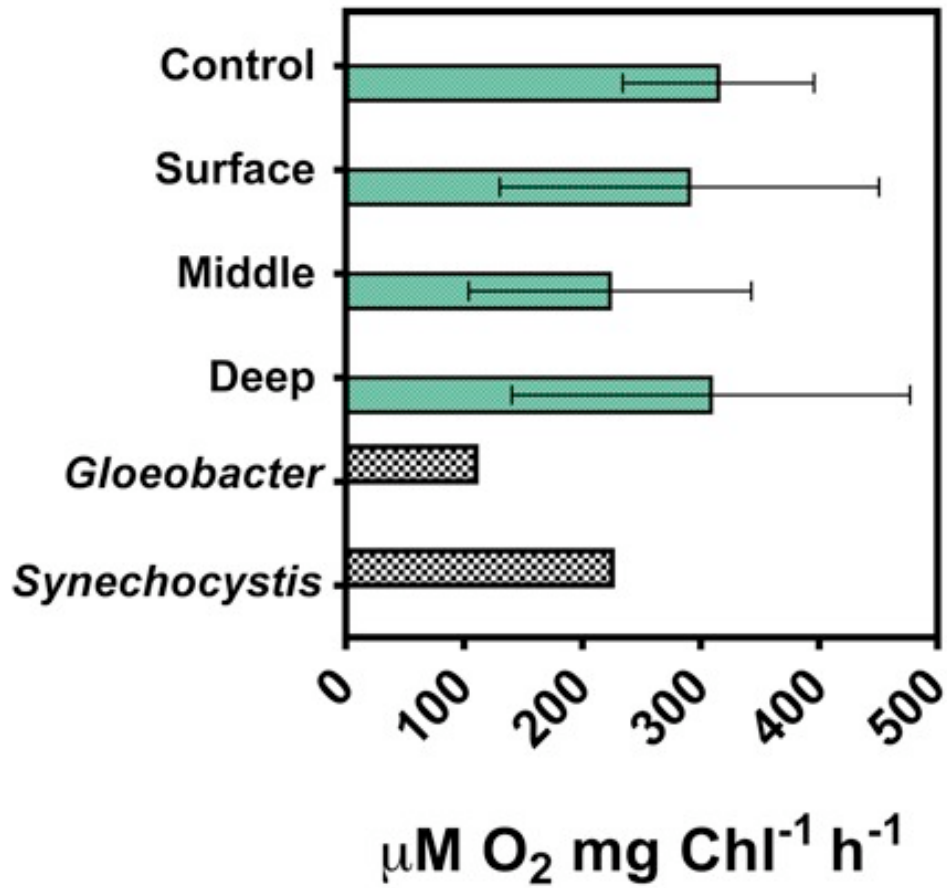


**FIG. 1** Typical morphology of free-living filaments of *Mastigocoleus* strain BC008, as seen with phase-contrast optics (A) and epifluorescence microscopy (Ex=488 nm) (C); Bar, 10  $\mu$ M. (B) Examples of calcite chips infested by an axenic culture of BC008. (D) Vertical cross-section of a calcite chip showing an extensive network of boring filaments. Deepest filaments are seen penetrating to depths of approximately 400  $\mu$ m. Surface micritization can be observed due to extensive reworking of the mineral matrix, consequence of borehole excavation and carbonate re-precipitation. Bar, 100  $\mu$ M.

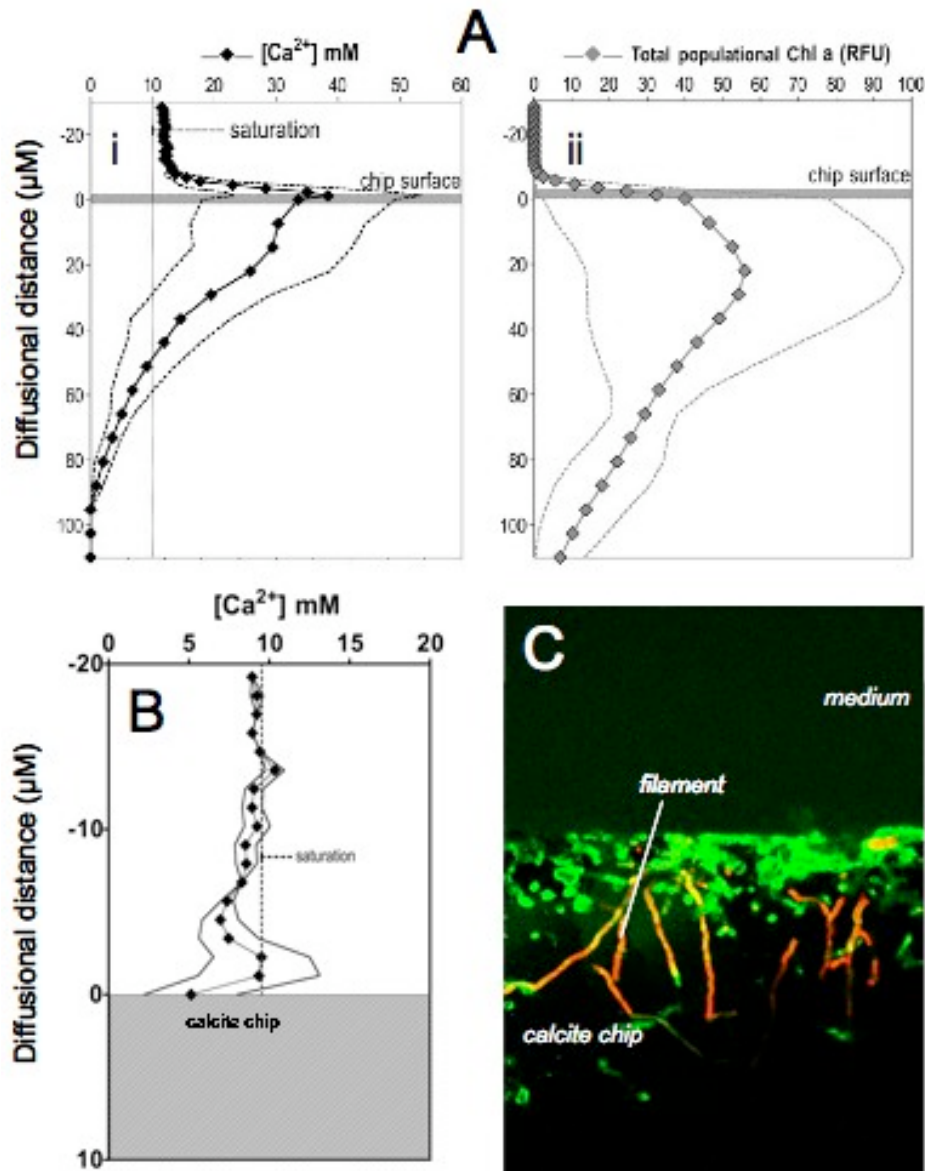


**FIG. 2** (A) Growth rate (doubling time, right axis) in liquid culture, and level of infestation attained on blocky calcite chips by BC008 at 5 weeks of incubation (left axis) as a function of the length of the light period when grown on a day-night cycle. (B) Cell-specific photosynthetic pigment content measured *in situ* during boring using fluorescence emission spectroscopy of confocal microscope optical sections with excitation at 488 nm. Lines show average emission spectra of single cells, for cells close to the boring front (deep) compared to cells close to the surface of the solid (surface). Insert shows data for Chl a-specific emission at 685 nm (error bars are 1 standard deviation), and the difference is not significant (t-test;  $p = 0.234$ ).

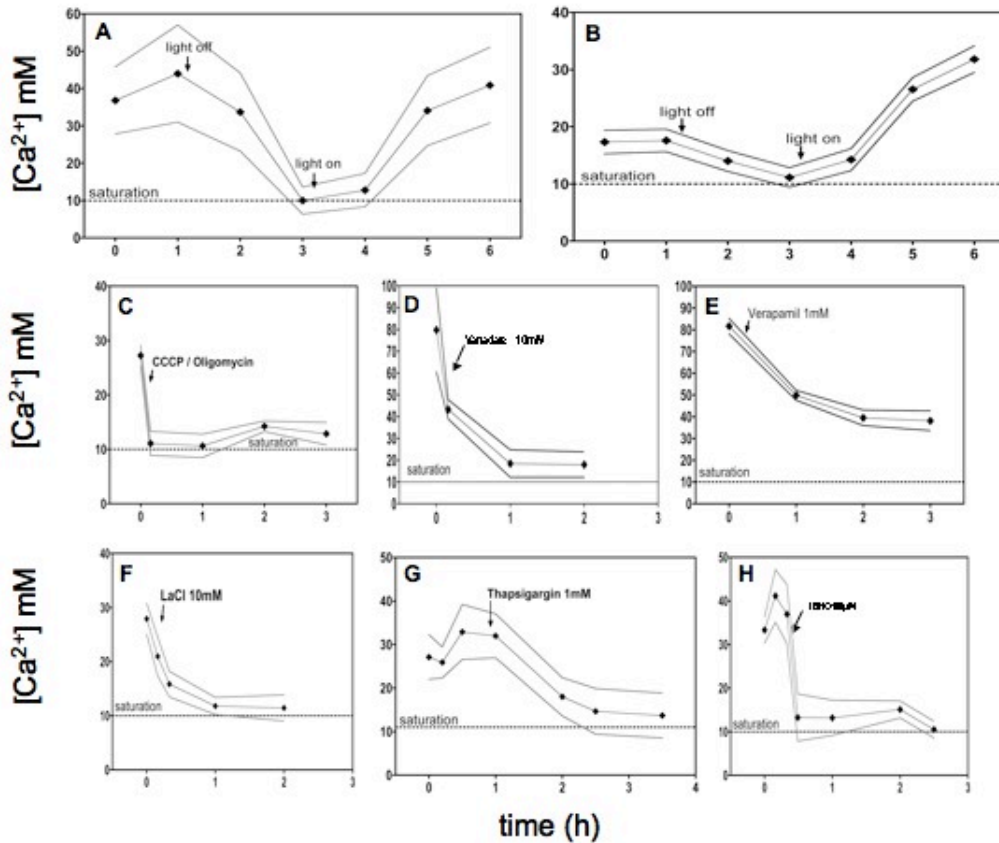




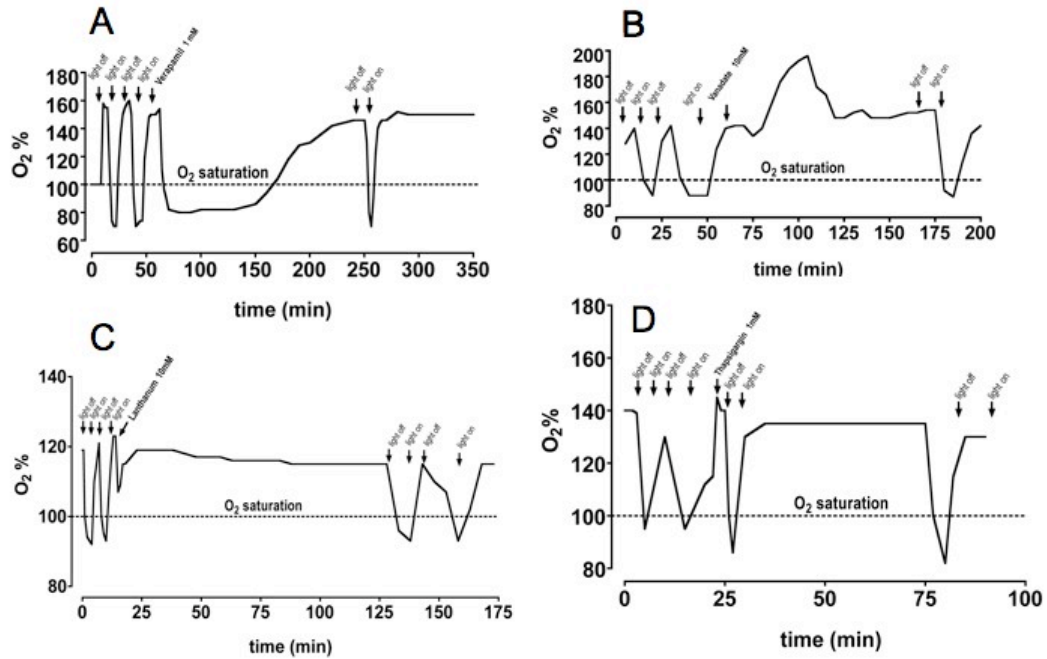
**FIG. 3** Photosynthetic rates of actively boring filaments exhumated from an infested calcite chip. Consecutive fractions (surface, middle and deep) correspond to 50  $\mu\text{m}$  in depth. Photosynthetic rates are not significantly different in any of the fractions (t-test,  $P=0.333$ ). Photosynthetic rates of 2 other cyanobacteria are presented for comparison. Light intensity = 500  $\mu\text{moles}$  of photons



**FIG. 4** (A) Typical *in situ* calcium microprofile of a BC008 infested chip measured in the LSCM. (I) Calcium concentration (in mM) and (II) Chlorophyll *a* values (as relative fluorescent units) are shown as a function of diffusional distance. Calcium supersaturation is observed at the surface of the infested chip where distal ends of the filaments and entrance of boring tunnels are located. Dotted line represents one standard deviation. (B) *In situ* imaging of calcium excretion by boring activity measured with LSCM. Image shows emission fluorescence of a vertical cross-section of an infested calcite chip. Release and accumulation of calcium at the surface of infested chip (green fluorescence,  $\lambda = 541$  nm) is observed at the distal end of boring filaments (red autofluorescence,  $\lambda = 685$  nm).



**FIG. 5** (A) Time courses showing calcium concentrations measured (as reported by CG5N) in the LSCM on one optical plane, at the surface of an infested chip. Dotted lines represent one standard deviation (of the population average) and points represent typical response in one individual filament. (A) Light/dark cycle with initial light intensity of 100  $\mu$ moles of photons (lamp of the microscope) followed by a recovery phase with light intensity of 100  $\mu$ moles of photons. (B) Light/dark cycle with initial light intensity of 30  $\mu$ moles of photons, followed by a recovery phase with light intensity of 100  $\mu$ moles of photons. (C) Effect of cellular energy decouplers CCCP/ oligomycin (1:1 cocktail at 2  $\mu$ M and 60  $\mu$ M respectively) and (D) sodium orthovanadate (10 mM) on boring activity. (E) Effect of calcium channel inhibitor verapamil (1 mM), (F) ATPase and calcium channel inhibitor lanthanum chloride (10 mM) and P-type  $Ca^{2+}$  ATPases inhibitors (G) thapsigargin (1 mM) and (H) TBHQ (100  $\mu$ M) on boring activity.



**FIG. 6** Controls showing the effect of calcium-transport inhibitors (A) sodium orthovanadate, (B) verapamil and (C) lanthanum chloride on photosynthesis of infested chips. Concentrations of the compounds are equal to the ones used in LCSM experiments. Oxygen values are shown as percent oxygen saturation (O<sub>2</sub> %) recorded with an oxygen optode in PES medium, and show initial and after treatment light/dark cycles to test for cell viability.

Table 1. Boring capability of strain BC008 in various substrates. Positive (+) or negative (-) infestation was measured both qualitatively and quantitatively by confirming boring success after 3 months of incubation. After removal of superficial growth, substrates were examined under the microscope for infestation and boring success quantified as Chl a / cm<sup>2</sup>. All mineral samples were confirmed pure by X-ray diffraction.

Substrate	Formula	Boring	Group
Calcite	CaCO <sub>3</sub>	+	CARBONATES
Aragonite	CaCO <sub>3</sub>	+	
Dolomite	CaMgCO <sub>3</sub>	-	
Magnesite	MgCO <sub>3</sub>	-	
Strontianite	SrCO <sub>3</sub>	+	
Marble	CaCO <sub>3</sub>	+	
Siderite	FeCO <sub>3</sub>	-	
Malachite	CuCO <sub>3</sub> .Cu(OH) <sub>2</sub>	-	
Ankerite	CaFe(CO <sub>3</sub> ) <sub>2</sub>	-	
Fluoroapatite	Ca <sub>5</sub> (PO <sub>4</sub> ) <sub>3</sub> F	-	PHOSPHATES
Vivianite	Fe <sub>3</sub> (PO <sub>4</sub> ) <sub>2</sub> .8(H <sub>2</sub> O)	-	
Brazilianite	NaAl <sub>3</sub> (PO <sub>4</sub> ) <sub>2</sub> (OH) <sub>4</sub>	-	
Andradite	Ca <sub>3</sub> Fe <sub>2</sub> (SiO <sub>4</sub> ) <sub>3</sub>	-	SILICATES
Gypsum	Ca <sub>2</sub> SO <sub>4</sub>	-	SULFATES
Barite	BaSO <sub>4</sub>	-	
Colemanite	CaB <sub>3</sub> O <sub>4</sub> (OH) <sub>3</sub> .H <sub>2</sub> O	-	OXIDES
Hematite	Fe <sub>2</sub> O <sub>3</sub>	-	

## CHAPTER 3

### UNIVERSALITY OF THE $\text{Ca}^{2+}$ ATPASE-MEDIATED CARBONATE BORING MECHANISM IN CYANOBACTERIAL EUENDOLITHS

## ABSTRACT

Recent work has shown that the filamentous cyanobacterial euendolith *Mastigocoleus testarum* (strain BC008) bores into carbonates using  $\text{Ca}^{2+}$ -ATPases to power  $\text{Ca}^{2+}$  uptake from the medium at the boring front, promoting dissolution of  $\text{CaCO}_3$  there. It is not known, however, if this is a common mechanism among euendolithic cyanobacteria, or a rather unique capability of this model strain. To test this we undertook a survey of, multispecies euendolithic microbial assemblages from carbonates collected in the Caribbean, Mediterranean, North and South Pacific marine coastal waters. Microscopic examination revealed the presence of a variety of euendolithic morphogenera, encompassing 3 out of the 5 major cyanobacterial taxonomic groups. 16S rRNA gene clone libraries confirmed the diversity of euendoliths and allowed us to categorize them into 8 distinct phylogenetic clades. Using real-time  $\text{Ca}^{2+}$  imaging under the laser-scanning confocal microscope, all samples showed the light-dependent formation of  $\text{Ca}^{2+}$  supersaturated zones in and around boreholes, confirming that they sustained active carbonate boring by phototrophs. In three out of four samples boring activity was sensitive to at least one of two inhibitors of  $\text{Ca}^{2+}$ -ATPase transporters (thapsigargin or tert-butylhydroquinone) indicating that the  $\text{Ca}^{2+}$ -ATPase mechanism of *Mastigocoleus* is widespread among cyanobacterial euendoliths, but perhaps not universal. Function/community structure correlations point to one particular clade of baeocyte-forming euendoliths as the potential exception.

## INTRODUCTION

Euendolithic cyanobacteria, also known as boring, microboring, excavating, perforating or tunneling cyanobacteria, can penetrate into a variety of calcareous substrates, such as shells, dead coral and limestone, by means of chemical dissolution. They can be found in diverse geographical locations worldwide (Al-Thukair and Golubic, 1991, Chacón, et al., 2006, Fremy, 1936, Golubic, 1975, Le Campion-Alsumard, et al., 1995, Raghukumar, et al., 1991, Vogel, et al., 2000) and are involved in the diagenesis or in some cases the lithification of the calcareous substrates that they colonize. In most instances, they weaken the structure of a solid substrate with their tunneling (Che, et al., 1996, Kaehler, 1999, Webb and Korrubel, 1994). In other cases, the re-precipitation of micrite, by-product of dissolution, forms the cement that binds carbonate sand grains in stromatolitic laminae (Reid, et al., 2000). A variety of euendoliths has been described (Golubic, 1969, Le Campion-Alsumard, et al., 1995, Zhang, 1987), during almost 2 centuries of naturalistic studies (Bornet, 1888, Lagerheim, 1886, Thuret, 1875).

The mechanism that allows cyanobacterial endoliths to bore, a subject of long-standing controversy, has been recently elucidated in the model filamentous strain, *Mastigocoleus testarum* BC008 (Chapter 2, this dissertation). It is based on the uptake and transcellular transport of  $\text{Ca}^{2+}$  mediated by P-type  $\text{Ca}^{2+}$ -ATPases. As it is understood, these enzymes help import free  $\text{Ca}^{2+}$  from the medium at the interstitial space between boring cell and mineral (“boring front”) reducing the concentration of the ion in the



interstitial space below that of saturation, and promotes the localized dissolution of the substrate at the boring front. Intracellular calcium is transported cell-to-cell along the filament, likely with the aid of other  $\text{Ca}^{2+}$  specific pumps or channels, and excreted at the farthest end from the boring front, maintaining internal calcium homeostasis (Chapter 2, this dissertation). This results in a strong supersaturation of  $\text{Ca}^{2+}$  around the boreholes. This mechanism shown in *M. testarum* BC008 differs from the previously tacitly accepted hypothesis of boring powered by acid deposition.

The Phylum Cyanobacteria are a diverse group of organisms, but only a small proportion of species are capable of boring (see Introduction, this dissertation). However, this selected group has representatives in several of the major taxonomic “orders” composing the Phylum. Because of this phylogenetic diversity, in it is only natural to question if the strategy of BC008 is universal among all. A mechanism that is common to all cyanobacterial microborers does not seem implausible. Still, for those species that bore, the information available has been mostly descriptive, with no physiological or molecular knowledge on the boring mechanism.

In fact explicit phylogenetic work on euendoliths is extremely restricted and practically non-existent (Chacón et al, 2006; Foster, et al., 2009, Ramírez-Reinat et al., unpublished), and thus the evolutionary history of this capacity remains largely unexplored.

The overarching goal of this work is to address the potential universality of the boring mechanism among cyanobacterial euendoliths. The boring mechanism was investigated empirically in complex microbial

assemblages, collected from distinct geographical locations worldwide, so as to encompass as diverse as possible a range of subjects, and compared to the one described in *M. testarum* BC008.

## MATERIALS AND METHODS

**Field samples.** Euendolith-infested carbonates (clam shells and dead coral skeleton pieces) were collected from four coastal regions: the Caribbean (San Juan, Puerto Rico, 18°45' N, 65°96' W), North Pacific (Baja California, 30° 92' N, 114°70' W), Mediterranean (L'Alguer, Italy, 40°33' N, 8°19' E) and South Pacific (Whakatane, New Zealand, 37°31' S, 177°11' E). Infested samples were selected guided by their for typical green to gray coloration. They were air-dried and transported to the laboratory where they were rehydrated in a mixture of Provasoli's Enriched Seawater (PES) medium (Provasoli, 1968) (pH=8.3) and filtered seawater in a 1:1 (v/v) ratio. Samples were kept at 25° C under constant light, provided by white fluorescent lamps, at a light intensity of 30  $\mu$ moles of photons, before analysis.

**Laser scanning confocal microscopy.** Small fragments, ranging from 2 to 6 mm<sup>2</sup> in size, broken off from large pieces of infested carbonate using sterile pliers and/or a sterilized hammer. Fragments were scrubbed briskly with a small paintbrush to remove any superficial biomass or biofilms, rinsed twice in sterile PES medium and prepared for confocal microscopy analysis as described in Chapter 2 of this dissertation. Briefly, fragments were incubated for 1 hour in PES medium with 1  $\mu$ M of Calcium Green-5N ([CG5N] Molecular Probes, Eugene, OR, USA) at room temperature under white

incandescent light at 30  $\mu$ moles of photons. After incubation, the fragments were fixed to custom-made slides with “superglue” (cyanoacrylate). Slides were then filled with PES containing CG5N at a final concentration of 1  $\mu$ M. A glass coverslip was placed on top of the ring, creating a chamber. The slides were then placed on the stage of a Leica TCS-SP2 Laser Scanning Confocal Microscope and observed under an oil immersion 40x objective. An epifluorescent mercury lamp, with visible light the 488nm and 546 nm regions, was used to evaluate the fragments for infestation and viability (presence of photosynthetic pigments in cells) prior to laser scanning. Visible laser lines of Ar/Kr (488nm) and Kr (546nm) were used to excite the fragments. CG5N and chlorophyll fluorescence were recorded on a single optical section focused on the surface of the carbonate, at the entrance of the boreholes (Fig. 1). Images were analyzed with the Leica Confocal Software (Leica Microsystems Inc., Bannockburn, IL, USA). Fragments were analyzed within a week of collection, to minimize potential changes in community composition.

**Testing for boring activity and its light-dependency.** To test for active boring we imaged  $[Ca^{2+}]$  *in situ* at the surface of infested fragments on a single optical section. This area at the entrance of boreholes has strongest  $[Ca^{2+}]$  supersaturation ( $>>10$  mM) in pure culture experiments using BC008. Fragments were illuminated with the stage illumination (white light, 50  $\mu$ moles of photons) for 1 hour before initial imaging. To demonstrate light dependency, a characteristic of boring by phototrophs, illumination was

turned off for at least one hour, and imaged again. To assess recovery, light was turned on once more and fragments incubated for ~1 hour before repeating measurements.

**Effects of calcium-transport inhibitors on boring.** To address the involvement of P-type  $\text{Ca}^{2+}$  ATPase enzymes in the boring mechanism of field euendoliths, the inhibitors thapsigargin (TG [Alexis Biochemicals, Lausen, Switzerland]) and tert-butyl hydroquinone (TBHQ [Spectrum Chemicals, Gardena, CA, USA]) were used at a final concentration of 1 mM. Carbonate fragments were incubated under constant light for 1 hour and single optical plane measurements at the surface of the carbonate were recorded, before addition of the inhibitors.  $[\text{Ca}^{2+}]$  dynamics were monitored thereafter for at least 1 hour.

**Exhumation of euendoliths and microscopic observations.** Euendoliths were exhumated from the carbonate samples used in the boring experiments using an EDTA dissolution method described in detail in Chapter 4 of this dissertation. Briefly, carbonate fragments were washed in sterile PES, and placed on a mesh basket on top of the column of a filtration apparatus. There, an iced-cooled, sterile solution of 100 mM ethylenediamine-tetraacetic acid (EDTA) adjusted to pH 5 was allowed to drip over the sample, slowly dissolving the carbonate matrix, driven by a peristaltic pump at a rate of  $0.5 \text{ mL min}^{-1}$ . Cells then exposed were removed by gently brushing the surface, allowed to flow with the dripping EDTA solution and

collected on a (2  $\mu$ M pore size) polycarbonate filter at the bottom of the column. Filters were washed with sterile distilled water (~5 mL) while still in the column, collected and placed in 5 mL of sterile PES medium. After gentle centrifugation (4,000 RPM, 10 min.) filters were removed and cells re-suspended in sterile PES medium. Wet mounts were prepared in glass slides for the observation of exhumated euendoliths, which was done under brightfield optics in a compound microscope. Cell diameter measurements were performed with a calibrated ocular micrometer.

**DNA extraction.** Nucleic acids were extracted from the exhumated biomass of the same samples used in physiological experiments and microscopy, using the UltraClean Soil DNA kit (MoBio Laboratories, Inc., Solana Beach, Calif.) according to the manufacturer's recommendations. After extraction, genomic DNA quantity and size was determined by electrophoresis on 1% agarose gels, and stained with ethidium bromide. Approximately 10 ng of DNA extract was used as template to generate small subunit ribosomal RNA gene (16S rRNA) amplicons by Polymerase Chain Reaction (PCR) amplification. 16S rRNA fragments (ca. 700 bp-long) were amplified, using the primer set CYA106F /CYA781R, specific for Cyanobacteria (Nübel, et al., 1997). The thermal cycle consisted of an initial denaturation at 94°C for 5 min, 35 cycles of 94°C for 1 min, 60°C for 1 min, and 72°C for 1 min, and a final extension at 72°C for 5 min. Quantification of PCR products was performed as explained previously for genomic DNA.

**Clone libraries.** To gage the diversity of euendoliths, nine clone libraries of the 16S rRNA gene PCR products were constructed separately for each fragment (stemming from individual geographical regions) used in the inhibitor experiments. These were generated by ligating 16S amplicons into TOPO 2.1 cloning vector and transforming chemically competent *E. coli* cells, following manufacturer's instructions (Invitrogen, CA, USA). 10 individual colonies were selected from each sample amplicate and grown in 3 ml of Luria Broth medium with kanamycin (50 µg/ml) overnight at 37°C in a shaking waterbath. A Qiagen Plasmid Prep kit was used to isolate the plasmids according to the manufacturers instructions (Qiagen Inc, CA, USA). EcoRI was used to check for the correct insert size. Double-stranded plasmid DNA was sequenced in an Applied Biosystems 3730 sequencer (Arizona State University).

**Phylogenetic reconstructions.** A total of 11 clones were obtained from Italy, 16 from Mexico, 10 from New Zealand and 8 from Puerto Rico. Sequences were aligned with MEGA 4.0 (Tamura, et al., 2007) and checked for non-coding bases, which accounted for 1% or less of the total sequence length and all non-coding ends were discarded. These new sequences were aligned alongside other cyanobacterial 16S rRNA partial sequences retrieved from NCBI (National Center for Biotechnology Information) database using the Basic Local Alignment Search Tool (BLAST). The phylogenetically closest cyanobacterial sequences according to BLAST were used to establish the initial alignment, and sequences representative of cyanobacteria (and plant

plastids) of all taxonomic groups were used thereafter to populate the alignment; a beta-proteobacterium sequence was used to root the phylogenetic tree. In all 93 taxa were used to construct a phylogenetic tree, which contains all clones from all sites. All positions containing gaps and missing data were eliminated. For this, 2 algorithms were used, the Neighbor-Joining (NJ) and the Maximum Parsimony (MP), both with 1,000 bootstrap replicates. Bootstrap values, or the percentage of replicate trees where a group of sequences clustered together, are shown next to the respective nodes. Letters were assigned to well-resolved clusters of clone sequences in the phylogenetic tree (Fig. 4) to aid in their identification, which were as well color-coded according to geographical region.

## RESULTS

**Morphology of exhumated euendoliths.** Morphogenera were identified diacritically and compared to traditional morphotaxa (Castenholz, 2001, Geitler, 1932). Fig. 1 illustrates non-exhaustively the diversity of morphogenera found in our samples. In the Italy samples (IT) (Fig. 1, upper left panel) we found pseudofilamentous, non-heterocystous forms, resembling *Hyella* or *Solentia* types, that range from 10 to 15  $\mu\text{m}$  in diameter and display a range of bluish to greenish colors. We also found abundant thin, filamentous, non-heterocystous, *Plectonema*-like forms of about 2-3  $\mu\text{m}$  in diameter. In the New Zealand fragments (NZ) (Fig. 1, upper right panel) we find an unidentified, thin, true branching, non-heterocystous form of about 2-3  $\mu\text{m}$  in diameter. In this fragment we also find commonly non-heterocystous, baeocyte forming *Pleurocapsa* or *Mysoxarcina*-like forms with variable

diameter (5-15  $\mu\text{m}$ ). In the Mexico (MX) samples (Fig. 1, lower left panel) non-heterocystous *Hyella*-like pseudofilaments, ranging from 10-15  $\mu\text{m}$  in diameter, and green-gray in color, were common accompanied by, 2-3  $\mu\text{m}$  thick, filamentous, non heterocystous *Plectonema*-like types, with somewhat elongated cells. Other thin, filamentous, non-heterocystous forms, with shorter cells, 2-3  $\mu\text{m}$  in diameter and blue green in color were seen there as well. Lastly, in the Puerto Rico fragments (PR) (Fig. 1, lower right panel), filamentous, true branching, heterocystous forms are observed, that range 5-10  $\mu\text{m}$  in diameter, with the typical morphology of *Mastigocoleus*. Other unidentified, filamentous, non-heterocystous forms, with apparent baeocyte formation, ranging from 4-10  $\mu\text{m}$  in diameter, were observed there as well.

**Boring activity and its light-dependence.** Incubations in the light were performed on all fragments to assess if calcium supersaturation, a proxy of boring activity by phototrophic euendoliths, was present at the surface of the substrate. Fig. 2 (left column) depicts the level of  $\text{Ca}^{2+}$  supersaturation and its dynamic response to sequential darkening and illumination. All samples exhibited significant supersaturation, with average  $[\text{Ca}^{2+}]$  ranging from 20 to 60 mM in the light. In all cases,  $[\text{Ca}^{2+}]$  decreased to calcite-saturation levels equal to those of the medium (for PES this is around 10 mM). After illumination, again in all cases, there was clear recovery of supersaturation. Thus all samples tested contained significant boring activity, most of which can be attributed to phototrophic organisms that require light to power calcium transport.



**Effect of Ca-ATPase inhibitors on boring activity.** Fig. 2 (center column) illustrates the effect to the Ca<sup>2+</sup>-ATPase inhibitor thapsigargin (TG) in calcium release due to boring activity. Average Ca<sup>2+</sup> supersaturation levels in all fragments before inhibition ranged from 40 to 70 mM. TG was effective in inhibiting boring activity only in the NZ and PR fragments, with final levels of free Ca<sup>2+</sup> reaching saturation levels (~10 mM) after the treatment. The IT and MX fragments were apparently not significantly affected. Fig. 2 (right column) illustrates the effects of the specific Ca<sup>2+</sup>-ATPase inhibitor, tert-butyl hydroquinone (TBHQ). Average Ca<sup>2+</sup> supersaturation levels in all fragments ranged from 32 to 75 mM initially. Treatment with TBHQ resulted in effective inhibiting of calcium release in the IT, NZ and PR samples. This effect was dose dependent, with IT responding to 5 mM TBHQ, but not to a previous 1 mM treatment (data not shown). The MX fragment did not respond to TBHQ (up to 10 mM). Thus all but the MX sample were sensitive to at least one of the two P-type ATPase inhibitors tested.

**Clone libraries and phylogenetic reconstruction.** The evolutionary history of clone sequences was inferred using the Neighbor-Joining (NJ) and Maximum Parsimony (MP) algorithms with 1,000 bootstrap replicates. Both algorithms generated trees with similar topologies; only the NJ tree is shown for the sake of simplicity. Fig. 4 illustrates the phylogenetic analysis of 93 16S rRNA partial sequences including 45 clones, 42 cyanobacteria, 3 plasmid sequences, and 1 member of the beta-proteobacteria (*Chromobacterium*

*violaceum* JCM 1249). Clone libraries stemming from individual fragments were numbered according to inhibitor treatment (No. 2, 3, 5 & 10 = TG; 1, 4, 6 = TBHQ; No. 9 (NZ) = TG & TBHQ). Regardless of treatment, no significant difference in diversity was observed between fragments from the same geographic locations. A total of 11 sequences stem from Italy (“Italy”), 16 sequences from Mexico (“Baja”), 10 sequences from New Zealand (“NZ”) and 8 sequences from Puerto Rico (“PR”). Eight clades (A, B, B<sub>1</sub>, C, D, E, F, and G) were assigned to clone sequences that cluster together. Clade A includes heterocystous cyanobacteria in the taxonomic groups IV (Order Nostocales) and V (Order Stigonematales); *Mastigocoleus* BC008 sequence is found within this clade. Clade B includes baeocyte-forming genera (*Mysoxarcina* / *Pleurocapsa* / *Staniera*) in Group II (Order Pleurocapsales). Clade B<sub>1</sub> contains sequences that fall within clade B, but are not well resolved and do not have any close neighboring sequence to compare to. Clade C contains Group II sequences and includes *Chroococccidiopsis* and *Solentia* HBC10, a boring cyanobacterium. Clade D includes a cluster that falls within Group II but does not have a close neighboring sequence to compare to. Clades E and F contain sequences exclusive to New Zealand, which fall within Group III (Order Oscillatoriales). Clade E contains *Leptolyngbya*-types, with its closest neighbor being *Leptolyngbya* ITAC101; clade F does not have a close neighboring sequence to compare to. Clade G includes *Leptolyngbya*-type sequences (Group III), with the closest neighbor being *Leptolyngbya* HBC1. Apart from the assigned clades, there are three clone sequences, all within the *Leptolyngbya* that stand alone: PR 10e, Baja 5h and Baja 6a. From these,

only Baja 5h has a close neighboring sequence pair (*Leptolyngya* PCC 7373 / *Phormidium* SAG 80.79).

## DISCUSSION

**Microborer diversity.** Microscopic observations of exhumated euendoliths revealed a broad diversity of morphogenera in our sample collection, encompassing 3 out of the 5 major cyanobacterial taxonomic groups (Group II, Order Pleurocapsales; Group III, Order Oscillatoriales; Group V, Stigonematales). Most common were pseudofilamentous, non-heterocystous, baeocyte-forming cyanobacteria (Group II), which could be seen found in all four of the geographical regions surveyed. This result is not surprising as it is from this Group II of the cyanobacteria that many morphogenera with microboring species, such as *Cyanosaccus* (Lukas and Golubic, 1981), *Hyella* (Al-Thukair and Golubic, 1991, Le Campion-Alsumard, 1991), *Hormathonema* (Ercegović, 1927, Golubic, 1969) and *Solentia* (Foster, et al., 2009, Stolz, et al., 2001) have been described (Castenholz et al., 1989).. The importance of this group is particularly evident in the Sard fragments, where all the forms we find can be assigned, at least morphologically, to this group. In the fragments from New Zealand and Mexico, forms assignable to Groups II and III were found. In Mexico, we find *Hyella* / *Solentia*-like cyanobacteria among others that closely resemble members of the genus *Plectonema*. In New Zealand we find *Pleurocapsa* / *Mysoxarcina*-like forms among *Plectonema*-like types.

*Plectonema* is another genus that contains boring species (e.g. *Plectonema terebrans*) (Le Campion-Alsumard, et al., 1995, Raghukumar, et

al., 1991). In the fragments from Puerto Rico, exhumated filaments displayed a variety of morphologies, with many filamentous, non-heterocystous types with apparent baeocyte formation seen (likely Group II), but we were unable to assign them accurately to a particular genus. Among the latter, we found filamentous, true branching forms that displayed lateral heterocysts (Group V, Stigonematales) resembling closely the morphological characters of *Mastigocoleus*, another genus with a single, microboring species (Montoya-Terreros, 2006, Webb and Korrubel, 1994).

This broad morphological diversity is partly consistent with the variety of clades detected according to total genomic DNA-based 16S rRNA clone libraries. Four out of eight clades (B, B<sub>1</sub>, C & D) were assigned to clusters of sequences that fall within baeocyte-forming (Group II) types, stemming from all four geographic regions. The relative abundance of sequences within this group, compared to other all phlotypes, indicates that the majority of euendoliths found are pseudofilamentous, non-heterocystous, baeocyte-forming types, which correlates with previous microscopic observations of *Hyella* and *Solentia*-like forms. Clade A includes one sequence found only in Puerto Rico and the sequence of the model boring organism *Mastigocoleus testarum* BC008, which was originally isolated from carbonates in this geographic region (Chacón et al., 2006). This finding its not surprising as it correlates with microscopic observations in which *Mastigocoleus*-types were seen. The only disagreement is in the relative diversity and abundance of *Leptolyngbya*-like, thin-filamentous cyanobacteria. Traditional studies only report a single species of microborer

among this group: *Plectonema terebrans*. Yet we found at least 3 distinct clades in our survey (E, F and G), and a few other singletons, which likely represent several different generic entities. Obviously traditional surveys have severely underestimated the diversity of thin-filamentous microborers. The phylogenetic diversity of boring *Leptolyngbya*-like members, as depicted by the phylogenetic reconstructions was unprecedented, and reinforces the need for more phylogenetic work done in euendolithic cyanobacteria. In many cases, finding a thin, filamentous, boring cyanobacterium automatically tags it as a member of the genus *Plectonema*. Our phylogenetic data suggest that many other species within Group III are capable of boring, with this diversity remaining largely unexplored.

Clone sequences from Mexico and Puerto Rico that stand by themselves in the tree, might correlate with the unidentified morphotypes that were seen under the microscope in both regions. A renewed and sustained effort to find cultivated isolates for some of these clades and unidentified forms will be necessary to fully describe the diversity of euendoliths in a comprehensive and useful manner.

**Universality of the boring mechanism.** Having established that all samples were active with respect to boring activity and that phototrophs accounted for most of the boring activity in these substrates, the molecular surveys discussed above insured that the diversity of microborers was large in all samples, and covered many if not all of the groups of cyanobacterial microborers known from the literature. Thus, the fact that in most instances

at least one of the P-type  $\text{Ca}^{2+}$  ATPase inhibitors could abolish boring activity in our samples, indicated that these enzymes are central to the process of boring in most cyanobacterial euendoliths, as they are in strain BC008. In this sense the mechanism seems to be quite widespread. Not unexpectedly, however, the degree of sensitivity differed among samples. We know from laboratory experiments, that inhibitors such as thapsigargin work in some organisms, and not in others (Pickles and Cuthbert, 1992, Scamps, et al., 2004). This is actually why our experimental design called for using 2 independent inhibitors. In our interpretation, sensitivity to at least one of the two denote the involvement of the target enzyme. Only in one case MX, none of the fragments responded to either TG or TBHQ, even in large concentrations. This lack of response prevents us from calling the mechanism universal. It may speak for the presence of a different boring mechanism in the euendoliths of this sample. If so, then we would need to postulate that a group of cyanobacteria that is highly represented in the MX clone libraries, but not in others, is probably responsible. Clade B<sub>1</sub> seems to be the only group fitting this criterion. Unfortunately no cultivated representatives are available to test this hypothesis.

Even cyanobacteria would rely on a single mechanisms, it is unknown if the ability to bore came from a common ancestor, or is a case of convergent evolution due to lateral transfer of “boring” genes. The evolution of boring as a survival strategy and its persistence in modern times, can be attributed to selective pressure, including the need for acquisition of nutrients, finding a niche with limited competition, escaping from adverse conditions on the

surface of rocks or the prevention of mineralization (Cockell and Herrera, 2008). More work that looks at presence, expression and regulation of genes involved in boring would shed light into the molecular basis of the phenomenon. The boring mechanism, elucidated conclusively in a variety of cultivated euendoliths, would provide the final answer.

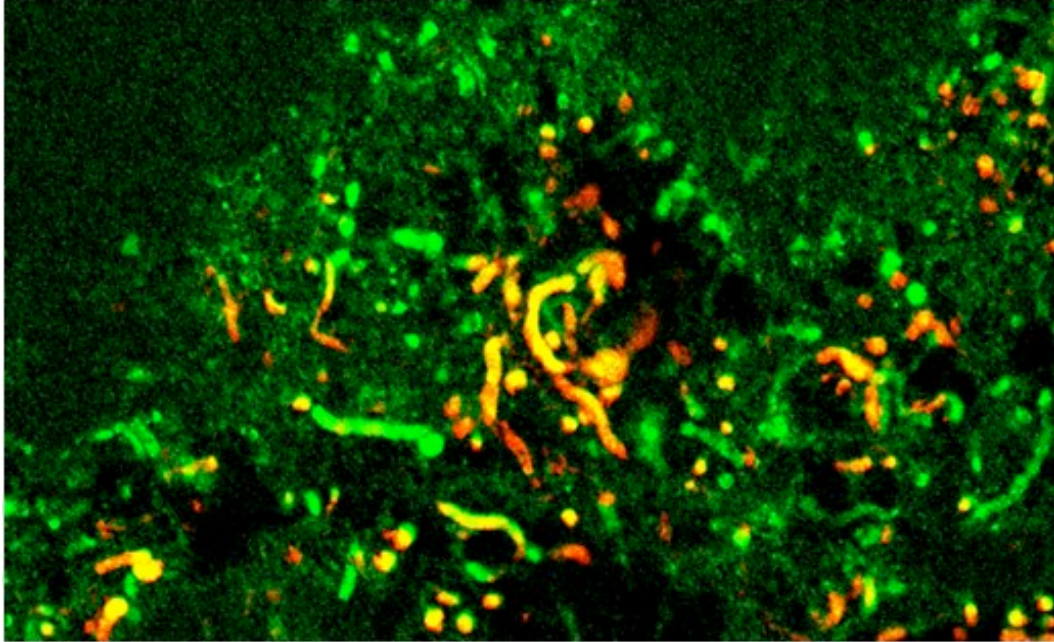
### **CONCLUSIONS**

An empirical analysis of the boring mechanism in geographically-distinct, complex euendolithic microbial assemblages demonstrate a similar physiological response to core experiments performed in *M. testarum* BC008, suggesting that the boring mechanism, as its understood in the latter, might be widespread, but perhaps not universal. Molecular work involving genes that regulate boring are in the horizon of future research.

### **ACKNOWLEDGEMENTS**

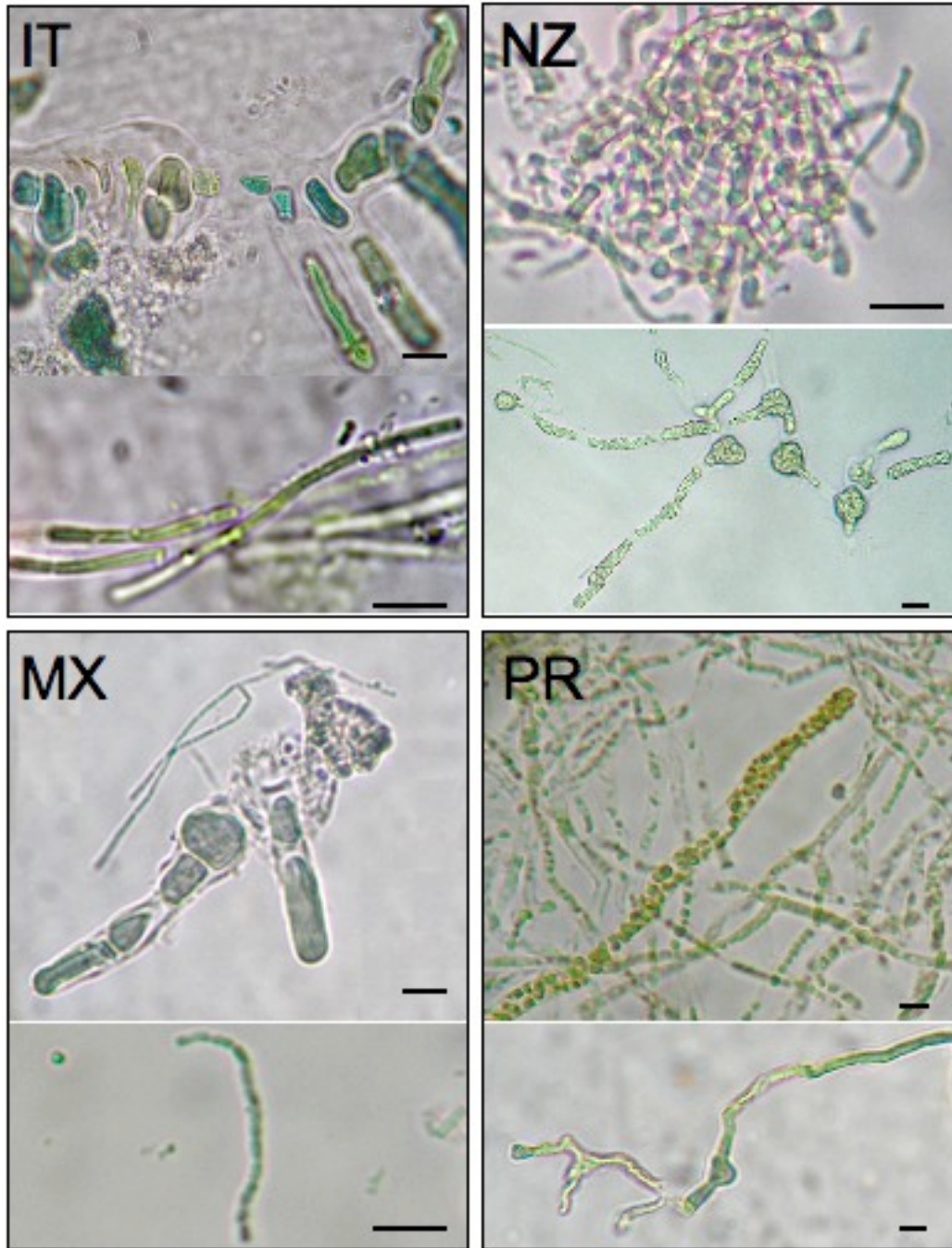
We would like to thank Dr. Dörte Hoffmann for assistance in the construction of clone libraries, as well as Ankita Kothari and Carmen M. Reinat for assistance with sample collection.

This work was supported by a National Science Foundation grant 0311945

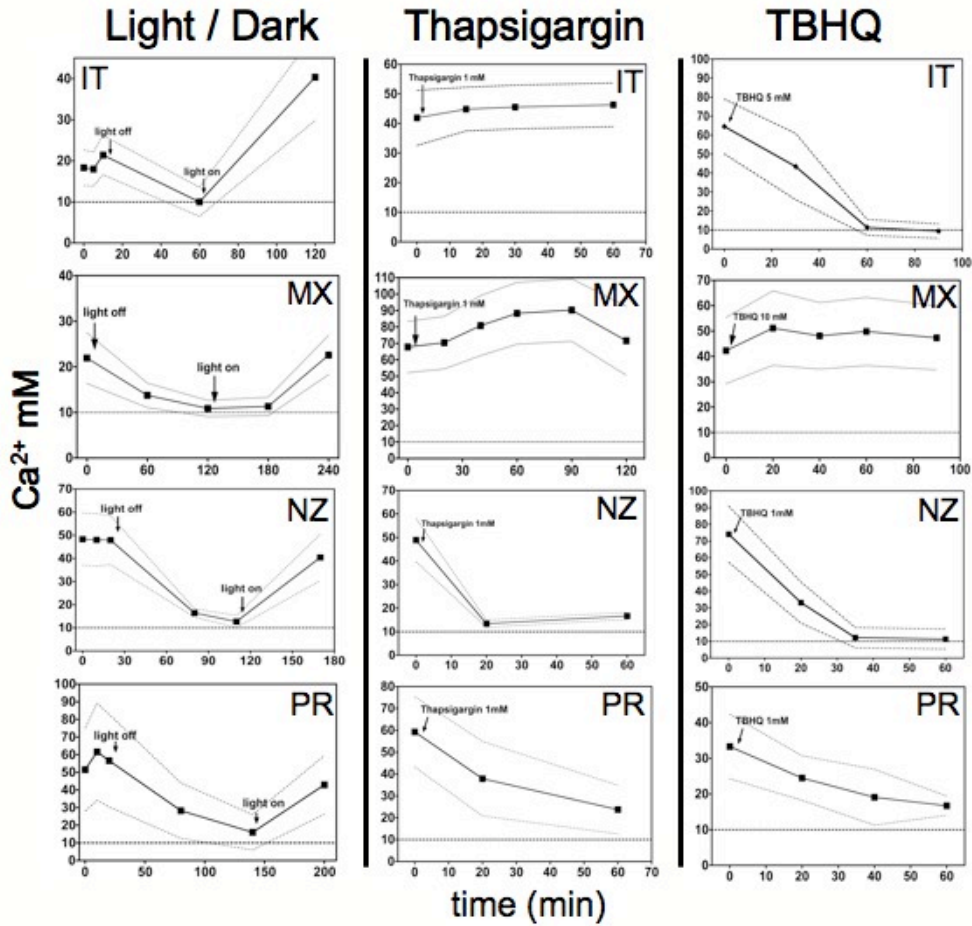


**FIG.1** Diversity of euendoliths in a shell fragment from New Zealand as imaged by *in situ* laser scanning confocal microscopy. Green fluorescence indicates free Ca<sup>2+</sup> as reported by the extracellular, calcium-sensitive fluorophore calcium green-5N (CG5N). Yellow and orange fluorescence indicates co-localization of CG5N and autofluorescent pigments; chlorophyll a and phycobilins fluoresce in red.

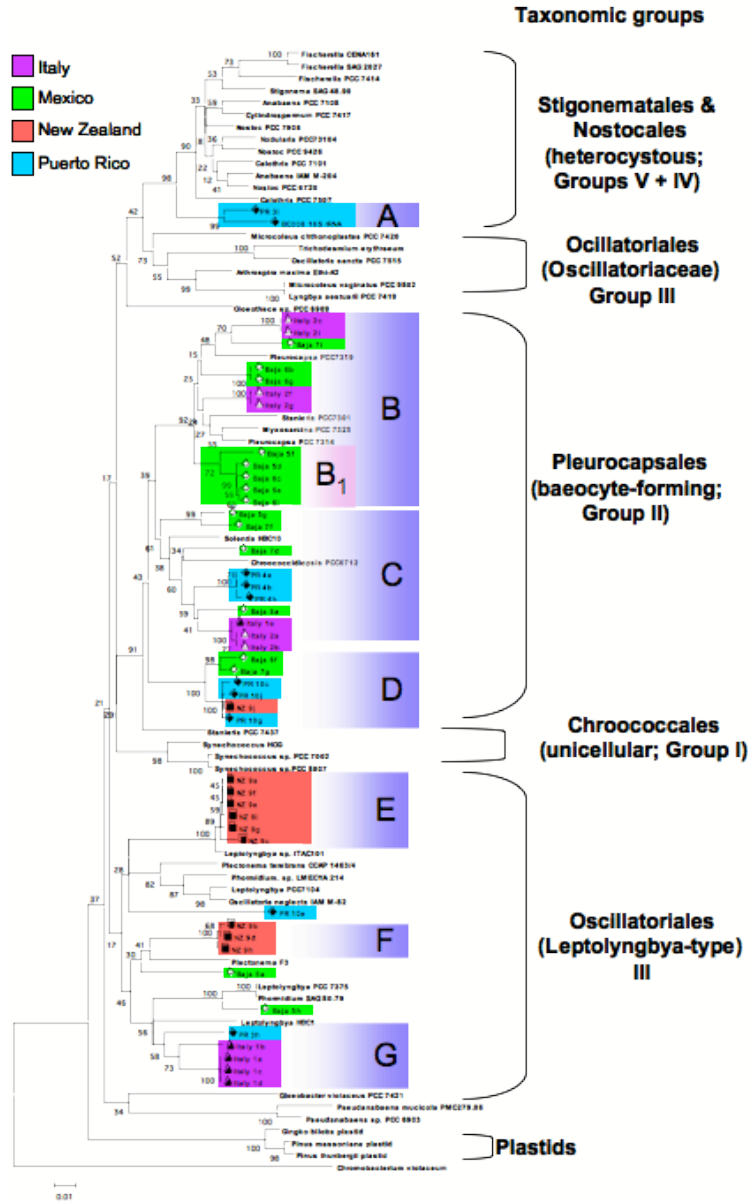




**FIG. 2** Morphological diversity of exhumated euendoliths. Upper, left panel, (IT); *Hyella*-like and *Plectonema*-like filamentous forms. Upper right panel, NZ; *Plectonema*-like and *Pleurocapsa*/*Mysoxarcina* filamentous forms. Lower left panel, MX; *Hyella*-like and *Plectonema*-like forms. Lower right panel, PR; Unknown morphotypes, apparent baeocyte-forming filamentous forms and *Mastigocoleus*-like filamentous forms. IT=Italy, MX=Mexico, NZ=New Zealand, PR=Puerto Rico. Bar, 10  $\mu$ m.



**FIG. 3** Time courses showing calcium concentration as reported by CG5N in one optical section, at the surface of infested carbonate fragments. Dotted lines represent one standard deviation of the population average. Leftmost column: light/dark cycle, with recovery. Center column: effect of P-type  $\text{Ca}^{2+}$  ATPases inhibitor thapsigargin (1 mM). Rightmost column: effect of P-type  $\text{Ca}^{2+}$  ATPases inhibitor TBHQ (1-10 mM). IT=Italy, MX=Mexico, NZ=New Zealand, PR=Puerto Rico.



**FIG. 4** Neighbor-Joining phylogenetic tree based on 88 16S rRNA sequences (final alignment = 661 bp). The sequence of *Chromobacterium violaceum* (ATCC12472) was used as the outgroup. Brackets illustrate phylotypes assigned to clustering sequences; roman numerals illustrate cyanobacterial groups. Denomination of particular strains corresponds to those in the database, and are not necessarily taxonomically correct. Bootstrap values of 1,000 trees are included and indicated at the nodes. Scale bar represent 1% estimated sequence divergence. IT=Italy, MX=Mexico, NZ=New Zealand, PR=Puerto Rico.

CHAPTER 4

A METHOD FOR THE EXHUMATION OF LIVE ENDOLITHS FROM  
CALCAREOUS SUBSTRATES

## ABSTRACT

Endoliths are microbes that live within a solid substrate, either in cavities, cracks or pores (e.g. chasmoliths, cryptoendoliths), by excavating tunnels (e.g. euendoliths) or after becoming entrapped in minerals that precipitate around them, as may happen in modern microbialites. These organisms cannot be sampled without destructive techniques. In calcareous or calcophosphatic substrates endoliths are commonly exhumated by acid-driven dissolution of the surrounding matrix, a process that can render morphologically sound but non-viable specimens, and their nucleic acids are hydrolyzed in the process. An alternative method based on substrate dissolution by the chelating agent ethylene-diamine-tetracetic acid (EDTA), preserves the morphological and genetic integrity of euendoliths, so that downstream genetic fingerprinting is possible (Wade and Garcia-Pichel, 2003). Here we optimized this approach to preserve not only the structural and genetic integrity, but also viability of exhumated specimens. This method allowed the exhumation of live microboring cyanobacteria (*Mastigocoleus testarum* BC008), which could demonstrably be analyzed downstream for gene expression and physiological activity, and the establishment of cultures.

## INTRODUCTION

Endolithic microorganisms, which may include fungi, lichens, algae, and cyanobacteria, live within a solid substrate, either by colonizing already available cracks and fissures (chasmoliths), pores (cryptoendoliths) or by making new cavities or tunnels (euendoliths) (Golubic, *et al.*, 1981). Calcareous and calcophosphatic substrates, such as shells (Nielsen, 1987),

coral skeleton (Le Campion-Alsumard, et al., 1995), bone (Ascenzi and Silvestrini, 1984) and limestones and dolostones (Danin, et al., 1983), are frequently inhabited by endoliths. In some cases microorganisms become endolithic as a result of entrapment by precipitating carbonate in alkaline environments. Examples of this occurrence include the case of modern microbialites (Defarge and Trichet, 1990, Dupraz and Strasser, 1999) or tufas (Merz-Preiss and Riding, 1999, Pentecost, 1985) where lithification happens as a consequence of sediment trapping and carbonate precipitation, a product of alkalization of the water by phototrophic consumption of CO<sub>2</sub> (Baumgartner, et al., 2009, Dupraz and Visscher, 2005, Garcia-Pichel et al., 2004, Laurenti and Montaggioni, 1995, Stolz, et al., 2001, Wierzchos, et al., 2006). Due to their intrinsic physical isolation, endoliths do not lend themselves readily to collection. Therefore, they must be exhumated from the substrate; a harsh process that involves either mechanical or chemical removal of the solid, and in many cases proves detrimental to the cells within. Generally, geomicrobiological studies of endolithic microbes, such as those inhabiting modern microbialites, are thus limited to microscopic, mineralogical, and biogeochemical analyses (Laval, *et al.*, 2000). In cases where the matrix that surrounds the endoliths is a carbonate (aragonite, calcite or dolomite...), dilute acetic acid or hydrochloric acid is used for dissolution (Golubic, 1969, Lagerheim, 1886). Liberating these organisms by acidification is useful as it generally renders specimens that retain their morphological characteristics, if their pigmentation may be altered, but hinders further molecular or physiological work due to hydrolysis of nucleic

acids.

A method published by Wade and Garcia-Pichel (2003) explored the exhumation of endoliths from modern microbialites by ethylene-diamine-tetra-acetic acid (EDTA) dissolution of the surrounding matrix. It proved useful in the isolation of cyanobacterial filaments of oncolites and microbialites, while preserving morphology and the integrity of their genetic material, at least for DNA (Wade and Garcia-Pichel, 2003). Even though it preserves the structural integrity of the cells and genetic material, the viability of the organisms was not implicitly studied. EDTA however has been known to damage the outer membrane of gram-negative bacteria (e.g. Alakomi, et al., 2003).

We optimized the EDTA dissolution method with respect to EDTA concentration and delivery, T and pressure, and tested it using *Mastigocoleus testarum* (strain BC008) boring on crystalline calcite for integrity of the transcriptional machinery, physiological activity, and viability. The detailed process is presented below, and demonstrated practically on video format (see attached movie).

## MATERIALS AND METHODS

### **Exhumation setup:**

1. A vacuum filtration apparatus (“VWR 25 mm Filter Holder”, VWR International, IL, USA) consisting of a 25 mm borosilicate glass filter holder with fritted glass support base, a 15mL graduated funnel, anodized aluminum clamp, and a No. 5 silicone stopper (or equivalent)

2. A small, 2.5 x 2.5 cm piece of stainless steel screen or equivalent as sample-holding basket
3. 25 mm diam. (2  $\mu$ m pore-size) polycarbonate filters
4. 25 mm diam. GF/F glass-fiber filters
5. A small, watercolor brush with plastic bristles (or equivalent)
6. Tweezers or forceps
7. Steel clamps, holders, jacks, or other supporting equipment
8. A bucket with ice
9. Sterile centrifuge tubes (15 mL or equivalent)
10. Sterile media of appropriate composition
11. A variable flow peristaltic pump
12. A centrifuge with a rotor capable of holding the sterile tubes
13. A 100mM solution of disodium ethylene-diamine -tetracetic acid ( $\text{Na}_2$ -EDTA), prepared with deionized water and adjusted to pH 5 with HCl. This solution is autoclaved and maintained at room temperature until use, to prevent precipitation.

## PROTOCOL

All components, including tubing, glassware, filters or any other material in contact with the samples are to be sterilized either by autoclaving (i.e. glass components, metal components and filters) or by dipping in 70% ethanol overnight (i.e. silicon tubing) as appropriate. Ethanol-sterilized components are to be rinsed in sterile, deionized water prior to use. The EDTA vessel is to be placed in the ice bath. The protocol will consist of four steps: (1) cleaning of the substrate in preparation for dissolution, (2)



dissolution of the matrix, (3) collection of exhumated specimens and (4) viability assessment. The accompanying illustrated guide (Figs. 1 and 2) shows stills of individual steps of the exhumation. Our substrate consists of chips of commercially available blocky calcite (WARD'S Natural Science, NY, USA) (Fig. 1-1), which we allowed to be infested by a strain of euendolithic cyanobacteria, *Mastigocoleus testarum* BC008 (Fig. 1-2).

**Step 1: Cleaning.** Infested chips are the substrate shown in this protocol, but the cleaning applies equally to other samples. Samples are thoroughly brushed while submerged in liquid medium to remove any surface growth (Fig. 1-3), and rinsed in fresh medium.

**Step 2: Dissolution of the substrate.** The sample is placed on the screen basket holder (Fig.1-5) on the upper part in the filtration tower. Ice-cold EDTA solution, drawn by a peristaltic pump with variable flow (VWR Mini-Pump, VWR International, West Chester, PA, USA), is allowed to drip over the sample (Fig. 1-6) at constant flow rate. Dripping at 0.5 mL / min allowed us to methodically remove layers of defined thickness from the sample. With chips of our size the dissolution proceeded at a rate of about 100  $\mu\text{m}$  per hour. This will of course depend on the size and porosity of the sample, and must be calibrated for each case. As filaments are exposed, these are gently brushed down into the filter tower, allowed to flow with the dripping EDTA solution, and are collected on the filter at the bottom. In our case, we carried out three, 30-min dissolution steps, collecting the biomass

after each. This yielded 3 fractions, each containing cells from the upper (0-50  $\mu\text{m}$ ), mid (50-100  $\mu\text{m}$ ) and deep (100-150  $\mu\text{m}$ ) layer of the chip.

**Step 3: Collection of specimens.** After exhumation, the polycarbonate filter is washed in place with 5 mL of distilled water (Fig. 2-7), which helps remove any EDTA or precipitates of Ca-EDTA before retrieval (Fig. 2-8). Filters are then placed in sterile media (Fig. 1-9) and vortexed/shaken to liberate the cells into suspension. After discarding the filters, specimens are collected by centrifugation at 4,000 RPM for 10 minutes, and the supernatant decanted. Lastly, cell pellets are re-suspended in fresh medium (Fig. 2-10).

**Step 4: Viability assessment.** We allowed our filaments to rest in the light for several hours (3-4). A Hansatech liquid-phase oxygen electrode chamber (Hansatech Instruments, Norfolk, England) was used to measure oxygen evolution from the suspended fractions (Fig. 2-11). The electrode 2-point was calibrated in medium, achieving 100%  $\text{O}_2$  saturation by stirring in the open chamber, and by adding sodium dithionite to establish 0%  $\text{O}_2$  saturation. Oxygen evolution rates were measured under white fluorescent illumination at 500  $\mu\text{moles}$  of photons (Fig. 2-12). Other forms of viability assessment can be devised as needed. Results of this experiments show that photosynthetic rates per unit biomass do not vary with depth and are similar to those of non-boring BC008 cultures (Chapter 2 of this dissertation). We have been successful in using this method to obtain viable cultures from exhumated BC008 by standard plating (not shown), as well as from other

endoliths exhumated from natural samples (McLennan and Ramírez-Reinat, unpublished). We have also been able to obtain good quality mRNA preparations for gene expression studies of BC008 cells exhumated in this manner (Garcia-Pichel et al, in the press).

## DISCUSSION

This method proves useful in the exhumation of live cyanobacterial euendoliths from calcareous substrates, by gently removing the surrounding matrix. A less concentrated solution than those previously published by Wade (500-675 mM) allowed effective, yet gentle dissolution of the samples. Doing away with the original method while slowing rates of dissolution probably helps with organismal viability as well. The continuous drip approach used here, partly makes up for that, in that it ensures a constant supply of fresh EDTA, prevents the formation of microlayers of high calcium and carbonate ion concentration. This enhances dissolution rate and prevents the deposition of Ca-EDTA precipitates on the sample, a by-product of the dissolution process. Cooling the solution likely reduced the damaging effects of EDTA, since, in our experience, extractions conducted at room temperature had reduced viability of cells. This protocol offers some improvements over other methods as it preserves both the morphology and viability of the cells. Most constrains in studying euendolithic organisms *in vivo* come from their difficult accessibility; this method removes those constrains.

This method should prove a useful tool in future studies of boring cyanobacteria or other endolithic organisms. It may also find application in other fields of biology where mineral/biological systems co-occur, such as the

biology of corals or other calcified animals or tissues. It may be of use in biomedical investigations of bone tissue or mineral calculi.

### **ACKNOWLEDGEMENTS**

We would like to thank Ipsita Dutta for assistance with the oxygen sensor, and Natalie Myers for for graciously providing me with filming equipment.

This work was supported by a National Science Foundation grant 0311945.

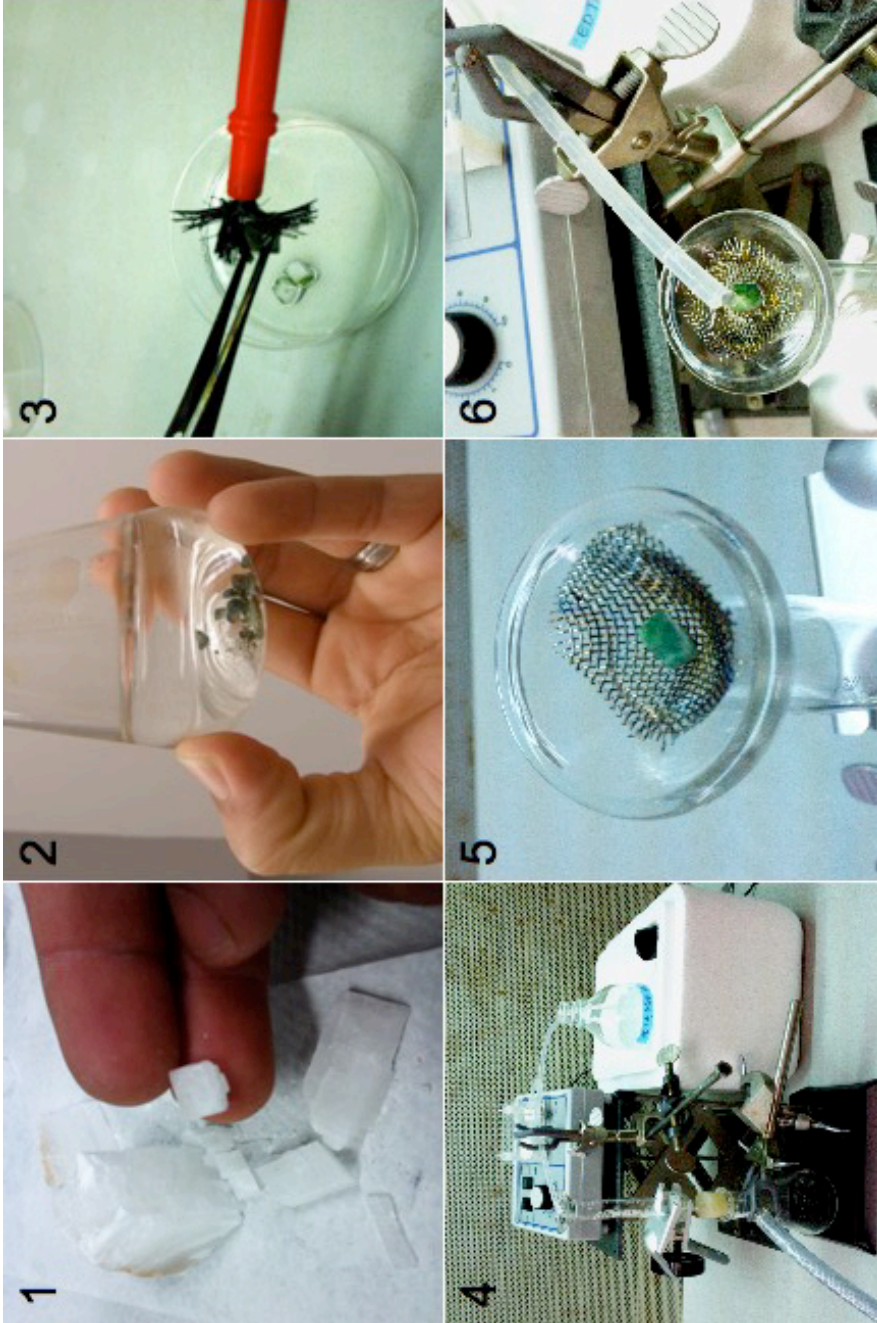


Fig. 1 Illustrated exhumation sequence. (1) Blocky calcite used as the substrate *M. testarum* strain BC008. (2) Calcite chips infested with strain BC008, ready for collection. (3) Cleaning of the calcite chips to remove superficial filaments. (4) Exhumation setup: filtration apparatus, peristaltic pump and EDTA solution. (5) Mesh holder with calcite chip (6) EDTA solution

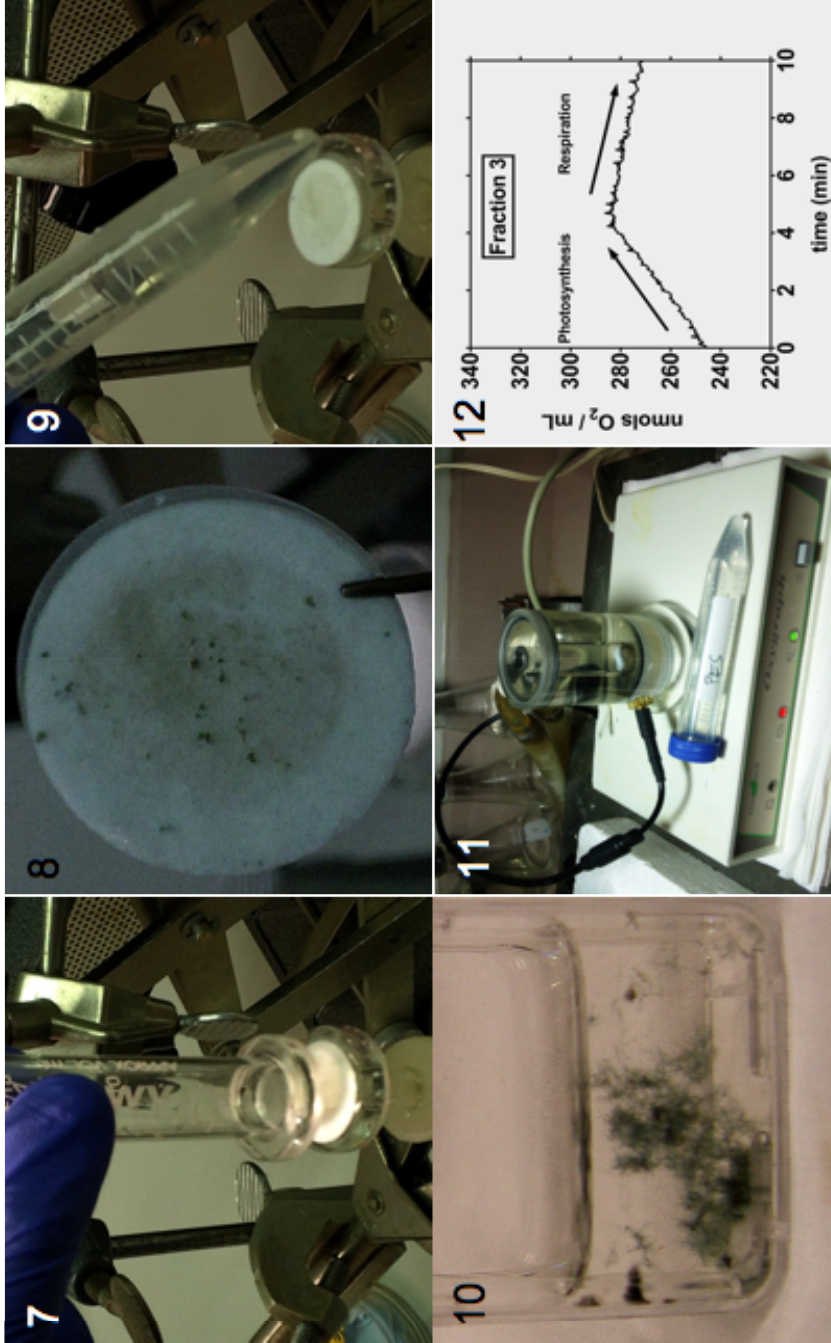


Fig. 2 Illustrated exhumation sequence, cont. (7) Rinsing and collection of polycarbonate filter. (8) Exhumated filaments of strain BC008. (9) Rinsing of filaments in sterile medium. (10) Filaments of strain BC008, placed in sterile medium after collection. (11) Oxygen chamber (12) Typical photosynthetic rates of exhumated BC008 filaments.

## REFERENCES

### INTRODUCTION

- Alexandersson, E.T.** 1975. Marks of Unknown Carbonate-Decomposing Organelles in Cyanophyte Borings. *Nature* **254**:212-238.
- Al-Thukair, A.A.** 2002. Effect of oil pollution on euendolithic cyanobacteria of the Arabian Gulf. *Environmental Microbiology* **4**:125-129.
- Al-Thukair, A.A., and Golubic, S.** 1991. 5 New Hyella Species from the Arabian Gulf. *Archiv für Hydrobiologie*:167-197.
- Al-Thukair, A.A., and Golubic, S.** 1991. New Endolithic Cyanobacteria from the Arabian Gulf, *Hyella immanis* Sp. Nov. *Journal of Phycology* **27**:766-780.
- Ascaso, C., and Wierzchos, J.** 2002. New approaches to the study of Antarctic lithobiontic microorganisms and their inorganic traces, and their application in the detection of life in Martian rocks. *International Microbiology* **5**:215-22.
- Barbosa, S.S., Byrne, M., and Kelaher, B.P.** 2008. Bioerosion caused by foraging of the tropical chiton *Acanthopleura gemmata* at One Tree Reef, southern Great Barrier Reef. *Coral Reefs* **27**:635-639.
- Bathurst, R.G.C.** 1980. Lithification of Carbonate Sediments. *Science Progress* **66**:451-471.
- Bentis, C.J., Kaufman, L., and Golubic, S.** 2000. Endolithic fungi in reef-building corals (Order : Scleractinia) are common, cosmopolitan, and potentially pathogenic. *Biological Bulletin* **198**:254-260.
- Berkelman, T., Garret-Engele, P., and Hoffman, N.E.** 1994. The *pacL* gene of *Synechococcus* sp. strain PCC 7942 encodes a Ca<sup>2+</sup>-transporting ATPase. *Journal of Bacteriology* **176**:4430-4436.
- Blake, J.A.** 1969. Systematics and Ecology of Shell-Boring Polychaetes from New England. *American Zoologist* **9**:813-820.
- Bornet, E. and Flahault, C.** 1888. Note sur deux nouveaux genres d'algues perforantes. *Journal de Botanique* **2**:162-163.
- Bornet, E. and Flahault, C.** 1889. Sur quelques plantes vivant dans le test calcaire des mollusques. *Bulletin Société Botanique de France* **36**:147-176.

- Borzi, A.** 1907. *Conspectus generum Stigonetacearum*. *Nuova Notarisia* **18**:38.
- Brock, T.D.** 1973. Lower pH limit for the existence of blue-green algae: evolutionary and ecological implications. *Science* **179**:480-483.
- Budd, D.A., and Perkins, R.D.** 1980. Bathymetric zonation and paleoecological significance of microborings in Puerto Rican shelf and slope sediments. *Journal of Sedimentary Research* **50**:881-903.
- Buschbaum, C., Buschbaum, G., Schrey, I., and Thieltges, D.W.** 2006. Shell-boring polychaetes affect gastropod shell strength and crab predation. *Marine Ecology-Progress Series* **329**:123-130.
- Campbell, S.** 1982. Precambrian endoliths discovered. *Nature* **299**:429-431.
- Campbell, S.** 1983. The modern distribution and geological history of calcium carbonate boring microorganisms, p. 99-104. In: Wesbroek, P., De Jong, E.W. (Eds.), *Biom mineralization and Biological Metal Accumulation*. Reidel Publishing, Boston.
- Carreiro-Silva, M., and Mcclanahan, T.R.** 2001. Echinoid bioerosion and herbivory on Kenyan coral reefs: the role of protection from fishing. *J Exp Mar Bio Ecol* **262**:133-153.
- Carriker, M.R., and Gruber, G.L.** 1999. Uniqueness of the gastropod accessory boring organ (ABO): Comparative biology, an update. *Journal of Shellfish Research* **18**:579-595.
- Chazottes, V., Cabioch, G., Golubic, S., and Radtke, G.** 2009. Bathymetric zonation of modern microborers in dead coral substrates from New Caledonia--Implications for paleodepth reconstructions in Holocene corals. *Palaeogeography, Palaeoclimatology, Palaeoecology* **280**:456-468.
- Chazottes, V., Le Campion-Alsumard, T. And Peyrot-Clausade, M.** 1995. Bioerosion rates on coral reefs: interactions between macroborers, microborers and grazers (Moorea, French Polynesia). *Palaeogeography, Palaeoclimatology, Palaeoecology* **113**:189-198.
- Che, L.M., Le Campion-Alsumard, T., Bouryesnault, N., Payri, C., Golubic, S., and Bezac, C.** 1996. Biodegradation of shells of the black pearl oyster, *Pinctada margaritifera* var *cumingii*, by microborers and sponges of French Polynesia. *Marine Biology* **126**:509-519.
- Ciferri, O.** 1983. *Spirulina, the Edible Microorganism*. *Microbiological Reviews* **47**:551-578.



- Criddle, D.N., Gerasimenko, J.V., Baumgartner, H.K., Jaffar, M., Voronina, S., Sutton, R., Petersen, O.H., and Gerasimenko, O.V.** 2007. Calcium signalling and pancreatic cell death: apoptosis or necrosis? *Cell Death and Differentiation* **14**:1285-1294.
- Danin, A., and Caneva, G.** 1990. Deterioration of Limestone Walls in Jerusalem and Marble Monuments in Rome Caused by Cyanobacteria and Cyanophilous Lichens. *International Biodeterioration* **26**:397-417.
- Desikachary, T.V.** 1953. *Iyengariella tirupatiensis* gen. et sp. nov. from South India. . *Phytomorphology* **3**:249–253.
- Diaz Del Castillo, B.** 1928. *Historia verdadera de la conquista de la Nueva España*, vol. 1. Madrid.
- Dirksen, R.T., and Beam, K.G.** 1995. Single calcium channel behavior in native skeletal muscle. *Journal of General Physiology* **105**:227-247.
- Dismukes, G.C., Klimov, V.V., Baranov, S.V., Kozlov, Y.N., Dasgupta, J., and Tyryshkin, A.** 2001. The origin of atmospheric oxygen on Earth: The innovation of oxygenic photosynthesis. *Proceedings of the National Academy of Sciences of the United States of America* **98**:2170-2175.
- Domínguez, D.C.** 2004. Calcium signalling in bacteria. *Molecular Microbiology* **54**:291-297.
- Drouet, F.** 1963. Ecophenes of *Schizothrix calcicola* (Oscillatoriaceae). *Proceedings of the Academy of Natural Sciences of Philadelphia* **115**:261-281.
- Dupraz, C., and Visscher, P.T.** 2005. Microbial lithification in marine stromatolites and hypersaline mats. *Trends in Microbiology* **13**:429-38.
- Ercegović, A.** 1927. Tri roda litofitskih cijanoficeja sa jadranske obale. *Acta Botanica Instituti Botanici Universitatis Zagrebensis* **2**:78-84.
- Flores, E., Herrero, A., Wolk, C.P., and Maldener, I.** 2006. Is the periplasm continuous in filamentous multicellular cyanobacteria? *Trends in Microbiology* **14**:439-443.
- Flourakis, M., and Prevarskaya, N.** 2009. Insights into Ca<sup>2+</sup> homeostasis of advanced prostate cancer cells. *Biochimica Et Biophysica Acta-Molecular Cell Research* **1793**:1105-1109.
- Flugel, E.** 2004. Bioerosion, boring and grazing organisms. In: *Microfacies of carbonate rocks: analysis, interpretation and application*, pp. 387-397. Springer-Verlag.

- Frémy, P.** 1936. Les algues perforantes. Mémoire de la Société Nationale des Sciences Naturelles et Mathématiques de Cherbourg **42**:275-300.
- Friedmann, E.I., Hua, M. And Ocampo-Friedmann, R.** 1993. Terraforming Mars: dissolution of carbonate rocks by cyanobacteria. Journal of the British Interplanetary Society **46**:291-292.
- Furuya, K., Enomoto, K., and Yamagishi, S.** 1993. Spontaneous calcium oscillations and mechanically and chemically induced calcium responses in mammary epithelial cells. Pflugers Arch **422**:295-304.
- Garbary, D.** 2007. The Margin of the Sea: Survival at the Top of the Tides, p. 173-191. In: Seckback, J. (Ed.), Algae and Cyanobacteria in Extreme Environments. Springer.
- Garcia-Pichel, F.** 2006. Plausible mechanisms for the boring on carbonates by microbial phototrophs. Sedimentary Geology **185**:205-213.
- Garcia-Pichel, F., Nubel, U., and Muyzer, G.** 1998. The phylogeny of unicellular, extremely halotolerant cyanobacteria. Arch Microbiol **169**:469-82.
- Garcia-Pichel, F., Sherry, N.D., and Castenholz, R.W.** 1992. Evidence for an ultraviolet sunscreen role of the extracellular pigment scytonemin in the terrestrial cyanobacterium *Chlorogloeopsis* sp. Photochem Photobiol **56**:17-23.
- Garcia-Pichel, F., Wingard, C.E., and Castenholz, R.W.** 1993. Evidence Regarding the UV Sunscreen Role of a Mycosporine-Like Compound in the Cyanobacterium *Gloeocapsa* sp. Appl Environ Microbiol **59**:170-176.
- Geisler, M., Richter, J., and Schumann, J.** 1993. Molecular cloning of a P-type ATPase gene from the cyanobacterium *Synechocystis* sp. PCC 6803. Homology to eukaryotic Ca(2+)-ATPases. Journal of Molecular Biology **234**:1284-1289.
- Golubić, S., and Le Campion-Alsumard, T.** 1973. Boring behavior of marine blue-green algae *Mastigocoleus testarum* Lagerheim and *Kyrtuthrix dalmatica* Ercegovic, as a taxonomic character. Aquatic Sciences - Research Across Boundaries **35**:157-161.
- Golubic, S., Campbell, S.E., Drobne, K., Cameron, B., Balsam, W.L., Cimerman, F., and Dubois, L.** 1984. Microbial Endoliths - a Benthic Overprint in the Sedimentary Record, and a Paleobathymetric Cross-Reference with Foraminifera. Journal of Paleontology **58**:351-361.

- Golubic, S., Perkins, R.D. And Lukas, K.J.** 1975. Boring Microorganisms and Borings in Carbonate Substrates. In: Frey, R.W. (Ed), *The Study of Trace Fossils*. Springer, Berlin, pp.229-259
- Golubic, S., Radtke, G., and Le Campion-Alsumard, T.** 2005. Endolithic fungi in marine ecosystems. *Trends Microbiol* **13**:229-235.
- Gomont, M.** 1892. Monographie des Oscillariees (Nostocacees homocystees). *Annales des Sciences Naturelles Botanique* **7**:265-368.
- Hammond, L.S.** 1981. An Analysis of Grain-Size Modification in Biogenic Carbonate Sediments by Deposit-Feeding Holothurians and Echinoids (Echinodermata). *Limnology and Oceanography* **26**:898-906.
- Herbert, G.S., Diet, G.P., Fortunato, H., Simone, L.R.L., and Sliko, J.** 2009. Extremely slow feeding in a tropical drilling ectoparasite, *Vitularia salebrosa* (King and Broderip, 1832) (Gastropoda: Muricidae), on molluscan hosts from Pacific Panama. *Nautilus* **123**:121-136.
- Herrera-Escalante, T., Lopez-Perez, R.A., and Leyte-Morales, G.E.** 2005. Bioerosion caused by the sea urchin *Diadema Mexicanum* (Echinodermata: Echinoidea) at Bahias de Huatulco, Western Mexico. *Rev Biol Trop* **53 Suppl 3**:263-273.
- Hoiczyk, E.** 2000. Gliding motility in cyanobacteria: observations and possible explanations. **174**:11-17.
- Hoiczyk, E., and Baumeister, W.** 1997. Oscillin, an extracellular, Ca<sup>2+</sup>-binding glycoprotein essential for the gliding motility of cyanobacteria. *Molecular Microbiology* **26**:699-708.
- Hoiczyk, E., and Baumeister, W.** 1998. The junctional pore complex, a prokaryotic secretion organelle, is the molecular motor underlying gliding motility in cyanobacteria. *Current Biology* **8**:1161-1168.
- Holmes, G., Ortiz, J.-C., and Schönberg, C.** 2009. Bioerosion rates of the sponge *Cliona orientalis* Thiele, 1900: spatial variation over short distances *Facies* **55**:203-211.
- Hong, C.Y., Chiang, B.N., Wu, P., Wei, Y.H., and Fong, J.C.** 1985. Involvement of calcium Ca<sup>2+</sup> in the caffeine stimulation of human sperm motility. *British Journal of Clinical Pharmacology* **19**:739-43.
- Jansen, H., and Ahrens, M.J.** 2004. Carbonate dissolution in the guts of benthic deposit feeders: A numerical model. *Geochimica Et Cosmochimica Acta* **68**:4077-4092.

- Johnson, H.E., King, S.R., Banack, S.A., Webster, C., Callanaupa, W.J., and Cox, P.A.** 2008. Cyanobacteria (*Nostoc commune*) used as a dietary item in the Peruvian highlands produce the neurotoxic amino acid BMAA. *Journal of Ethnopharmacology* **118**:159-165.
- Kabakov, A.Y., and Hilgemann, D.W.** 1995. Modulation of Na<sup>+</sup>/ Ca<sup>2+</sup> exchange current by EGTA calcium buffering in giant cardiac membrane patches. *Biochimica Biophysica Acta* **1240**:142-148.
- Kaehler, S.** 1999. Incidence and distribution of phototrophic shell-degrading endoliths of the brown mussel *Perna perna*. *Marine Biology* **135**:505-514.
- Knoll, A.H., Golubic, S., Green, J., and Swett, K.** 1986. Organically preserved microbial endoliths from the late Proterozoic of East Greenland. *Nature* **321**:856-7.
- Knoll, A.H., Swett, K., and Burkhardt, E.** 1989. Paleoenvironmental distribution of microfossils and stromatolites in the Upper Proterozoic Backlundtoppen Formation, Spitsbergen. *Journal of Paleontology* **63**:129-45.
- Kretsinger, R.H., and Nelson, D.J.** 1976. Calcium in biological systems. *Coordination Chemistry Reviews* **18**:29-124.
- Kumar, H.D.** 2004. Management of nutritional and health needs of malnourished and vegetarian people in India. *Complementary and Alternative Approaches to Biomedicine* **546**:311-321.
- Kupriyanova, E.V., Lebedeva, N.V., Dudoladova, M.V., Gerasimenko, L.M., Alekseeva, S.G., Pronina, N.A., and Zavarzin, G.A.** 2003. Carbonic Anhydrase Activity of Alkalophilic Cyanobacteria from Soda Lakes. *Russian Journal of Plant Physiology* **50**:532-539.
- Lagerheim, G.** 1886. Note sur le *Mastigocoleus*, nouveau genre des algues marines de l'ordre des *Phycochromacees*. *Notarisia* **1**:65-69.
- Lamenti, G., Tiano, P., and Tomaselli, L.** 2000. Biodeterioration of ornamental marble statues in the Boboli Gardens (Florence, Italy). *Journal of Applied Phycology* **12**:427-433.
- Laurenti, A., and Montaggioni, L.** 1995. The Role of Microbial Activity in Marine Reef Lithification (Tahiti, French-Polynesia). *Comptes Rendus De L'Academie Des Sciences* **320**:845-852.
- Le Campion-Alsumard, T.** 1970. Cyanophycées marines endoliths colonisant les surfaces rochenses dénudées (Etages Supralittoral et

Mediolittoral de la region de Marseilles). Schweizerische Zeitschrift für Allgemeine Mikrobiologie **2**:45-47.

**Le Campion-Alsumard, T.** 1991. 3 Hyella Taxa (Endolithic Cyanophytes) from Tropical Environments (Lizard-Island, Great-Barrier-Reef). Archiv für Hydrobiologie **64**:159-166.

**Le Campion-Alsumard, T., Golubic, S., and Hutchings, P.** 1995. Microbial Endoliths in Skeletons of Live and Dead Corals - Porites Lobata (Moorea, French-Polynesia). Marine Ecology-Progress Series **117**:149-157.

**Lee, S.J., Golubic, S., and Verrecchia, E.** 1999. Epibiotic relationships in Mesoproterozoic fossil record: Gaoyuzhuang Formation, China. Geology **27**:1059-1062.

**Lynch, G.S., Fary, C.J., and Williams, D.A.** 1997. Quantitative measurement of resting skeletal muscle [Ca<sup>2+</sup>]<sub>i</sub> following acute and long-term downhill running exercise in mice. Cell Calcium **22**:373-383.

**May, J.A., and Perkins, R.D.** 1979. Endolithic Infestation of Carbonate Substrates Below the Sediment-Water Interface. Journal of Sedimentary Petrology **49**:357-378.

**Mikhodyuk, O., Zavarzin, G., and Ivanovsky, R.** 2008. Transport systems for carbonate in the extremely natronophilic cyanobacterium Euhalothece sp. Microbiology **77**:412-418.

**Miller, S.R., and Castenholz, R.W.** 2000. Evolution of thermotolerance in hot spring cyanobacteria of the genus Synechococcus. Applied and Environmental Microbiology **66**:4222-4229.

**Montoya-Terreros, H., Gomez-Carrion, J. and Benavente-Palacios, M.** 2006. Natural populations and culture of the marine microalga Mastigocoleus testarum Lagerheim ex Bornet et Flahault (Cyanophyta, Nostochopsaceae), the first record for the Peruvian flora. Arnaldoa **13**:258-269.

**Moon, Y.J., Park, Y.M., Chung, Y.H., and Choi, J.S.** 2004. Calcium is involved in photomovement of cyanobacterium Synechocystis sp. PCC 6803. Photochemistry and Photobiology **79**:114-119.

**Nava, H., and Carballo, J.L.** 2008. Chemical and mechanical bioerosion of boring sponges from Mexican Pacific coral reefs. Journal of Experimental Biology **211**:2827-2831.

- Neumann, A.C.** 1966. Observations on Coastal Erosion in Bermuda and Measurements of Boring Rate of Sponge *Cliona Lampa*. *Limnology and Oceanography* **11**:92-108.
- Norris, V., Grant, S., Freestone, P., Canvin, J., Sheikh, F.N., Toth, I., Trinei, M., Modha, K., and Norman, R.I.** 1996. Calcium  $Ca^{2+}$  signalling in bacteria. *Journal of Bacteriology* **178**:3677-3682.
- Norris, V., Seror, S.J., Casaregola, S., and Holland, I.B.** 1988. A single calcium flux triggers chromosome replication, segregation and septation in bacteria: a model. *Journal of Theoretical Biology* **134**:341-350.
- Omelson, C.R., Pollard, W.H., and Ferris, F.G.** 2007. Inorganic species distribution and microbial diversity within high arctic cryptoendolithic habitats. *Microbial Ecology* **54**:740-752.
- Ong, L., and Holland, K.N.** 2010. Bioerosion of coral reefs by two Hawaiian parrotfishes: species, size differences and fishery implications. *Marine Biology* **157**:1313-1323.
- Ordal, G.W.** 1977. Calcium  $Ca^{2+}$  ion regulates chemotactic behaviour in bacteria. *Nature* **270**:66-67.
- Ortegacalvo, J.J., Arino, X., Hernandezmarine, M., and Saizjimenez, C.** 1995. Factors Affecting the Weathering and Colonization of Monuments by Phototrophic Microorganisms. *Science of the Total Environment* **167**:329-341.
- Ourribane, M., Chellai, E.H., and Zaghib-Turki, D.** 2000. Microbialites and micro-encrusters role in the reefs lithification: examples of the Maghrebian Atlas reefs during the Upper Jurassic. *Comptes Rendus De L' Academie Des Sciences* **330**:407-414.
- Paerl, H.W., Steppe, T.F., and Reid, R.P.** 2001. Bacterially mediated precipitation in marine stromatolites. *Environmental Microbiology* **3**:123-130.
- Pandey, P.K., Gour, R.K., and Bisen, P.S.** 1999. Energy-dependent  $Ca^{2+}$  efflux from the cells of *Nostoc calcicola* Breb: Role of modifying factors. *Current Microbiology* **39**:254-258.
- Pandey, K.D., Shukla, S.P., Shukla, P.N., Giri, D.D., Singh, J.S., Singh, P., and Kashyap, A.K.** 2004. Cyanobacteria in Antarctica: ecology, physiology and cold adaptation. *Cellular and Molecular Biology* **50**:575-84.

- Pari, N., Peyrot-Clausade, M., Le Campion-Alsumard, T., Hutchings, P., Chazottes, V., Golubic, S., Le Campion, J., and Fontaine, M.F.** 1998. Bioerosion of experimental substrates on high islands and on atoll lagoons (French Polynesia) after two years of exposure. *Marine Ecology-Progress Series* **166**:119-130.
- Pentecost, A.** 1992. Growth and distribution of endolithic algae in some North Yorkshire streams (UK). *British Phycological Journal* **27**:145 - 151.
- Peyrot-Clausade, M., Chabanet, P., Conand, C., Fontaine, M.F., Letourneur, Y., and Harmelin-Vivien, M.** 2000. Sea urchin and fish bioerosion on La Reunion and Moorea reefs. *Bulletin of Marine Science* **66**:477-485.
- Porn-Ares, M.I., Ares, M.P.S., and Orrenius, S.** 1998. Ca<sup>2+</sup> signalling and the regulation of apoptosis. *Toxicology in Vitro* **12**:539-543.
- Proteau, P.J., Gerwick, W.H., Garciapichel, F., and Castenholz, R.** 1993. The Structure of Scytonemin, an Ultraviolet Sunscreen Pigment from the Sheaths of Cyanobacteria. *Experientia* **49**:825-829.
- Rasmussen, K.A., and Frankenberg, E.W.** 1990. Intertidal Bioerosion by the Chiton *Acanthopleura-Granulata* - San-Salvador, Bahamas. *Bulletin of Marine Science* **47**:680-695.
- Reid, R.P., and Macintyre, I.G.** 2000. Microboring Versus Recrystallization: Further Insight into the Micritization Process. *Journal of Sedimentary Research* **70**:24-28.
- Reid, R.P., Visscher, P.T., Decho, A.W., Stolz, J.F., Bebout, B.M., Dupraz, C., Macintyre, I.G., Paerl, H.W., Pinckney, J.L., Prufert-Bebout, L., Steppe, T.F., and Desmarais, D.J.** 2000. The role of microbes in accretion, lamination and early lithification of modern marine stromatolites. *Nature* **406**:989-92.
- Riascos, J.M., Guzman, N., Laudien, J., Oliva, M.E., Heilmayer, O., and Ortlieb, L.** 2009. Long-term parasitic association between the boring polychaete *Polydora biocipitalis* and *Mesodesma donacium*. *Diseases of Aquatic Organisms* **85**:209-215.
- Rodríguez, H., Rivas, J., Guerrero, M.G., and Losada, M.** 1989. Nitrogen-Fixing Cyanobacterium with a High Phycoerythrin Content. *Applied and Environmental Microbiology* **55**:758-760.

- Roney, B.R., Li, R.H., Banack, S.A., Murch, S., Honegger, R., and Cox, P.A.** 2009. Consumption of faecal Nostoc soup: A Potential for BMAA exposure from Nostoc cyanobacteria in China? *Amyotrophic Lateral Sclerosis* **10**:44-49.
- Rotjan, R.D., and Lewis, S.M.** 2005. Selective predation by parrotfishes on the reef coral *Porites astreoides*. *Marine Ecology-Progress Series* **305**:193-201.
- Schneider, J., and Le Campion-Alsumard, T.** 1999. Construction and destruction of carbonates by marine and freshwater cyanobacteria. *European Journal of Phycology* **34**:417-426.
- Schreiber, R.** 2005. Ca<sup>2+</sup> signaling, intracellular pH and cell volume in cell proliferation. *Journal of Membrane Biology* **205**:129-137.
- Seeler, J.S., and Golubic, S.** 1991. *Iyengariella-Endolithica* Sp Nova, a Carbonate Boring Stigonematalean Cyanobacterium from a Warm Spring-Fed Lake - Nature to Culture. *Archiv für Hydrobiologie*:399-410.
- Sharp, J.H.** 1969. Blue-Green Algae and Carbonates-Schizothrix calcicola and Algal Stromatolites from Bermuda. *Limnology and Oceanography* **14**:568-578.
- Sheppard, C.R., Spalding, M., Bradshaw, C., and Wilson, S.** 2002. Erosion vs. recovery of coral reefs after 1998 El Nino: Chagos reefs, Indian Ocean. *Ambio* **31**:40-48.
- Snyder, M.A., Stock, J.B., and Koshland, D.E., Jr.** 1981. Role of membrane potential and Ca<sup>2+</sup> in chemotactic sensing by bacteria. *J Mol Biol* **149**:241-57.
- Soule, T., Stout, V., Swingley, W.D., Meeks, J.C., and Garcia-Pichel, F.** 2007. Molecular genetics and genomic analysis of scytonemin biosynthesis in *Nostoc punctiforme* ATCC 29133. *Journal of Bacteriology* **189**:4465-72.
- Sperti, G., and Colucci, W.S.** 1991. Ca<sup>2+</sup> influx modulates DNA synthesis and proliferation in A7r5 vascular smooth muscle cells. *Eur J Pharmacol* **206**:279-84.
- Tan, F.C., Goll, D.E., and Otsuka, Y.** 1988. Some properties of the millimolar Ca<sup>2+</sup> - dependent proteinase from bovine cardiac muscle. *Journal of Molecular and Cellular Cardiology* **20**:983-97.



- Takabe, T., Incharoensakdi, A., Arakawa, K., and Yokota, S.** 1988. CO<sub>2</sub> Fixation Rate and RuBisCO Content Increase in the Halotolerant Cyanobacterium, *Aphanothece halophytica*, Grown in High Salinities. *Plant Physiology* **88**:1120-4.
- Thuret, G.** 1875. Essai de classification des Nostochinees. *Annales des Sciences Natureles* **6**:375-379.
- Toh, P.S.Y., Yew, S.P., Yong, K.H., Sudesh, K., and Abed, R.M.M.** 2009. Phototactic Motility of *Synechocystis* Sp. *Uniwig* (Cyanobacteria) from Brackish Environment *Journal of Phycology* **46**:102-111.
- Toro-Farmer, G., Cantera, J.R., Londono-Cruz, E., Orozco, C., and Neira, R.** 2004. [Distribution patterns and bioerosion of the sea urchin *Centrostephanus coronatus* (Diadematoida: Diadematidae), at the reef of Playa Blanca, Colombian Pacific. *Revista de Biologia Tropical* **52**:67-76.
- Torrecilla, I., Leganes, F., Bonilla, I., and Fernandez-Pinas, E.** 2001. Ca<sup>2+</sup> transients in response to salinity and osmotic stress in the nitrogen-fixing cyanobacterium *Anabaena* sp PCC7120, expressing cytosolic apoaequorin. *Plant Cell and Environment* **24**:641-648.
- Tribollet, A., Godinot, C., Atkinson, M., and Langdon, C.** 2009. Effects of elevated pCO<sub>2</sub> on dissolution of coral carbonates by microbial euendoliths. *Global Biogeochemical Cycles* **23**:1-7
- Tribollet, A.** 2008. Dissolution of dead corals by euendolithic microorganisms across the northern Great Barrier Reef (Australia). *Microbial Ecology* **55**:569-80.
- Tribollet, A., and Golubic, S.** 2005. Cross-shelf differences in the pattern and pace of bioerosion of experimental carbonate substrates exposed for 3 years on the northern Great Barrier Reef, Australia. *Coral Reefs* **24**:422-434.
- Tribollet, A., Langdon, C., Golubic, S., and Atkinson, M.** 2006. Endolithic microflora are major primary producers in dead carbonate substrates of Hawaiian coral reefs. *Journal of Phycology* **42**:292-303.
- Villar, S.E., Edwards, H.G., and Cockell, C.S.** 2005. Raman spectroscopy of endoliths from Antarctic cold desert environments. *Analyst* **130**:156-62.

- Vogel, K., and Brett, C.E.** 2009. Record of microendoliths in different facies of the Upper Ordovician in the Cincinnati Arch region USA: The early history of light-related microendolithic zonation. *Palaeogeography Palaeoclimatology Palaeoecology* **281**:1-24.
- Vogel, K., Gektidis, M., Golubic, S., Kiene, W.E., and Radtke, G.** 2000. Experimental studies on microbial bioerosion at Lee Stocking Island, Bahamas and One Tree Island, Great Barrier Reef, Australia: implications for paleoecological reconstructions. *Lethaia* **33**:190-204.
- Wade, B.D., and Garcia-Pichel, F.** 2003. Evaluation of DNA extraction methods for molecular analyses of microbial communities in modern calcareous microbialites. *Geomicrobiology Journal* **20**:549-561.
- Waditee, R., Hibino, T., Tanaka, Y., Nakamura, T., Incharoensakdi, A., and Takabe, T.** 2001. Halotolerant cyanobacterium *Aphanothece halophytica* contains an Na(+)/H(+) antiporter, homologous to eukaryotic ones, with novel ion specificity affected by C-terminal tail. *J Biol Chem* **276**:36931-8.
- Ward, D. and Castenholz, R.** 2002. Cyanobacteria in Geothermal Habitats. In: B. A. Whitton & M. Potts (Eds.) *The Ecology of Cyanobacteria: Their Diversity in Time and Space*. Kluwer Academic Publishers.
- Waterbury, J.B., Watson, S.W., Guillard, R.R.L., and Brand, L.E.** 1979. Widespread Occurrence of a Unicellular, Marine, Planktonic, Cyanobacterium. *Nature* **277**:293-294.
- Wayne, T.A.** 1987. Responses of a Mussel to Shell-Boring Snails - Defensive Behavior in *Mytilus Edulis*. *Veliger* **30**:138-147.
- Webb, S.C., and Korrubel, J.L.** 1994. Shell Weakening in Marine Mytilids Attributable to Blue-Green-Alga *Mastigocoleus* Sp. (Nostochopsidaceae). *Journal of Shellfish Research* **13**:11-17.
- Wilde, D.W., Knight, P.R., Sheth, N., and Williams, B.A.** 1991. Halothane Alters Control of Intracellular Ca<sup>2+</sup> Mobilization in Single-Rat Ventricular Myocytes. *Anesthesiology* **75**:1075-1086.
- Wisshak, M., Gektidis, M., Freiwald, A., and Lundälv, T.** 2005. Bioerosion along a bathymetric gradient in a cold-temperate setting (Kosterfjord, SW Sweden): an experimental study. *Facies* **51**:93-117.
- Wynn-Williams, D.D., and Edwards, H.G.M.** 2000. Antarctic ecosystems as models for extraterrestrial surface habitats. *Planetary and Space Science* **48**:1065-1075.

- Young, H.R., and Nelson, C.S.** 1988. Endolithic Biodegradation of Cool-Water Skeletal Carbonates on Scott Shelf, Northwestern Vancouver-Island, Canada. *Sedimentary Geology* **60**:251-267.
- Young, L.G., and Nelson, L.** 1974. Ca<sup>2+</sup> ions and control of the motility of sea urchin spermatozoa. *Journal of Reproduction and Fertility* **41**:371-378.
- Zhang, Y.A.G., S.** 1987. Endolithic microfossils (cyanophyta) from early Proterozoic stromatolites, Hebei, China. *Acta Micropalaentologica Sinica* **4**:1-12.
- Zhao, M., Hollingworth, S., and Baylor, S.M.** 1996. Properties of tri- and tetracarboxylate Ca<sup>2+</sup> indicators in frog skeletal muscle fibers. *Biophysical Journal* **70**:896-916.
- Zubia, M., and Peyrot-Clausade, M.** 2001. Internal bioerosion of *Acropora formosa* in Reunion (Indian Ocean): microborer and macroborer activities. *Oceanologica Acta* **24**:251-262.
- Zundeleovich, A., Lazar, B., and Ilan, M.** 2007. Chemical versus mechanical bioerosion of coral reefs by boring sponges-lessons from *Pione cf. vastifica*. *Journal of Experimental Biology* **210**:91-96

## **CHAPTER 1**

- Alfaro, A.C., Webb, S.C., and Barnaby, C.** 2008. Variability of growth, health, and population turnover within mussel beds of *Perna canaliculus* in northern New Zealand. *Marine Biology Research* **4**:376 - 383.
- Aline, T.** 2008. Dissolution of dead corals by euendolithic microorganisms across the northern Great Barrier Reef (Australia). *Microb Ecol* **55**:569-80.
- Al-Thukair, A.A., and Golubic, S.** 1991. 5 New *Hyella* Species from the Arabian Gulf. *Archiv Fur Hydrobiologie*:167-197.
- Bathurst, R.G.** 1974. Marine Diagenesis of Shallow-Water Calcium-Carbonate Sediments. *Annual Review of Earth and Planetary Sciences* **2**:257-274.
- Berman-Frank, I., Lundgren, P., and Falkowski, P.** 2003. Nitrogen fixation and photosynthetic oxygen evolution in cyanobacteria. *Research in Microbiology* **154**:157-164.
- Castenholz, R. W.** 2001. Phylum BX. Cyanobacteria. *In* *Bergey's Manual of Systematic Bacteriology*, 2nd edn, vol. 1, pp. 473–487.

- Chacón, E., Berrendero, E., and Pichel, F.G.** 2006. Biogeological signatures of microboring cyanobacterial communities in marine carbonates from Cabo Rojo, Puerto Rico. *Sedimentary Geology* **185**:215-228.
- Chazottes, V., Cabioch, G., Golubic, S., and Radtke, G.** 2009. Bathymetric zonation of modern microborers in dead coral substrates from New Caledonia-Implications for paleodepth reconstructions in Holocene corals. *Palaeogeography Palaeoclimatology Palaeoecology* **280**:456-468.
- Che, L.M., Le Campion-Alsumard, T., Bouryesnault, N., Payri, C., Golubic, S., and Bezac, C.** 1996. Biodegradation of shells of the black pearl oyster, *Pinctada margaritifera* var *cumingii*, by microborers and sponges of French Polynesia. *Marine Biology* **126**:509-519.
- Cockell, C.S., and Herrera, A.** 2008. Why are some microorganisms boring? *Trends in Microbiology* **16**:101-106.
- Countway, P.D., Gast, R.J., Savai, P., and Caron, D.A.** 2005. Protistan diversity estimates based on 18S rDNA from seawater incubations in the western North Atlantic. *Journal of Eukaryotic Microbiology* **52**:95-106.
- Danin, A., Gerson, R., Marton, K., and Garty, J.** 1982. Patterns of Limestone and Dolomite Weathering by Lichens and Blue-Green-Algae and Their Paleoclimatic Significance. *Palaeogeography Palaeoclimatology Palaeoecology* **37**:221-233.
- Desikachary, T.V.** 1959. *Cyanophytae*. Indian Council of Agricultural Research, New Delhi. 686p.
- Duguid, S.M.A., Kyser, T.K., James, N.P., and Rankey, E.C.** 2010. Microbes and Ooids. *Journal of Sedimentary Research* **80**:236-251.
- Dunphy, B.J., and Wells, R.M.G.** 2001. Endobiont infestation, shell strength and condition index in wild populations of New Zealand abalone, *Haliotis iris*. *Marine and Freshwater Research* **52**:781-786.
- Dvornyk, V., Vinogradova, O., and Nevo, E.** 2003. Origin and evolution of circadian clock genes in prokaryotes. *Proceedings of the National Academy of Sciences of the United States of America* **100**:2495-2500.

- Friedmann, E.I., Hua, M. And Ocampo-Friedmann, R.** 1993. Terraforming Mars: dissolution of carbonate rocks by cyanobacteria. *Journal of the British Interplanetary Society* **46**:291-292.
- Forsterra, F., and Haussermann, V.** 2008. Unusual symbiotic relationships between microendolithic phototrophic organisms and azooxanthellate cold-water corals from Chilean fjords. *Marine Ecology Progress Series* **370**:121-125.
- Garcia-Pichel, F.** 2006. Plausible mechanisms for the boring on carbonates by microbial phototrophs. *Sedimentary Geology* **185**:205-213.
- Geitler, L.** 1932. Cyanophyceae, p. 916-931. *In* Rabenhorst's Kryptogamenflora von Deutschland. Österreich und der Schweiz, vol. 14. Akad Verlag, Leipzig.
- Ghirardelli, L.A.** 2002. Endolithic microorganisms in live and dead thalli of coralline red algae (Corallinales, Rhodophyta) in the northern Adriatic Sea. *Acta Geologica Hispanica* **37**:53-60
- Golubic, S., Brent, G., and Le Campion-Alsumard, T.** 1970. Scanning Electron Microscopy of Endolithic Algae and Fungi Using a Multipurpose Casting-Embedding Technique. *Lethaia* **3**:203-209.
- Golubic, S., Perkins, R.D. And Lukas, K.J., Editors.** 1975. Boring Microorganisms and Borings in Carbonate Substrates, vol. Springer-Verlag, Berlin.
- Golubic, S., and Seong-Joo, L.** 1999. Early cyanobacterial fossil record: preservation, palaeoenvironments and identification. *European Journal of Phycology* **34**:339-348.
- Hoffmann, L.** 1990. Presence of Mastigocladopsis-Jogensis (Cyanophyceae, Mastigocladopsidaceae) in Corsica (France). *Cryptogamie Algologie* **11**:219-224.
- Horath, T., Neu, T.R., and Bachofen, R.** 2006. An endolithic microbial community in dolomite rock in central Switzerland: characterization by reflection spectroscopy, pigment analyses, scanning electron microscopy, and laser scanning microscopy. *Microb Ecol* **51**:353-64.
- Kaehler, S.** 1999. Incidence and distribution of phototrophic shell-degrading endoliths of the brown mussel *Perna perna*. *Marine Biology* **135**:505-514.
- Knoll, A.H., Golubic, S., Green, J., and Swett, K.** 1986. Organically preserved microbial endoliths from the late Proterozoic of East Greenland. *Nature* **321**:856-7.

- Komárek, J., and Anagnostidis, K.** 1999. Cyanoprokaryota. *In* Ettl, H., Gärtner, G., Heynig, H. & Mollenhauer, D. (ed.), Süßwasserflora von Mitteleuropa, vol. 19. Spektrum, Akad. Verlag, Heidelberg; Berlin.
- Lagerheim, G.** 1886. Note sur le Mastigocoleus, nouveau genre des algues marines de l'ordre des Phycchromacees. *Notarisia* **1**:65-69.
- Le Campion-Alsumard, T.** 1991. 3 Hyella Taxa (Endolithic Cyanophytes) from Tropical Environments (Lizard-Island, Great-Barrier-Reef). *Archiv für Hydrobiologie*:159-166.
- Le Campion-Alsumard, T., Golubic, S., and Hutchings, P.** 1995. Microbial Endoliths in Skeletons of Live and Dead Corals - Porites Lobata (Moorea, French-Polynesia). *Marine Ecology-Progress Series* **117**:149-157.
- Lorne, J., Scheffer, J., Lee, A., Painter, M., and Miao, V.P.** 2000. Genes controlling circadian rhythm are widely distributed in cyanobacteria. *FEMS Microbiol Lett* **189**:129-33.
- Macintyre, I.G., Prufert-Bebout, L., and Reid, R.P.** 2000. The role of endolithic cyanobacteria in the formation of lithified laminae in Bahamian stromatolites. *Sedimentology* **47**:915-921.
- Montoya-Terreros, H., Gomez-Carrion, J. and Benavente-Palacios, M.** 2006. Natural populations and culture of the marine microalga *Mastigocoleus testarum* Lagerheim ex Bornet et Flahault (Cyanophyta, Nostochopsaceae), the first record for the Peruvian flora. *Arnaldoa* **13**:258-269.
- Nagy, M.L., Perez, A., and Garcia-Pichel, F.** 2005. The prokaryotic diversity of biological soil crusts in the Sonoran Desert (Organ Pipe Cactus National Monument, AZ). *FEMS Microbiology Ecology* **54**:233-45.
- Nielsen, C.S.** 1956. Notes on Stigonemataceae from Southeastern United States. *Transactions of the American Microscopical Society* **75**:427-436.
- Perkins, R.D., and Tsentas, C.I.** 1976. Microbial Infestation of Carbonate Substrates Planted on St-Croix Shelf, West-Indies. *Geological Society of America Bulletin* **87**:1615-1628.
- Poly, F., Ranjard, L., Nazaret, S., Gourbiere, F., and Monrozier, L.J.** 2001. Comparison of nifH gene pools in soils and soil microenvironments with contrasting properties. *Applied Environmental Microbiology* **67**:2255-62.

- Provasoli, L.** 1968. Media and prospects for the cultivation of marine algae  
In: Watanabe, A. and Hattori, A., Eds. Cultures and Collection of  
Algae. Japanese Society of Plant Physiology, Hakone.
- Radtke, G., and Golubic, S.** 2005. Microborings in mollusk shells, Bay of  
Safaga, Egypt: Morphometry and ichnology. *Facies* **51**:125-141.
- Raghukumar, C., Sharma, S., and Lande, V.** 1991. Distribution and  
Biomass Estimation of Shell-Boring Algae in the Intertidal at Goa,  
India. *Phycologia* **30**:303-309.
- Rajaniemi, P., Hrouzek, P., Kastovska, K., Willame, R., Rantala,  
A., Hoffmann, L., Komarek, J., and Sivonen, K.** 2005.  
Phylogenetic and morphological evaluation of the genera *Anabaena*,  
*Aphanizomenon*, *Trichormus* and *Nostoc* (Nostocales, Cyanobacteria).  
*International Journal of Systematic and Evolutionary Microbiology*  
**55**:11-26.
- Reid, R.P., Visscher, P.T., Decho, A.W., Stolz, J.F., Bebout, B.M.,  
Dupraz, C., Macintyre, L.G., Paerl, H.W., Pinckney, J.L.,  
Prufert-Bebout, L., Steppe, T.F., and Desmarais, D.J.** 2000.  
The role of microbes in accretion, lamination and early lithification of  
modern marine stromatolites. *Nature* **406**:989-992.
- Seong-Joo, L., and Golubic, S.** 1998. Multi-trichomous cyanobacterial  
microfossils from the Mesoproterozoic Gaoyuzhuang Formation,  
China: Paleoecological and taxonomic implications. *Lethaia* **31**:169-  
184.
- Sigler, W.V., Bachofen, R., and Zeyer, J.** 2003. Molecular  
characterization of endolithic cyanobacteria inhabiting exposed  
dolomite in central Switzerland. *Environ Microbiol* **5**:618-27.
- Silva, P.C., Basson, P.W. And Moe, R.L.** 1996. Catalogue of the benthic  
marine algae of the Indian Ocean, p. 78. UC Publications in Botany,  
vol. 79. University of California Press.
- Sinha, R.P., Richter, P., Faddoul, J., Braun, M., and Hader, D.P.**  
2002. Effects of UV and visible light on cyanobacteria at the cellular  
level. *Photochemical & Photobiological Sciences* **1**:553-559.
- Stackebrandt, E. and Goebel B. M.** 1994. Taxonomic note: a place for  
DNA-DNA reassociation and 16S rRNA sequence analysis in the  
present species definition in bacteriology. *International Journal of  
Systematic Bacteriology* **44**:846-849.

- Stockfors, M., and Peel, J.S.** 2005. Euendoliths and cryptoendoliths within late Middle Cambrian brachiopod shells from North Greenland. *GFF* **127**:187-194.
- Stolz, J.F., Feinstein, T.N., Salsi, J., Visscher, P.T., and Reid, R.P.** 2001. TEM analysis of microbial mediated sedimentation and lithification in modern marine stromatolites. *American Mineralogist* **86**:826-833.
- Tamura, K., Dudley, J., Nei, M., and Kumar, S.** 2007. MEGA4: Molecular evolutionary genetics analysis (MEGA) software version 4.0. *Molecular Biology and Evolution* **24**:1596-1599.
- Tiwari, D.N.** 1978. Heterocysts of the Blue-Green-Alga *Nostochopsis-Lobatus*- Effects of Cultural Conditions. *New Phytologist* **81**:653-656.
- Tomitani, A., Knoll, A.H., Cavanaugh, C.M., and Ohno, T.** 2006. The evolutionary diversification of cyanobacteria: Molecular-phylogenetic and paleontological perspectives. *Proceedings of the National Academy of Sciences of the United States of America* **103**:5442-5447.
- Tribollet, A.** 2008. The boring microflora in modern coral reef ecosystems: a Review of its roles. *In* Wisshak, M.A.T., L. (ed.), *Current Developments in Bioerosion*. Springer-Verlag, Berlin.
- Tribollet, A., and Golubic, S.** 2005. Cross-shelf differences in the pattern and pace of bioerosion of experimental carbonate substrates exposed for 3 years on the northern Great Barrier Reef, Australia. *Coral Reefs* **24**:422-434.
- Tribollet, A., Langdon, C., Golubic, S., and Atkinson, M.** 2006. Endolithic microflora are major primary producers in dead carbonate substrates of Hawaiian coral reefs. *Journal of Phycology* **42**:292-303.
- Tribollet, A., and Payri, C.** 2001. Bioerosion of the coralline alga *Hydrolithon onkodes* by microborers in the coral reefs of Moorea, French Polynesia. *Oceanologica Acta* **24**:329-342.
- Van De Meene, A.M.L., Hohmann-Marriott, M.F., Vermaas, W.F.J., and Roberson, R.W.** 2006. The three-dimensional structure of the cyanobacterium *Synechocystis* sp PCC 6803. *Archives of Microbiology* **184**:259-270.
- Vischer, W.** 1937. Die Kultur der Heterokonten, p. 190-201. *In* Rabenhorst, L. (ed.), *Kryptogamenflora von Deutschland, Osterreich und der Schweiz*, vol. 11. Akademische Verlagsgesellschaft, Leipzig.



- Vogel, K., and Brett, C.E.** 2009. Record of microendoliths in different facies of the Upper Ordovician in the Cincinnati Arch region USA: The early history of light-related microendolithic zonation. *Palaeogeography Palaeoclimatology Palaeoecology* **281**:1-24.
- Vogel, K., Gektidis, M., Golubic, S., Kiene, W.E., and Radtke, G.** 2000. Experimental studies on microbial bioerosion at Lee Stocking Island, Bahamas and One Tree Island, Great Barrier Reef, Australia: implications for paleoecological reconstructions. *Lethaia* **33**:190-204.
- Wade, B.D., and Garcia-Pichel, F.** 2003. Evaluation of DNA Extraction Methods for Molecular Analyses of Microbial Communities in Modern Calcareous Microbialites. *Geomicrobiology Journal* **20**:549 - 561.
- Webb, S.C., and Korrubel, J.L.** 1994. Shell Weakening in Marine Mytilids Attributable to Blue-Green-Alga *Mastigocoleus* Sp. (*Nostochopsidaceae*). *Journal of Shellfish Research* **13**:11-17.
- Weckesser, J., Hofmann, K., Jürgens, U.J., Whitton, B.A., and Raffelsberger, B.** 1988. Isolation and Chemical-Analysis of the Sheaths of the Filamentous Cyanobacteria *Calothrix-Parietina* and *C-Scopulorum*. *Journal of General Microbiology* **134**:629-634.
- Yeates, T.O., Kerfeld, C.A., Heinhorst, S., Cannon, G.C., and Shively, J.M.** 2008. Protein-based organelles in bacteria: carboxysomes and related microcompartments. *Nature Reviews Microbiology* **6**:681-91.
- Young, H.R., and Nelson, C.S.** 1988. Endolithic Biodegradation of Cool-Water Skeletal Carbonates on Scott Shelf, Northwestern Vancouver-Island, Canada. *Sedimentary Geology* **60**:251-267.
- Zehr, J.P., Mellon, M.T., and Hiorns, W.D.** 1997. Phylogeny of cyanobacterial *nifH* genes: Evolutionary implications and potential applications to natural assemblages. *Microbiology-Uk* **143**:1443-1450.

## **CHAPTER 2**

- Al-Thukair, A.A., and Golubic, S.** 1991. 5 New *Hyella* Species from the Arabian Gulf. *Archiv für Hydrobiologie*:167-197.
- Andersen, C.L., Holland, I.B., and Jacq, A.** 2006. Verapamil, a Ca<sup>2+</sup> channel inhibitor acts as a local anesthetic and induces the sigma E dependent extra-cytoplasmic stress response in *E. coli*. *Biochimica Biophysica Acta* **1758**:1587-1595.
- Avery, S.V., and Tobin, J.M.** 1992. Mechanisms of Strontium Uptake by Laboratory and Brewing Strains of *Saccharomyces-Cerevisiae*. *Applied and Environmental Microbiology* **58**:3883-3889.

- Berman-Frank, I., Lundgren, P., Chen, Y.B., Kupper, H., Kolber, Z., Bergman, B., and Falkowski, P.** 2001. Segregation of nitrogen fixation and oxygenic photosynthesis in the marine cyanobacterium *Trichodesmium*. *Science* **294**:1534-1537.
- Bourget, C.** 1982. Verapamil: a calcium-channel blocker. *Dimensions of Critical Care Nursing* **1**:134-138.
- Campbell, S.** 1983. The modern distribution and geological history of calcium carbonate boring microorganisms, p. 99-104. *In* Wesbroek, P., De Jong, E.W. (ed.), *Biom mineralization and Biological Metal Accumulation*. Reidel Publishing, Boston.
- Eberhard, M., and Erne, P.** 1991. Calcium-Binding to Fluorescent Calcium Indicators - Calcium Green, Calcium Orange and Calcium Crimson. *Biochemical and Biophysical Research Communications* **180**:209-215.
- Entman, M.L., Hansen, J.L., and Cook, J.W., Jr.** 1969. Calcium metabolism in cardiac microsomes incubated with lanthanum ion. *Biochem Biophys Res Commun* **35**:258-264.
- Fernandez-Belda, F.** 1988. Lanthanum as a calcium-substituting ion for binding to sarcoplasmic reticulum ATPase. *Archives of Biochemistry and Biophysics* **267**:770-775.
- Fremy, P.** 1936. Les algues perforantes. *Memoires de la Societe Nationale des Sciences Naturelles et Mathematiques de Cherbourg* **42**:275-300.
- Friedmann, E.I., Hua, M., and Ocampo-Friedmann, R.** 1993. Terraforming Mars: dissolution of carbonate rocks by cyanobacteria. *Journal of the British Interplanetary Society* **46**:291-292.
- Fujimori, T., and Jencks, W.P.** 1990. Lanthanum inhibits steady-state turnover of the sarcoplasmic reticulum calcium ATPase by replacing magnesium as the catalytic ion. *Journal Biological Chemistry* **265**:16262-16270.
- Garcia-Pichel, F.** 2006. Plausible mechanisms for the boring on carbonates by microbial phototrophs. *Sedimentary Geology* **185**:205-213.
- Geisler, M., Koenen, W., Richter, J., and Schumann, J.** 1998. Expression and characterization of a *Synechocystis* PCC 6803 P-type ATPase in *E. coli* plasma membranes. *Biochimica Biophys ica Acta* **1368**:267-275.

- Golubic, S., Brent, G., and Lecampio.T.** 1970. Scanning Electron Microscopy of Endolithic Algae and Fungi Using a Multipurpose Casting-Embedding Technique. *Lethaia* **3**:203-209.
- Golubic, S., Campbell, S.E., Drobne, K., Cameron, B., Balsam, W.L., Cimerman, F., and Dubois, L.** 1984. Microbial Endoliths - a Benthic Overprint in the Sedimentary Record, and a Paleobathymetric Cross-Reference with Foraminifera. *Journal of Paleontology* **58**:351-361.
- Gordon, J.A.** 1991. Use of vanadate as protein-phosphotyrosine phosphatase inhibitor. *Methods in Enzymology* **201**:477-482.
- Gukovskaya, A.S., Gukovsky, S., and Pandol, S.J.** 2000. Endoplasmic reticulum Ca(2+)-ATPase inhibitors stimulate membrane guanylate cyclase in pancreatic acinar cells. *American Journal of Physiology* **278**:363-371.
- Haigler, S.A.** 1969. Boring Mechanism of *Polydora Websteri* Inhabiting *Crassostrea Virginica*. *American Zoologist* **9**:821-828.
- Hanel, A.M., and Jencks, W.P.** 1990. Phosphorylation of the calcium-transporting adenosinetriphosphatase by lanthanum ATP: rapid phosphoryl transfer following a rate-limiting conformational change. *Biochemistry* **29**:5210-5220.
- Harrison, S.M., and Bers, D.M.** 1989. Correction of Proton and Ca Association Constants of EGTA for Temperature and Ionic-Strength. *American Journal of Physiology* **256**:1250-1256.
- Hirose, S., Yaginuma, N., and Inada, Y.** 1974. Disruption of charge separation followed by that of the proton gradient in the mitochondrial membrane by CCCP. *Journal of Biochemistry* **76**:213-216.
- Kasianowicz, J., Benz, R., and Mclaughlin, S.** 1984. The kinetic mechanism by which CCCP (carbonyl cyanide m-chlorophenylhydrazone) transports protons across membranes. *Journal of Membrane Biology* **82**:179-190.
- Kirischuk, S., Voitenko, N., Kostyuk, P., and Verkhratsky, A.** 1996. Calcium signalling in granule neurones studied in cerebellar slices. *Cell Calcium* **19**:59-71.
- Knight, H., Trewavas, A.J., and Knight, M.R.** 1997. Calcium signalling in *Arabidopsis thaliana* responding to drought and salinity. *Plant Journal* **12**:1067-78.

- Konigshof, P., and Glaub, I.** 2004. Traces of microboring organisms in Palaeozoic conodont elements. *Geobios* **37**:416-424.
- Koyama, K., Suzuki, H., Noguchi, T., Akimoto, S., Tsuchiya, T., and Mimuro, M.** 2008. Oxygen evolution in the thylakoid-lacking cyanobacterium *Gloeobacter violaceus* PCC 7421. *Biochim Biophys Acta* **1777**:369-78.
- Lagerheim, G.** 1886. Note sur le *Mastigocoleus*, nouveau genre des algues marines de l'ordre des *Phycochromacees*. *Notarisia* **1**:65-69.
- Lanini, L., Bachs, O., and Carafoli, E.** 1992. The calcium pump of the liver nuclear membrane is identical to that of endoplasmic reticulum. *Journal of Biological Chemistry* **267**:11548-11552.
- Lattanzio, F.A., and Bartschat, D.K.** 1991. The Effect of Ph on Rate Constants, Ion Selectivity and Thermodynamic Properties of Fluorescent Calcium and Magnesium Indicators. *Biochemical and Biophysical Research Communications* **177**:184-191.
- Le Campion-Alsumard, T.** 1991. 3 *Hyella* Taxa (Endolithic Cyanophytes) from Tropical Environments (Lizard-Island, Great-Barrier-Reef). *Archiv für Hydrobiologie*:159-166.
- Le Campion-Alsumard, T., Golubic, S., and Hutchings, P.** 1995. Microbial Endoliths in Skeletons of Live and Dead Corals - *Porites Lobata* (Moorea, French-Polynesia). *Marine Ecology-Progress Series* **117**:149-157.
- Moreno, I., Norambuena, L., Maturana, D., Toro, M., Vergara, C., Orellana, A., Zurita-Silva, A., and Ordenes, V.R.** 2008. AtHMA1 is a thapsigargin-sensitive Ca<sup>2+</sup>/heavy metal pump. *Journal of Biological Chemistry* **283**:9633-9641.
- Nakata, M., Ishiyama, T., Akamatsu, S., Hirose, Y., Maruoka, H., Suzuki, R., and Tatsuta, K.** 1995. Synthetic Studies on Oligomycins - Synthesis of the Oligomycin-B Spiroketal and Polypropionate Portions. *Bulletin of the Chemical Society of Japan* **68**:967-989.
- Petersen, O.H., Michalak, M., and Verkhratsky, A.** 2005. Calcium signalling: Past, present and future. *Cell Calcium* **38**:161-169.
- Phillippe, M., Kim, J., Freij, M., and Saunders, T.** 1995. Effects of 2,5-di(tert-butyl)-1,4-hydroquinone, an endoplasmic reticulum Ca(2+)-ATPase inhibitor, on agonist-stimulated phasic myometrial contractions. *Biochemical and Biophysical Research Communications* **207**:891-896.

- Rajdev, S., and Reynolds, I.J.** 1993. Calcium Green-5n, a Novel Fluorescent-Probe for Monitoring High Intracellular Free Ca<sup>2+</sup> Concentrations Associated with Glutamate Excitotoxicity in Cultured Rat-Brain Neurons. *Neuroscience Letters* **162**:149-152.
- Robinson, I.M., Cheek, T.R., and Burgoyne, R.D.** 1992. Ca<sup>2+</sup> influx induced by the Ca(2+)-ATPase inhibitors 2,5-di-(t-butyl)-1,4-benzohydroquinone and thapsigargin in bovine adrenal chromaffin cells. *Biochemical Journal* **288** :457-63.
- Rogers, T.B., Inesi, G., Wade, R., and Lederer, W.J.** 1995. Use of thapsigargin to study Ca<sup>2+</sup> homeostasis in cardiac cells. *Bioscience Reports* **15**:341-9.
- Shainkin-Kestenbaum, R., Winikoff, Y., Kol, R., Chaimovitz, C., and Sarov, I.** 1989. Inhibition of growth of *Chlamydia trachomatis* by the calcium antagonist verapamil. *Journal of General Microbiology* **135**:1619-23.
- Stal, L.J., and Krumbein, W.E.** 1987. Temporal Separation of Nitrogen-Fixation and Photosynthesis in the Filamentous, Nonheterocystous Cyanobacterium *Oscillatoria* Sp. *Archives of Microbiology* **149**:76-80.
- Teixeira, C.E., Corrado, A.P., De Nucci, G., and Antunes, E.** 2004. Role of Ca<sup>2+</sup> in vascular smooth muscle contractions induced by Phoneutria nigriventer spider venom. *Toxicon* **43**:61-8.
- Tribollet, A., Langdon, C., Golubic, S., and Atkinson, M.** 2006. Endolithic microflora are major primary producers in dead carbonate substrates of Hawaiian coral reefs. *Journal of Phycology* **42**:292-303.
- Tucker, T., and Fettiplace, R.** 1995. Confocal imaging of calcium microdomains and calcium extrusion in turtle hair cells. *Neuron* **15**:1323-1335.
- Uhrik, B., and Zacharova, D.** 1988. Intracellular Site of Sr<sup>2+</sup> and Ba<sup>2+</sup> Accumulation in Frog Twitch Muscle-Fibers as Determined by Electron-Probe X-Ray-Microanalysis. *General Physiology and Biophysics* **7**:569-581.
- Vasington, F.D.** 1966. Accumulation of Ca<sup>2+</sup> and Sr<sup>2+</sup> by Rat-Liver Mitochondria - Preferential Loss of Adenosine Triphosphate-Dependent Mechanism for Sr<sup>2+</sup> Accumulation. *Biochimica Et Biophysica Acta* **113**:414-416.
- Vogel, K., Gektidis, M., Golubic, S., Kiene, W.E., and Radtke, G.** 2000. Experimental studies on microbial bioerosion at Lee Stocking

Island, Bahamas and One Tree Island, Great Barrier Reef, Australia: implications for paleoecological reconstructions. *Lethaia* **33**:190-204.

**Zhao, M.D., Hollingworth, S., and Baylor, S.M.** 1996. Properties of tri- and tetracarboxylate Ca<sup>2+</sup> indicators in frog skeletal muscle fibers. *Biophysical Journal* **70**:896-916.

### **CHAPTER 3**

**Al-Thukair, A.A., and Golubic, S.** 1991. 5 New *Hyella* Species from the Arabian Gulf. *Archiv für Hydrobiologie*:167-197.

**Al-Thukair, A.A., and Golubic, S.** 1991. New Endolithic Cyanobacteria from the Arabian Gulf. 1. *Hyella immanis* Sp. Nov. *Journal of Phycology* **27**:766-780.

**Bornet, E. and Flahault, C.** 1888. Note sur deux nouveaux genres d'algues perforantes. *Journal de Botanique* **2**:162-163.

**Castenholz, R. W.** 2001. Phylum BX. Cyanobacteria. *In* *Bergey's Manual of Systematic Bacteriology*, 2nd edn, vol. 1, pp. 473–487.

**Castenholz, R. W. & Waterbury, J. B. (1989).** Cyanobacteria. Preface. *In* Buchanan, R. E. & Gibbons, N. E. (Eds) *Bergey's Manual of Systematic Bacteriology*, vol. 3, pp. 1710±1806. Baltimore: Williams & Wilkins.

**Chacón, E., Berrendero, E., and Garcia-Pichel, F.** 2006. Biogeological signatures of microboring cyanobacterial communities in marine carbonates from Cabo Rojo, Puerto Rico. *Sedimentary Geology* **185**:215-228.

**Che, L.M., Le Campion-Alsumard, T., Bouryesnault, N., Payri, C., Golubic, S., and Bezac, C.** 1996. Biodegradation of shells of the black pearl oyster, *Pinctada margaritifera* var *cumingii*, by microborers and sponges of French Polynesia. *Marine Biology* **126**:509-519.

**Cockell, C.S., and Herrera, A.** 2008. Why are some microorganisms boring? *Trends in Microbiology* **16**:101-106.

**Desikachary, T.V.** 1959. Cyanophytae. Indian Council of Agricultural Research, New Delhi. 686p.

**Ercegović, A.** 1927. Tri roda litofitskih cijanoficeja sa jadranske obale. *Acta Botanica Instituti Botanici Universitatis Zagrebensis* **2**:78-84.

- Foster, J.S., Green, S.J., Ahrendt, S.R., Golubic, S., Reid, R.P., Hetherington, K.L., and Bebout, L.** 2009. Molecular and morphological characterization of cyanobacterial diversity in the stromatolites of Highborne Cay, Bahamas. *ISME Journal* **3**:573-87.
- Fremy, P.** 1936. Les algues perforantes. *Memoires de la Societe Nationale des Sciences Naturelles et Mathematiques de Cherbourg* **42**:275-300.
- Garcia-Pichel, F.** 2006. Plausible mechanisms for the boring on carbonates by microbial phototrophs. *Sedimentary Geology* **185**:205-213.
- Geitler, L.** 1932. Cyanophyceae, p. 916-931. *In* Rabenhorst's Kryptogamenflora von Deutschland. Österreich und der Schweiz, vol. 14. Akad Verlag, Leipzig.
- Golubic, S.** 1969. Distribution, Taxonomy, and Boring Patterns of Marine Endolithic Algae. *American Zoologist* **9**:747-751.
- Golubic, S., Perkins, R.D. And Lukas, K.J.** 1975. Boring Microorganisms and Borings in Carbonate Substrates. *In* Frey, R.W. (Ed), *The Study of Trace Fossils*. Springer, Berlin, pp.229-259
- Kaehler, S.** 1999. Incidence and distribution of phototrophic shell-degrading endoliths of the brown mussel *Perna perna*. *Marine Biology* **135**:505-514.
- Lagerheim, G.** 1886. Note sur le *Mastigocoleus*, nouveau genre des algues marines de l'ordre des *Phycochromaceae*. *Notarisia* **1**:65-69.
- Le Campion-Alsumard, T.** 1991. 3 *Hyella* Taxa (Endolithic Cyanophytes) from Tropical Environments (Lizard-Island, Great-Barrier-Reef). *Archiv für Hydrobiologie*:159-166.
- Le Campion-Alsumard, T., Golubic, S., and Hutchings, P.** 1995. Microbial Endoliths in Skeletons of Live and Dead Corals - *Porites Lobata* (Moorea, French-Polynesia). *Marine Ecology Progress Series* **117**:149-157.
- Lukas, K.J., and Golubic, S.** 1981. New Endolithic Cyanophytes from the North-Atlantic Ocean. 1. *Cyanosaccus piriformis* Gen. Et. Sp. Nov. *Journal of Phycology* **17**:224-229.
- Montoya-Terreros, H., Gomez-Carrión, J. and Benavente-Palacios, M.** 2006. Natural populations and culture of the marine microalga *Mastigocoleus testarum* Lagerheim ex Bornet et Flahault (Cyanophyta, Nostochopsaceae), the first record for the Peruvian flora. *Arnaldoa* **13**:258-269.

- Nübel, U., Garcia-Pichel, F., and Muyzer, G.** 1997. PCR primers to amplify 16S rRNA genes from cyanobacteria. *Applied and Environmental Microbiology* **63**:3327-32.
- Pickles, R.J., and Cuthbert, A.W.** 1992. Failure of thapsigargin to alter ion transport in human sweat gland epithelia while intracellular Ca<sup>2+</sup> concentration is raised. *Journal of Biological Chemistry* **267**:14818-14825.
- Provasoli, L.** 1968. Media and prospects for the cultivation of marine algae  
In: Watanabe, A. and Hattori, A., Eds. *Cultures and Collection of Algae*. Japanese Society of Plant Physiology, Hakone.
- Raghukumar, C., Sharma, S., and Lande, V.** 1991. Distribution and Biomass Estimation of Shell-Boring Algae in the Intertidal at Goa, India. *Phycologia* **30**:303-309.
- Reid, R.P., Visscher, P.T., Decho, A.W., Stolz, J.F., Bebout, B.M., Dupraz, C., Macintyre, I.G., Paerl, H.W., Pinckney, J.L., Prufert-Bebout, L., Steppe, T.F., and Desmarais, D.J.** 2000. The role of microbes in accretion, lamination and early lithification of modern marine stromatolites. *Nature* **406**:989-92.
- Scamps, F., Roig, A., Boukhaddaoui, H., Andre, S., Puech, S., and Valmier, J.** 2004. Activation of P-type calcium channel regulates a unique thapsigargin-sensitive calcium pool in embryonic motoneurons. *European Journal of Neuroscience* **19**:977-982.
- Schneider, J., and Le Campion-Alsumard, T.** 1999. Construction and destruction of carbonates by marine and freshwater cyanobacteria. *European Journal of Phycology* **34**:417-426.
- Stolz, J.F., Feinstein, T.N., Salsi, J., Visscher, P.T., and Reid, R.P.** 2001. TEM analysis of microbial mediated sedimentation and lithification in modern marine stromatolites. *American Mineralogist* **86**:826-833.
- Thuret, G.** 1875. Essai de classification des Nostochinees. *Annales des Sciences Natureles* **6**:375-379.
- Vogel, K., Gektidis, M., Golubic, S., Kiene, W.E., and Radtke, G.** 2000. Experimental studies on microbial bioerosion at Lee Stocking Island, Bahamas and One Tree Island, Great Barrier Reef, Australia: implications for paleoecological reconstructions. *Lethaia* **33**:190-204.
- Webb, S.C., and Korrubel, J.L.** 1994. Shell Weakening in Marine Mytilids Attributable to Blue-Green-Alga *Mastigocoleus* Sp. (Nostochopsidaceae). *Journal of Shellfish Research* **13**:11-17.



**Zhang, Y.A.G., S.** 1987. Endolithic microfossils (cyanophyta) from early Proterozoic stromatolites, Hebei, China. *Acta Micropalaentol. Sin.* **4**:1-12.

#### **CHAPTER 4**

**Alakomi, H.-L., Paananen, A., Suihko, M.-L., Helander, I.M., and Saarela, M.** 2006. Weakening Effect of Cell Permeabilizers on Gram-Negative Bacteria Causing Biodeterioration. *Applied and Environmental Microbiology* **72**:4695-4703.

**Alakomi, H.-L., Saarela, M., and Helander, I.M.** 2003. Effect of EDTA on *Salmonella enterica* serovar Typhimurium involves a component not assignable to lipopolysaccharide release. *Microbiology* **149**:2015-2021.

**Ascenzi, A., and Silvestrini, G.** 1984. Bone-Boring Marine Microorganisms - an Experimental Investigation. *Journal of Human Evolution* **13**:531-536.

**Baumgartner, L.K., Dupraz, C., Buckley, D.H., Spear, J.R., Pace, N.R., and Visscher, P.T.** 2009. Microbial Species Richness and Metabolic Activities in Hypersaline Microbial Mats: Insight into Biosignature Formation Through Lithification. *Astrobiology* **9**:861-874.

**Danin, A., Gerson, R., and Garty, J.** 1983. Weathering Patterns on Hard Limestone and Dolomite by Endolithic Lichens and Cyanobacteria - Supporting Evidence for Eolian Contribution to Terra Rossa Soil. *Soil Science* **136**:213-217.

**Defarge, C., and Trichet, J.** 1990. Role of Organic Substrates Inherited from Living Organisms in the Mineralization of Modern Calcareous Microbialites (Kopara from French-Polynesia) - Implications Concerning the Intervention of Sedimentary Organic-Matter in Geological Processes. *Comptes Rendus De L Academie Des Sciences* **310**:1461-1467.

**Dupraz, C., and Strasser, A.** 1999. Microbialites and micro-encrusters in shallow coral bioherms (Middle to Late Oxfordian, Swiss Jura Mountains). *Facies* **40**:101-129.

**Dupraz, C., and Visscher, P.T.** 2005. Microbial lithification in marine stromatolites and hypersaline mats. *Trends in Microbiology* **13**:429-438.

- Garcia-Pichel, F., Al-Horani, F., Ludwig, R., Farmer, J., Wade, B.** 2004 Balance between calcification and bioerosion in modern stromatolites. *Geobiology* 2:49-57
- Golubic, S.** 1969. Distribution, Taxonomy, and Boring Patterns of Marine Endolithic Algae. *American Zoologist* 9:747-751.
- Golubic, S., Friedmann, I., and Schneider, J.** 1981. The Lithobiontic Ecological Niche, with Special Reference to Microorganisms. *Journal of Sedimentary Petrology* 51:475-478.
- Lagerheim, G.** 1886. Note sur le Mastigocoleus, nouveau genre des algues marines de l'ordre des Phycochromacees. *Notarisia* 1:65-69.
- Laurenti, A., and Montaggioni, L.** 1995. The Role of Microbial Activity in Marine Reef Lithification (Tahiti, French-Polynesia). *Comptes Rendus De L' Academie Des Sciences* 320:845-852.
- Laval, B., Cady, S.L., Pollack, J.C., Mckay, C.P., Bird, J.S., Grotzinger, J.P., Ford, D.C., and Bohm, H.R.** 2000. Modern freshwater microbialite analogues for ancient dendritic reef structures. *Nature* 407:626-629.
- Le Campion-Alsumard, T., Golubic, S., and Hutchings, P.** 1995. Microbial Endoliths in Skeletons of Live and Dead Corals - Porites Lobata (Moorea, French-Polynesia). *Marine Ecology Progress Series* 117:149-157.
- Merz-Preiss, M., and Riding, R.** 1999. Cyanobacterial tufa calcification in two freshwater streams: ambient environment, chemical thresholds and biological processes. *Sedimentary Geology* 126:103-124.
- Nielsen, R.** 1987. Marine-Algae within Calcareous Shells from New Zealand. *New Zealand Journal of Botany* 25:425-438.
- Pentecost, A.** 1985. Association of Cyanobacteria with Tufa Deposits - Identity, Enumeration, and Nature of the Sheath Material Revealed by Histochemistry. *Geomicrobiology Journal* 4:285-298.
- Stolz, J.F., Feinstein, T.N., Salsi, J., Visscher, P.T., and Reid, R.P.** 2001. TEM analysis of microbial mediated sedimentation and lithification in modern marine stromatolites. *American Mineralogist* 86:826-833.
- Wade, B.D., and Garcia-Pichel, F.** 2003. Evaluation of DNA extraction methods for molecular analyses of microbial communities in modern calcareous microbialites. *Geomicrobiology Journal* 20:549-561.

**Wierzchos, J., Berlanga, M., Ascaso, C., and Guerrero, R.** 2006. Micromorphological characterization and lithification of microbial mats from the Ebro Delta (Spain). *International Microbiology* **9**:289-295.

